Thermal regime and sublimation rates of subsurface ice in Antarctica and on Mars under current and past environmental conditions: Insights from modeling and ground data

Lu Liu

A dissertation

submitted in partial fulfillment of the

requirements for the degree of

Doctor of Philosophy

University of Washington

2014

Reading Committee:

Ronald S. Sletten, Chair

Bernard Hallet

Edwin D. Waddington

Stephen E. Wood

Program Authorized to Offer Degree:

Department of Earth and Space Sciences

University of Washington

ABSTRACT

Thermal regime and sublimation rates of subsurface ice in Antarctica and on Mars under current and past environmental conditions: Insights from modeling and ground data

Lu Liu

Chair of the Supervisory Committee:

Research Associate Professor Ronald S. Sletten

Department of Earth and Space Sciences

Subsurface ice is common in regions where mean annual temperatures are below the freezing point of water. Once present, this ice may persist for long periods of time even under unfavorable environmental conditions. Subsurface ice is fundamentally important as a source of water for plants and microbes, a proxy for paleoclimatic information, and a major component controlling the periglacial landscape. This dissertation examines the stability and persistence of ground ice both in the Dry Valleys of Antarctica, a small part of the continent that is not covered in ice, and at the equatorial region on Mars. This research was initially motivated by claims that the ice buried under several decimeters of dry regolith in Beacon Valley is more than 1 Ma old and perhaps over 8.1 Ma, thereby making it the oldest known ice on Earth. My study uses numerical modeling to determine the short-term and long-term rates of sublimation of ground ice; the latter bears directly on the longevity of subsurface ice. The modeling utilizes extensive soil and environmental data from a well-characterized site in Beacon Valley. One component of the model

is to reconstruct subsurface temperatures based on measured surface temperatures. It is validated using ground temperature measurements. Both thermal and sublimation components of the model are then coupled, along with environmental data from the Curiosity Rover, to numerically simulate the sublimation of ground ice in Gale Crater, and to consider the potential for ground ice to have persisted there for long periods of time.

The contemporary sublimation rate of ground ice in Beacon Valley, Antarctica is modeled using a vapor diffusion model constrained by 12 years of climate and soil temperature data, and field data of episodic snow cover and snowmelt events that have not been represented in previous models of the ground ice sublimation. The model is extended to reconstruct the sublimation history over the last 200 ka using paleotemperatures estimated from ice core data from nearby Taylor Dome, and a relationship between atmospheric temperature and humidity derived from our meteorological records. This study provides a realistic estimate of the long-term sublimation history in Beacon Valley. Sublimation occurs throughout the modeled period; however, the rates are slow enough that the residual buried ice is likely older than 1 Ma.

I also studied the subsurface thermal regime and soil thermal properties in Beacon Valley and, using temperature-dependent thermal properties, numerically solved the heat diffusion equation using the finite volume method. The modeled temperatures approximate closely the measured temperatures at all depths with average differences ranging from 0.01°C to 0.03°C. The latent heat from documented episodic snowmelt events or modeled changes in ice content due to condensation or sublimation have negligible effects on the temperature. This study validates that our model is applicable to ground conditions in the cold, dry environments in general, including other regions in Antarctica, high mountain ranges in the central Asian and South America, and on Mars.

The heat and vapor diffusion models developed for Beacon Valley were then applied to Gale Crater, Mars to study the ground temperature and stability of ice that formed potentially during the last high obliquity phase of Mars. This study of subsurface heat and vapor transport is made use of one year of extensive ground-based measurements by Curiosity′s Rover Environmental Monitoring Station (REMS). As in Beacon Valley, ground ice is currently unstable along the Curiosity traverse; furthermore, also analogous to Beacon Valley, Gale Crater may have relict ground ice from as recently as ~0.5 Ma during the last high obliquity period. Similarly, modeling the sublimation rates, adjusted for Mars conditions, shows that water vapor loss deceases increasingly with depth as overlying dry regolith thickens. My study suggests ground ice that may have formed ~0.5 Ma ago could persist within meters of the surface; this finding may be important for future mission considerations.

Overall, my studies advance our understanding of the thermal regime and long-term stability of subsurface ice in frigid, hyperarid environments.

No matter what you do, be good at it.

ACKNOWLEDGEMENTS

I wish to express my deepest gratitude to my committee members; I would never have been able to finish my dissertation without the guidance from them. First of all, I would like thank my advisor, Dr. Ronald Sletten, for making this amazing experience possible and for his excellent guidance and patience, and for caring and providing me with a wonderful environment for doing research. I am truly fortunate to have worked with, and learned from, such an expert both in the field and in the laboratory. I also highly appreciate the rest of my committee members, Dr. Bernard Hallet, Dr. Edwin Waddington, Dr. John Stone, and Dr. Stephen Wood for their guidance and advice to help me develop my scientific background and advance my research in the polar subsurface environment. I would also like to recognize Dr. John Berg, my Graduate School Representative, for his constructive input and readiness to help.

I would like to specially thank Dr. Birgit Hagedorn at the University of Alaska-Anchorage for her support, collaborative research on the ground-ice sublimation, and her expert mentoring during my fieldwork. My sincere thanks to my fellow graduate students including Jon Toner, Zoe Harrold, Yan Hu, Batbaatar Jigjidsuren, Jon Bapst, and Nick Cuozzo for their support and going throughout this pleasant journey and great experience with me at the University of Washington.

The research presented in this dissertation was funded by the National Science Foundation (under Grants No. 0541054, 0636998, 1341680), NASA Mars Science Laboratory awarded via Malin Space Science Systems, and Kenneth C. Robbins Graduate Fellowship, Joseph A. Endowed Vance Fellowship, the Dr. Howard A. Coombs Scholarship, and David A. Johnston Award from the Department of Earth and Space Sciences at the University of Washington. I am also grateful to Antarctic Support Services, PHI, and our colleagues in Christchurch for superb logistical support in the Dry Valleys.

Last but not the least, I wish to express my greatest appreciation to my family in China for their support and encouragement. Finally, I would like to thank my husband, Jiajia Song, for his love and support. He is always there to cheer me up and stand by me through the good, as well as the difficult, times.

Table of Contents

LIST OF FIGURES

LIST OF TABLES

Chapter 1. Introduction

1.1. Overview and Background

Permafrost and associated subsurface ice cover approximately 20% of Earth's land surfaces [*Brown et al.*, 2002; *Gruber*, 2012] and all of Mars [*Jakosky and Mellon*, 2004]. The interest in subsurface ice is manifold, ranging from ground ice as an important reservoir of water for life [*Gleick*, 1993], as a proxy for paleoclimatic information [*Schirrmeister et al.*, 2002; *Stuiver et al.*, 1981], and as a major component controlling the periglacial landscape [*Black and Berg*, 1963; *Pewe*, 1959; *Sletten et al.*, 2003].

Ground ice stability is of interest in a number of environments including the Arctic, Antarctic, and Mars. The interest in the Arctic centers on the stability of permafrost and ground ice in a changing climate [*Kane et al.*, 1991; *Roth and Boike*, 2001; *Scherler et al.*, 2010; *Schuur et al.*, 2008]. In the frigid, hyperarid McMurdo Dry Valleys (MDV) of Antarctica, the formation and persistence of subsurface ice remain enigmatic, resulting in numerous papers investigating ground ice dynamics [*Hagedorn et al.*, 2007; *Hindmarsh et al.*, 1998; *McKay et al.*, 1998; *Schörghofer*, 2005; 2009] and its long-term stability [*Ng et al.*, 2005; *Schäfer et al.*, 2000; *Stone et al.*, 2000; *Sugden et al.*, 1995]. The MDV are one of our best terrestrial analogs for studying Martian ground ice [*Anderson et al.*, 1972; *Heldmann et al.*, 2013; *Sletten et al.*, 2003], which probably plays an important role in the formation and dynamics of many Martian landforms [*Anderson et al.*, 1972; *Mangold*, 2010; *Mellon et al.*, 2008; *Squyres and Carr*, 1986]. On Mars, the distribution and stability of subsurface ice has also been studied extensively [*Fanale*, 1976; *Fanale et al.*, 1986; *Mellon et al.*, 2004; *Mellon and Jakosky*, 1993; 1995; *Mellon et al.*, 1997; *Paige*, 1992; *Schörghofer*, 2007; *Schörghofer and Aharonson*, 2005]. Under current conditions on Mars, ground ice is present near the polar regions and absent at mid- and low-latitudes.

1.1.1. Beacon Valley

The McMurdo Dry Valleys (MDV) is the largest ice free area in Antarctica, with a combined area of approximately 4800 km^2 [*Doran et al.*, 2002]. The MDV get their name from the extremely low humidity and lack of a snow or ice cover. The hyperarid conditions are primarily the result of foehn winds [*Nylen et al.*, 2004; *Speirs et al.*, 2010] and a precipitation rate that is lower than the evaporation rate [*Fountain et al.*, 2009]; any ice present at the surface sublimates slowly. Despite these hyperarid conditions, ice-cemented permafrost is common throughout the MDV [*Bockheim et al.*, 2007].

One of the MDV that holds particular interest is Beacon Valley due to a massive ice body is buried 0.1 to 0.5 m below a layer of sublimation till and eolian material. This ice has received much attention initially spurred in the report by *Sugden et al.* [1995] that it was over 8.1 Ma old based on the age of tephra found in a sand wedge above the ice. If correct, this would make it the oldest known ice on Earth. The age of this buried ice was immediately questioned on theoretical grounds based on models of sublimation [*Hindmarsh et al.*, 1998]. They suggested that the sublimation rate of the ice would be too high to allow the ice to persist close to the surface after such a long time period. If this enigma is explained, it would help further our understanding of similar situations on Mars where ground ice is present.

In addition, microbes were detected in Beacon Valley ice samples [*Bidle et al.*, 2007]. That study suggests that microorganisms had been encased in the ice since sometime during the Miocene epoch; however, the growth of microbes was extremely slow and suggested that the viability of the cells was severely compromised. The finding suggest that life may be found in other environments where ground ice has persisted, possibly at depth in ancient ice.

1.1.2. Mars

Mars is of particular interest to astrobiologists because not only it is close to Earth and had many similarities with Earth including the presence of water ice. If liquid water existed once on Mars, it is possible that life could have existed on the planet. Even if the water is currently frozen, it is possible that extinct life could be preserved and discovered by future Mars missions. For example, the recent Mars Science Laboratory (MSL) was designed to undertake the search for past and present habitable environments at Gale Crater [*Grotzinger et al.*, 2012], where is found to be a loosely defined, a habitable environment that has liquid water, a source of carbon (to enable organism metabolism), and a source of energy (to fuel organism metabolism) – in other words, the essential ingredients for life as we know it on Earth.

There is an ongoing search for ice in the equatorial regions on Mars. Near the equator, water ice is unstable with respect to the atmosphere [*Clifford and Hillel*, 1983; *Mellon and Jakosky*, 1993; *Mellon et al.*, 1997; *Schörghofer and Aharonson*, 2005]; if ice exists in these regions, it is sublimating and the water vapor is diffusing through the regolith, dissipating into the atmosphere. Sublimation of any ground ice that formed in the past progressively lowers the ice table and eventually removes the ice altogether. There is, however, strong evidence that water ice once existed in these regions, and there are many observations of Martian surface morphological features that are consistent with the presence of subsurface ice [*Balme and Gallagher*, 2009; *Head et al.*, 2003; *Lanagan et al.*, 2001; *Oehler*, 2013; *Reiss et al.*, 2006; *Squyres and Carr*, 1986; *Yakovlev*, 2012]. Moreover, the Curiosity landing site, below Mt Sharp in Gale Crater, is predicted to be a hemispheric maximum for snowmelt on Mars [*Kite et al.*, 2013]. The combination of these factors may suggest the possibility for remnant ground ice in Martian equatorial regions.

1.2. Research Objectives

The overall objective of my dissertation is to study the stability of subsurface ice in a cold, hyper-arid region, e.g., Beacon Valley, Antarctica, and use this work as a basis for examining the persistence of potential ground ice in Gale Crater on Mars. The 3 main chapters of my dissertation are described briefly below. Each chapter is written as a stand-alone paper.

Chapter 2 presents an enhanced vapor diffusion model of ground ice at Beacon Valley, Antarctica that includes, for the first time, field measurements of episodic snow cover and snowmelt events. A realistic model of the long-term sublimation rates is extended back in time using a temperature proxy over the last 200 ka based on data from a nearby glacier ice core, and a correlation between relative humidity and air temperature developed from our field data.

In Chapter 3, we study the Beacon soil thermal properties and develop a two-layer 1-D heat transport model to study subsurface temperatures at Beacon Valley. This model is validated with measured soil temperatures. A model for the ground thermal behavior is necessary to study the stability of equatorial ground ice at Gale Crater on Mars since ground temperatures are not available there.

In Chapter 4, the persistence of subsurface ice at Gale Crater is studied using a coupled heat and vapor transport model that is constrained by climate data collected by Curiosity Rover (i.e. air temperature, relative humidity, and ground surface temperature). This model enables us to consider closely the potential persistence of ground ice that may have formed during last high obliquity 0.5 Ma ago [*Mellon and Jakosky*, 1995].

Each of these objectives is discussed in the next three chapters. Each chapter is written in the style of manuscript and have, or will be, submitted for publication. Chapter 2 has been

published in the Journal Geophysical Research: Earth Surfaces. Chapters 3 and 4 will be submitted shortly.

1.3. References

Anderson, D. M., L. W. Gatto, and F. C. Ugolini (1972), An antarctic analog of Martian permafrost terrain, *Antarctic Journal of the U.S.*(7), 114-116.

Balme, M., and C. Gallagher (2009), An equatorial periglacial landscape on Mars, *Earth and Planetary Science Letters*, *285*(1), 1-15.

Bidle, K. D., S. Lee, D. R. Marchant, and P. G. Falkowski (2007), Fossil genes and microbes in the oldest ice on Earth, *P Natl Acad Sci USA*, *104*(33), 13455-13460, doi:DOI 10.1073/pnas.0702196104.

Black, R. F., and T. E. Berg (1963), Hydrothermal regimen of patterned ground, Victoria Land, Antarctica, *International Association of Science, Hydrology Commission of Snow and Ice*, 121-127.

Bockheim, J. G., I. B. Campbell, and M. McLeod (2007), Permafrost distribution and active-layer depths in the McMurdo dry valleys, Antarctica, *Permafrost and Periglacial Processes*, *18*(3), 217-227, doi:10.1002/Ppp.588.

Brown, J., O. Ferrians Jr, J. Heginbottom, and E. Melnikov (2002), Circum-Arctic Map of Permafrost and Ground-Ice Conditions, version 2, *Boulder, Colorado USA, National Snow and Ice Data Center*.

Clifford, S. M., and D. Hillel (1983), The stability of ground ice in the equatorial region of Mars, *Journal of Geophysical Research*, *88*(B3), 2456-2474, doi:10.1029/JB088iB03p02456.

Doran, P. T., C. P. McKay, G. D. Clow, G. L. Dana, A. G. Fountain, T. Nylen, and W. B. Lyons (2002), Valley floor climate observations from the McMurdo dry valleys, Antarctica, 1986-

2000, *Journal of Geophysical Research-Atmospheres*, *107*(D24), 4772, doi:10.1029/2001jd002045.

Fanale, F. P. (1976), Martian Volatiles - Their Degassing History and Geochemical Fate, *Icarus*, *28*(2), 179-202, doi:10.1016/0019-1035(76)90032-4.

Fanale, F. P., J. R. Salvail, A. P. Zent, and S. E. Postawko (1986), Global distribution and migration of subsurface ice on Mars, *Icarus*, *67*(1), 1-18.

Fountain, A. G., T. H. Nylen, A. Monaghan, H. J. Basagic, and D. Bromwich (2009), Snow in the McMurdo Dry Valleys, Antarctica, *International Journal of Climatology*, *30*(5), 633-642, doi:10.1002/Joc.1933.

Gleick, P. H. (1993), *Water in crisis: a guide to the world's fresh water resources*, Oxford University Press, Inc.

Grotzinger, J. P., J. Crisp, A. R. Vasavada, R. C. Anderson, C. J. Baker, R. Barry, D. F. Blake, P. Conrad, K. S. Edgett, and B. Ferdowski (2012), Mars Science Laboratory mission and science investigation, *Space science reviews*, *170*(1-4), 5-56.

Gruber, S. (2012), Derivation and analysis of a high-resolution estimate of global permafrost zonation, *The Cryosphere*, *6*(1), 221-233.

Hagedorn, B., R. S. Sletten, and B. Hallet (2007), Sublimation and ice condensation in hyperarid soils: Modeling results using field data from Victoria Valley, Antarctica, *Journal of Geophysical Research-Earth Surface*, *112*(F3), F03017, doi:10.1029/2006jf000580.

Head, J. W., J. F. Mustard, M. A. Kreslavsky, R. E. Milliken, and D. R. Marchant (2003), Recent ice ages on Mars, *Nature*, *426*(6968), 797-802.

Heldmann, J. L., W. Pollard, C. P. McKay, M. M. Marinova, A. Davila, K. E. Williams, D. Lacelle, and D. T. Andersen (2013), The high elevation Dry Valleys in Antarctica as analog sites for subsurface ice on Mars, *Planet Space Sci*, *85*, 53-58, doi:10.1016/j.pss.2013.05.019.

Hindmarsh, R. C. A., F. M. Van der Wateren, and A. L. L. M. Verbers (1998), Sublimation of ice through sediment in Beacon Valley, Antarctica, *Geografiska Annaler Series a-Physical Geography*, *80A*(3-4), 209-219.

Jakosky, B. M., and M. T. Mellon (2004), Water on mars, *Physics Today*, *57*(4), 71-76.

Kane, D. L., L. D. Hinzman, and J. P. Zarling (1991), Thermal Response of the Active Layer to Climatic Warming in a Permafrost Environment, *Cold Regions Science and Technology*, *19*(2), 111-122.

Kite, E. S., I. Halevy, M. A. Kahre, M. J. Wolff, and M. Manga (2013), Seasonal melting and the formation of sedimentary rocks on Mars, with predictions for the Gale Crater mound, *Icarus*, *223*(1), 181-210, doi:10.1016/j.icarus.2012.11.034.

Lanagan, P. D., A. S. McEwen, L. P. Keszthelyi, and T. Thordarson (2001), Rootless cones on Mars indicating the presence of shallow equatorial ground ice in recent times, *Geophysical Research Letters*, *28*(12), 2365-2367, doi:10.1029/2001gl012932.

Mangold, N. (2010), Ice sublimation as a geomorphic process: A planetary perspective, *Geomorphology*, *126*(1-2), 1-17.

McKay, C. P., M. T. Mellon, and E. I. Friedmann (1998), Soil temperatures and stability of ice-cemented ground in the McMurdo Dry Valleys, Antarctica, *Antarctic Science*, *10*(1), 31-38.

Mellon, M. T., R. E. Arvidson, J. J. Marlow, R. J. Phillips, and E. Asphaug (2008), Periglacial landforms at the Phoenix landing site and the northern plains of Mars, *Journal of Geophysical Research-Planets*, *113*, E00A23, doi:10.1029/2007je003039.

Mellon, M. T., W. C. Feldman, and T. H. Prettyman (2004), The presence and stability of ground ice in the southern hemisphere of Mars, *Icarus*, *169*(2), 324-340, doi:10.1016/J.Jicarus.10.022.

Mellon, M. T., and B. M. Jakosky (1993), Geographic Variations in the Thermal and Diffusive Stability of Ground Ice on Mars, *Journal of Geophysical Research-Planets*, *98*(E2), 3345-3364.

Mellon, M. T., and B. M. Jakosky (1995), The Distribution and Behavior of Martian Ground Ice during Past and Present Epochs (Vol 100, Pg 11781, 1995), *Journal of Geophysical Research-Planets*, *100*(E11), 23367-23370.

Mellon, M. T., B. M. Jakosky, and S. E. Postawko (1997), The persistence of equatorial ground ice on Mars, *Journal of Geophysical Research-Planets*, *102*(E8), 19357-19369, doi:10.1029/97je01346.

Ng, F., B. Hallet, R. S. Sletten, and J. O. Stone (2005), Fast-growing till over ancient ice in Beacon Valley, Antarctica, *Geology*, *33*(2), 121-124, doi:10.1130/G21064.1.

Nylen, T. H., A. G. Fountain, and P. T. Doran (2004), Climatology of katabatic winds in the McMurdo dry valleys, southern Victoria Land, Antarctica, *Journal of Geophysical Research-Atmospheres*, *109*(D3), D03114, doi:10.1029/2003jd003937.

Oehler, D. Z. (2013), A Periglacial Analog for Landforms in Gale Crater, Mars, in *44th Lunar and Planetary Science Conference*, edited.

Paige, D. A. (1992), The thermal stability of near-surface ground ice on Mars, *Nature*, *356*(6364), 43-45.

Pewe, T. L. (1959), Sand-Wedge Polygons (Tesselations) in the Mcmurdo Sound Region, Antarctica - a Progress Report, *Am J Sci*, *257*(8), 545-552.

Reiss, D., S. Gasselt, E. Hauber, G. Michael, R. Jaumann, and G. Neukum (2006), Ages of rampart craters in equatorial regions on Mars: Implications for the past and present distribution of ground ice, *Meteoritics & Planetary Science*, *41*(10), 1437-1452.

Roth, K., and J. Boike (2001), Quantifying the thermal dynamics of a permafrost site near Ny-Alesund, Svalbard, *Water Resources Research*, *37*(12), 2901-2914.

Schäfer, J. M., H. Baur, G. H. Denton, S. Ivy-Ochs, D. R. Marchant, C. Schluchter, and R. Wieler (2000), The oldest ice on Earth in Beacon Valley, Antarctica: new evidence from surface exposure dating, *Earth and Planetary Science Letters*, *179*(1), 91-99.

Scherler, M., C. Hauck, M. Hoelzle, M. Stähli, and I. Völksch (2010), Meltwater infiltration into the frozen active layer at an alpine permafrost site, *Permafrost and Periglacial Processes*, *21*(4), 325-334.

Schirrmeister, L., C. Siegert, T. Kuznetsova, S. Kuzmina, A. Andreev, F. Kienast, H. Meyer, and A. Bobrov (2002), Paleoenvironmental and paleoclimatic records from permafrost deposits in the Arctic region of Northern Siberia, *Quatern Int*, *89*, 97-118, doi:10.1016/S1040-6182(01)00083-0.

Schörghofer, N. (2005), A physical mechanism for long-term survival of ground ice in Beacon Valley, Antarctica, *Geophysical Research Letters*, *32*(19), L19503, doi:10.1029/2005gl023881.

Schörghofer, N. (2007), Dynamics of ice ages on Mars, *Nature*, *449*(7159), 192-U192, doi:10.1038/Nature06082.

Schörghofer, N. (2009), Buffering of Sublimation Loss of Subsurface Ice by Percolating Snowmelt: A Theoretical Analysis, *Permafrost and Periglacial Processes*, *20*(3), 309-313, doi:10.1002/Ppp.646.

Schörghofer, N., and O. Aharonson (2005), Stability and exchange of subsurface ice on Mars, *Journal of Geophysical Research-Planets*, *110*, E05003, doi:10.1029/2004je002350.

Schuur, E. A. G., et al. (2008), Vulnerability of permafrost carbon to climate change: Implications for the global carbon cycle, *Bioscience*, *58*(8), 701-714, doi:10.1641/B580807.

Sletten, R. S., B. Hallet, and R. C. Fletcher (2003), Resurfacing time of terrestrial surfaces by the formation and maturation of polygonal patterned ground, *Journal of Geophysical Research-Planets*, *108*(E4), 8044, doi:10.1029/2002je001914.

Speirs, J. C., D. F. Steinhoff, H. A. McGowan, D. H. Bromwich, and A. J. Monaghan (2010), Foehn Winds in the McMurdo Dry Valleys, Antarctica: The Origin of Extreme Warming Events, *Journal of Climate*, *23*(13), 3577-3598, doi:10.1175/2010jcli3382.1.

Squyres, S. W., and M. H. Carr (1986), Geomorphic evidence for the distribution of ground ice on Mars, *Science*, *231*(4735), 249-252.

Stone, J. O., R. S. Sletten, and B. Hallet (2000), Old ice, going fast: Cosmogenic isotope measurements on ice beneath the floor of Beacon Valley, Antarctica *Eos Transactions, American Geophysical Union, Fall Meeting Supplement, Abstract H52C–21 81*(48).

Stuiver, M., I. C. Yang, G. H. Denton, and T. B. Kellogg (1981), Oxygen isotope ratios of Antarctic permafrost and glacier ice, *Antarctic Research Series*, *33*, 131-139.

Sugden, D. E., D. R. Marchant, N. Potter, R. A. Souchez, G. H. Denton, C. C. Swisher, and J. L. Tison (1995), Preservation of Miocene Glacier Ice in East Antarctica, *Nature*, *376*(6539), 412-414.

Yakovlev, V. (2012), The Ice Nature of the Gale Crater Central Structure, paper presented at Lunar and Planetary Institute Science Conference Abstracts.

Chapter 2. An enhanced model of the contemporary and long-term (200 ka) sublimation of the massive subsurface ice in Beacon Valley, Antarctica

The content of this chapter was published in

Liu, L., R. S. Sletten, B. Hagedorn, B. Hallet, C. P. McKay, and J. O. Stone (2015), An enhanced model of the contemporary and long-term (200 ka) sublimation of the massive subsurface ice in Beacon Valley, Antarctica, *Journal of Geophysical Research: Earth Surface*, 120, doi:10.1002/2014JF003415.

2.1. Abstract

A massive ice body buried under several decimeters of dry regolith in Beacon Valley, Antarctica, is believed to be more than 1 Ma old and perhaps over 8.1 Ma; however, vapor diffusion models suggest that subsurface ice in this region is not stable under current climate conditions. To better understand the controls on sublimation rates and stability of this massive ice, we have modeled vapor diffusion using 12 years of climate and soil temperature data from 1999 to 2011, including field measurements of episodic snow cover and snowmelt events that have not been represented in previous models of ground ice sublimation. The model is then extended to reconstruct the sublimation history over the last 200 ka using paleotemperatures estimated from ice core data from nearby Taylor Dome and a relationship between atmospheric temperature and humidity derived from our meteorological records. The model quantifies the impact of episodic snow events; they account for a nearly 30% reduction in the massive ice loss. The sublimation rate of ground ice averages 0.11 mm a^{-1} between 1999 and 2011 in Beacon Valley. Parameterized with

past environmental conditions and assuming the same regolith thickness, the modeled sublimation rate of ground ice in Beacon Valley averages 0.09 mm a^{-1} for the last 200 ka, comparable to the long-term average rate estimated independently from various studies based on cosmogenic isotopes. This study provides a realistic estimate of the long-term sublimation history and supports the inference that the buried ice in Beacon Valley is older than 1 Ma.

2.2. Introduction

Permafrost, defined as ground being below 0 ℃ for at least two consecutive years [*Washburn*, 1979], covers approximately 20% of Earth′s land surfaces [*Brown et al.*, 2002; *Gruber*, 2012] and all of Mars [*Jakosky and Mellon*, 2004]. Permafrost may be dry or may contain ice ranging from a few percent interstitial ice cement to massive subsurface ice. In the McMurdo Dry Valleys (MDV) of Antarctica, ice is widespread within decimeters of the ground surface [*Bockheim*, 2002; *Campbell and Claridge*, 2006].

Subsurface ice is fundamentally important as a reservoir of water [*Gleick*, 1993], a proxy for paleoclimatic information [*Schirrmeister et al.*, 2002], and a major component controlling the periglacial landscape [*Black and Berg*, 1963; *Pewe*, 1959; *Sletten et al.*, 2003]. Furthermore, subsurface ice in the upper elevations of the MDV is an instructive analog for Martian subsurface ice [*Heldmann et al.*, 2013; *Sletten et al.*, 2003]. Detected on Mars a few centimeters below the surface at mid-latitude and high-latitude regions [*Mellon et al.*, 2008; *Mellon et al.*, 2004], subsurface ice plays an important role in the formation of many Martian landforms [*Anderson et al.*, 1972; *Mangold*, 2010; *Mellon et al.*, 2008; *Squyres and Carr*, 1986]. In the Martian equatorial region, subsurface ice is not expected based on models of ice stability under current climate conditions [*Clifford and Hillel*, 1983; *Mellon et al.*, 2004; *Schörghofer and Aharonson*, 2005], but morphological observations suggest the past presence of shallow subsurface water ice [*Balme and Gallagher*, 2009; *Lanagan et al.*, 2001; *Oehler*, 2013; *Reiss et al.*, 2006]. Hence, the stability of subsurface ice is of fundamental interest to both terrestrial and planetary science communities.

Beacon Valley contains a massive body of buried glacial ice 0.1 to 0.5 m below a layer of sublimation till and eolian material. This ice has received much attention initially spurred in the

report by *Sugden et al.* [1995] that it was over 8.1 Ma old based on the age of tephra found in a sand wedge above the ice. The age of this buried ice was immediately questioned on theoretical grounds based on models of sublimation [*Vanderwateren and Hindmarsh*, 1995]. Subsequently, reanalysis of cosmogenically dated cobbles that are deposited from the ice body as it sublimates [*Marchant et al.*, 2002; *Schäfer et al.*, 2000] suggests that the sublimation till overlying the ice is only several hundred thousand years old [*Ng et al.*, 2005]. Considering the cold and hyperarid climate conditions [*Doran et al.*, 2002; *Fountain et al.*, 2010] and the modeled rates of sublimation [*Ng et al.*, 2005; *Vanderwateren and Hindmarsh*, 1995], ice would sublimate to a depth of 20 to 40 m in soil and sediments within 300 ka, and yet it is typically found within 0.5 m of the ground surface in the upper MDV. Interest in the survival and age of buried massive Beacon ice, as well as the difference between current sublimation rates of the massive subsurface ice modeled using site-specific environmental data, and the long-term rates inferred from cosmogenic nuclide data, continue to focus attention on this ice.

Sublimation rates of 0.1−0.5 mm a^{-1} for subsurface ice in the upper elevations of the MDV have been obtained using models of water vapor diffusion, constrained by meteorological data including air temperature, relative humidity, and soil temperature [*Hagedorn et al.*, 2007; *Hindmarsh et al.*, 1998; *Kowalewski et al.*, 2006; *McKay*, 2009; *McKay et al.*, 1998; *Schörghofer*, 2005]. These rates suggest that interstitial ground ice should sublimate fairly quickly and that the top tens of meters of the soil should be free of ice within 100 ka, which is inconsistent with subsurface ice being pervasive within decimeters of the surface throughout the upper elevations of the MDV.

Slower long-term sublimation of subsurface ice in the upper elevations of the MDV has been suggested in a number of studies of cosmogenic nuclides and stable isotopes. *J. O. Stone et*

al. (manuscript in preparation, 2015) estimated a sublimation rate of subsurface ice to be 0.02−0.03 mm a^{-1} for at least the last ~200 ka in Beacon Valley using cosmogenic ^{10}Be profiles in ice and quartz grains along 8 m of an ice core collected at the study site. Based on the concentration of cosmogenic ^{10}Be and ^{26}Al in bulk sediment samples from three glacial deposits in the Quartermain Mountains, *Morgan et al.* [2011] suggested that ice sublimated at rates of 0.0007−0.012 mm a^{-1}; however, these rates are less constrained because they are sensitive to the assumed cosmogenic nuclide production profile, and the erosion history of the overlying till, for which the authors calculated similar rates of 0.0004−0.0012 mm a^{-1}. *Ng et al.* [2005] determined a minimum sublimation rate of 0.007 mm a^{-1} of ice using ^{3}He data from cobbles in Beacon Valley till. In addition, *Lacelle et al.* [2011] used a sublimation and molecular diffusion model in University Valley, 300 m above Beacon Valley, to account for the observed $\delta^{18}O$ profile in subsurface ice. Their model suggests an average ice sublimation rate of 0.0002 mm a^{-1}; however, the diffusion coefficients of the isotopes in dirty ice are poorly known, thus making the rate estimates relatively uncertain.

Two hypotheses have been advanced for the discrepancy in sublimation rates between vapor diffusion and cosmogenic isotope studies. First, the current cold and dry climate conditions in the upper elevations of the MDV, used in the vapor diffusion models, are not representative of past climate conditions. *McKay et al.* [1998], *Schörghofer* [2005], and *Kowalewski et al.* [2006; 2012] suggest that either a slight decrease in air temperature or increase in relative humidity would be sufficient to stabilize subsurface ice; however, treating changes in temperature and humidity independently is not realistic because they change concurrently. This change has not been taken into account in these estimates. Second, *McKay et al.* [1998] suggested that water recharge from snowmelt could offset, at least to a certain extent, the modeled ice loss due to sublimation. As

shown by *Schörghofer* [2009], this meltwater could act as a buffer between the subsurface ice and atmosphere, thereby slowing net sublimation. *McKay* [2009] concluded that a recurring snow cover every 2 years could account for the near-surface presence of subsurface ice at an elevation of ~1600 m in University Valley. *Gooseff et al.* [2003] showed a higher water content under seasonal snow patches and *Hagedorn et al.* [2007] modeled retarded sublimation of subsurface ice under snow cover. *Hagedorn et al.* [2010] quantitatively estimated ice recharge from snowmelt at a rate of ~0.4 mm a^{-1} over 10 ka in Victoria Valley soil using $\delta^{18}O$ profiles. Recharge at this rate is sufficient to compensate for the modeled sublimation rate of the ice-cemented permafrost in Victoria Valley and thereby maintain the ice-rich permafrost a few decimeters below the surface [*Hagedorn et al.*, 2010]. Our study addresses both the hypotheses presented above by using field-derived data as discussed next.

A 1-D mass balance model of vapor diffusion and ice condensation/sublimation, similar to that of *Hagedorn et al.* [2007], was developed to examine the stability of massive subsurface ice in Beacon Valley. The model is constrained by hourly measurements made from 1999 to 2011 of local climate parameters (air temperature and humidity), soil temperatures down to a depth of 0.60 m, and episodic snow cover and snowmelt events based on field measurements and time-lapse photography. In addition, a regional temperature-humidity correlation was developed using in situ measurements in Beacon Valley and the long-term temperature history was reconstructed based on ice core records; this enables us to model the sublimation rate realistically for the past 200 ka and provides a sound basis for considering the long-term stability of subsurface ice in this cold, hyperarid environment.

2.3. Study Site and Methods

2.3.1. Study Site

Beacon Valley (77º49′S, 161º39′E) is the southernmost of the MDV and the largest ice-free valley in the Quartermain Mountains (Figure 2.1). Beacon Valley trends northeast-southwest and is approximately 3 km wide and 12 km long. The floor of middle Beacon Valley where the ancient massive subsurface ice was found is approximately 1350 m above sea level. This massive subsurface ice contains approximately 10 wt% rock debris, commonly concentrated in bands up to 15-cm thick [*Marchant et al.*, 2002; *Sugden et al.*, 1995]. Sublimation of the ice has produced a sublimation till that, together with eolian material, mantles the ancient massive subsurface ice in central Beacon Valley (Figure 2.1 insert). On the valley floor, a network of contraction-crack polygons with diameters of 10 to 20 m is well developed [*Sletten et al.*, 2003]. This study is based on local climate data (air temperature and relative humidity) and subsurface temperatures from a site approximately midway between a polygon center and a trough (5.9 m from the adjacent trough) with a total regolith thickness of 0.30 m.

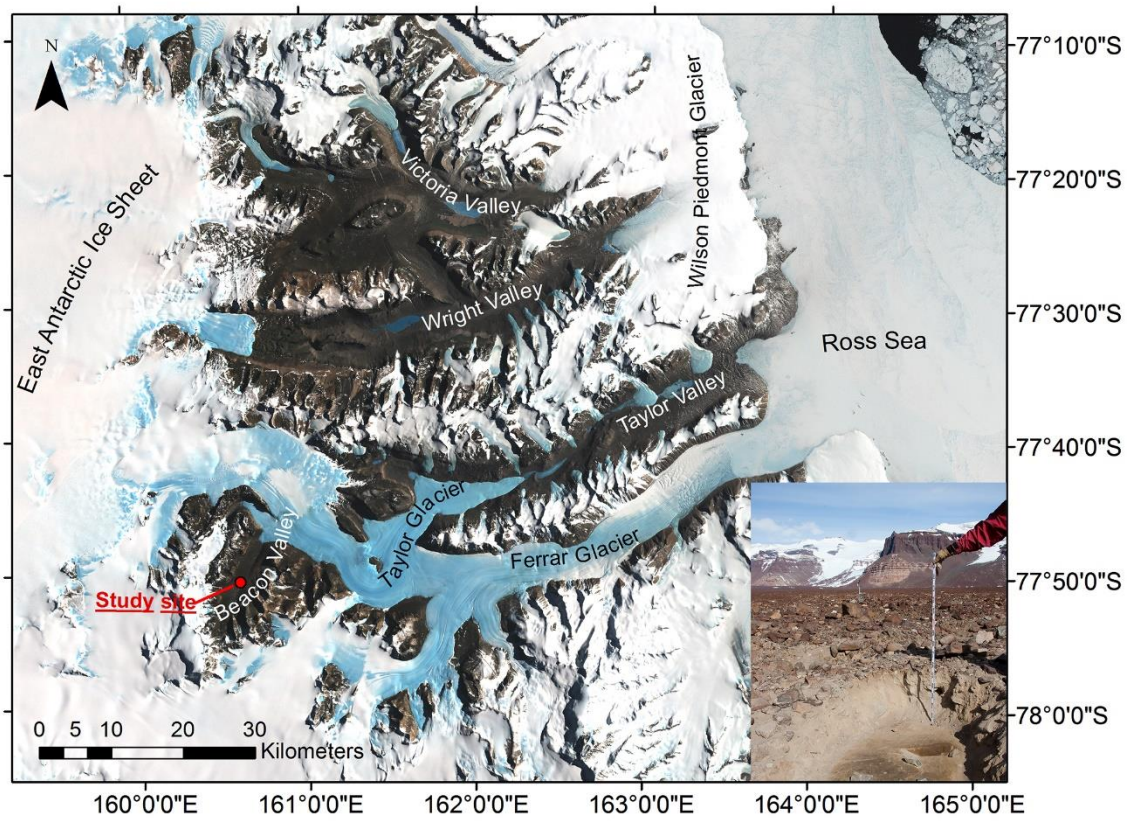

Figure 2.1. The McMurdo Dry Valleys (MDV) lie between the McMurdo Sound region of the Ross Sea and the East Antarctic Ice Sheet. Insert: buried massive ice lies beneath several decimeters of regolith in Beacon Valley, Antarctica.

2.3.2. Field Data Collection

Air temperature and relative humidity (RH) were measured with a Vaisala HMP45C probe every 10 seconds, averaged hourly, and recorded using a Campbell CR10X data logger. Because the HMP45C records temperatures only above −40.0°C, an internal temperature sensor is used to measure lower temperatures. The HMP45C probe reports humidity relative to liquid water; therefore, RH values recorded at sub-zero temperatures have been converted to RH values with respect to ice using the relationship for saturated vapor pressure from *Lowe* [1977]. The error for the HMP45C temperature is ±0.2°C at 20.0°C and increases linearly to ±0.4°C at −40.0°C. The

accuracy of HMP45C RH probe at 20.0°C is ±2% RH between 0% and 90% RH and ±3% between 90% and 100% RH. The temperature dependence of humidity accuracy is ±0.05% RH/°C. Thermistors, assembled at University of Washington and calibrated to within ±0.02°C, were installed in the regolith at depths: 0.02 m, 0.10 m, 0.20 m, and 0.30 m (regolith-ice boundary); and in the ice at 0.45 m, and 0.60 m. Archived data are available as described at: http://gcmd.nasa.gov/r/d/[GCMD]UW_Dry_Valley_Datalogging.

A digital camera (Model CC640, Campbell Scientific, Inc.) was installed at the study site to monitor the snow-cover condition every 3 h continuously for 2 years (January 2009 to January 2011). During the austral winters when there is 24 h darkness (May to August), the surface is assumed to be covered with snow. In actuality, during this period, there is virtually no ice sublimation/condensation and the surface-snow cover has little impact on the sublimation rate of the subsurface ice [*Hagedorn et al.*, 2007].

To document snowmelt infiltration, the electrical conductivity (EC) was measured hourly between a pair of bare wires installed 0.05 m below the surface and recorded hourly. A sharp increase in soil EC indicates soil wetting.

Records of oxygen ($\delta^{18}O$) and deuterium (δD) isotopes in the ice core from Taylor Dome, 30 km west of Beacon Valley, provide an estimate of past temperatures in that region for the last 200 ka [*Steig et al.*, 2000]. The present mean annual surface temperature at Taylor Dome is −41.2°C [*Clow and Waddington*, 1996] and at Beacon Valley is −22.9°C. This temperature difference, due to the elevation difference and geographic locations, is assumed to persist when reconstructing past temperature conditions for Beacon Valley for the last 200 ka.

2.3.3. Model Description

A 1-D water vapor diffusion model is used to determine the rate of ice exchange between massive subsurface ice and the atmosphere under current climate conditions in Beacon Valley. Water vapor diffusion in the atmosphere-soil-ice system is driven by water vapor density gradients; water vapor diffuses toward regions of lower vapor density. Water vapor density, ρ_v (molecules m^{-3} air) is calculated from the water vapor pressure (e in Pa) and temperature (T in K) using the ideal gas law:

$$\rho_v = \frac{e}{RT} \tag{2.1}$$

where R is the gas constant. The flux of water vapor F (molecules m^{-2} s^{-1}) can be calculated using Fick′s first law:

$$F = -\frac{\varepsilon}{\tau} D_v \frac{\partial \rho_v}{\partial z} \tag{2.2}$$

where D_v is the diffusion coefficient of water vapor in free air (m^2 s^{-1}), porosity ε is used to account for the cross-sectional area of diffusion, and tortuosity τ is for the characteristic length of the diffusion pathway. The diffusion coefficient for water vapor in free air at the given soil temperatures is calculated using an empirical fit to experimental measurements made at 1 atm pressure over a wide range of temperatures [*Fuller et al.*, 1966]:

$$D_v = 1.176 \times 10^{-9} \times {T_{av}}^{1.75} \tag{2.3}$$

where T_{av} is the average temperature for each soil layer. D_v ranges between 1.6×10^{-5} and 2.2×10^{-5} m^2 s^{-1} (Table 2.1). The porosity ε is estimated based on intrinsic density ρ_i (kg m^{-3}) and the dry bulk density ρ_b (kg m^{-3}) of the soil:

$$\varepsilon = 1 - \frac{\rho_{\mathrm{b}}}{\rho_{\mathrm{i}}} \tag{2.4}$$

Table 2.1. Characteristic soil parameters used in this study.

Parameter	Unit	Value	Note
Intrinsic density (ρ_{i})	kg m^{-3}	2570	Measured
Bulk density (ρ_{b})	kg m^{-3}	1780	Measured
Porosity (ε)	–	0.31 – 0.32	Equations (2.4) and (2.5)
Tortuosity (τ)	–	2.25 – 2.33	Equation (2.6)
Diffusion coefficient (D_{v})	m^2 s^{-1}	1.6×10^{-5} to 2.2×10^{-5}	Equation (2.3)

If ice is present in soil, the porosity ($\varepsilon_{\mathrm{icy}}$) is calculated as the difference between the porosity of the dry soil $\varepsilon_{\mathrm{dry}}$ and volumetric ice content (Table 2.1):

$$\varepsilon_{\mathrm{icy}} = \varepsilon_{\mathrm{dry}} - \frac{\theta m_{\mathrm{w}}}{\mathrm{Av}1000\rho_{\mathrm{ice}}} \tag{2.5}$$

where θ is the amount of condensed water (molecules m$_{\mathrm{soil}}^{-3}$), m_{w} (kg) is the mass of water molecules, Av is the Avogadro number (6.02×10^{23} molecules mol^{-1}), and ρ_{ice} is the density of ice (917 and 920 kg m^{-3} at 0.0°C and −20.0°C, respectively). Tortuosity τ is estimated, using an empirical fit of modeled porous solids by *Zalc et al.* [2004], as a cosecant function of porosity ε (Table 2.1):

$$\tau = \csc(\varepsilon/0.7) \tag{2.6}$$

The water vapor density at depth changes over time as a function of the divergence in the water-vapor flux *dF/dz*. Mass conservation can be expressed as [*Hindmarsh et al.*, 1998; *Schörghofer and Aharonson*, 2005]:

$$\varepsilon \frac{\partial \rho_{\mathrm{v}}}{\partial t} = -\left(\frac{\partial F}{\partial z} + \frac{\partial \theta}{\partial t} + \frac{\partial \sigma}{\partial t}\right) \tag{2.7}$$

where σ and θ are the amounts of condensed ice and adsorbed water (molecules m_{soil}^{-3}), respectively. Instantaneous vapor transport was calculated without considering water adsorption because adsorption accounts for a very small quantity of water vapor as discussed in *Schörghofer and Aharonson* [2005] and *Hagedorn et al.* [2007]. The density of water vapor in the air is calculated from the air temperature and relative humidity, and the vapor density at the soil-ice boundary is calculated from soil temperatures assuming saturated vapor densities. In dry soil, water vapor condenses when temperature drops below the frost point, and the water vapor density is assumed to equal the saturated vapor density for the measured soil temperature as long as ice is present. In such situations, the vapor density depends on soil temperature and the convergence in the water-vapor flux leads to ice formation [*Hindmarsh et al.*, 1998].

The water vapor transport between the massive subsurface ice and the atmosphere was modeled by solving equations (2.2) and (2.7) using an explicit finite difference approach in MATLAB. The initial condition assumes a linear gradient in water vapor density between the soil-ice boundary and the air above the soil. The model steps through with hourly time steps to calculate the water vapor flux and the mass balance of water vapor and ice. Water vapor flux is defined as positive when vapor diffuses into the soil and negative when transport is toward the atmosphere.

2.4. Results and Discussions

2.4.1. Meteorology

Hourly measurements of temperature and RH in Beacon Valley from March 1999 to January 2011 are shown in Figure 2.2. The air temperature averaged −22.9°C; it reached a maximum of 2.6°C and a minimum of −47.9°C. Summertime air temperatures rarely rise above

0°C (Figure 2.2a) and precipitation is <50 mm water equivalent per year [*Fountain et al.*, 2010]. Over the 12 year period of our records, the annual mean air temperature has stayed roughly constant (within ±2.0°C, Table S2.1 in the supporting information). Wintertime air temperatures are highly variable due to warm katabatic winds that can abruptly warm the air by several tens of degrees Celsius and lower the RH [*Nylen et al.*, 2004]; recently these winds have been suggested to be the foehn type rather than katabatic [*Speirs et al.*, 2010].

The soil temperature at 0.02 m below the surface is up to 10.0 ± 2°C warmer than the air in the summer due to solar radiation (Figure 2.2c and Table S2.1 in the supporting information). Soil temperature oscillations dampen with depth. In the winter, soil temperatures are strongly and sporadically affected by warm katabatic winds. At the soil-ice boundary, temperature ranged from −3.0°C to −41.2°C.

The saturated water vapor density in the soil is positively correlated with temperature; therefore, the temperature gradient is critical in determining the direction of the water vapor flux as vapor moves toward the colder region. Soil is warmer at the surface during the summer, but during the winter the temperature gradient reverses so that the soil is colder at the surface (Figure 2.2c). Warm winds during the winter can also warm the soil at depth and temporarily reverse the temperature gradient, which would temporarily switch the direction of water vapor flux.

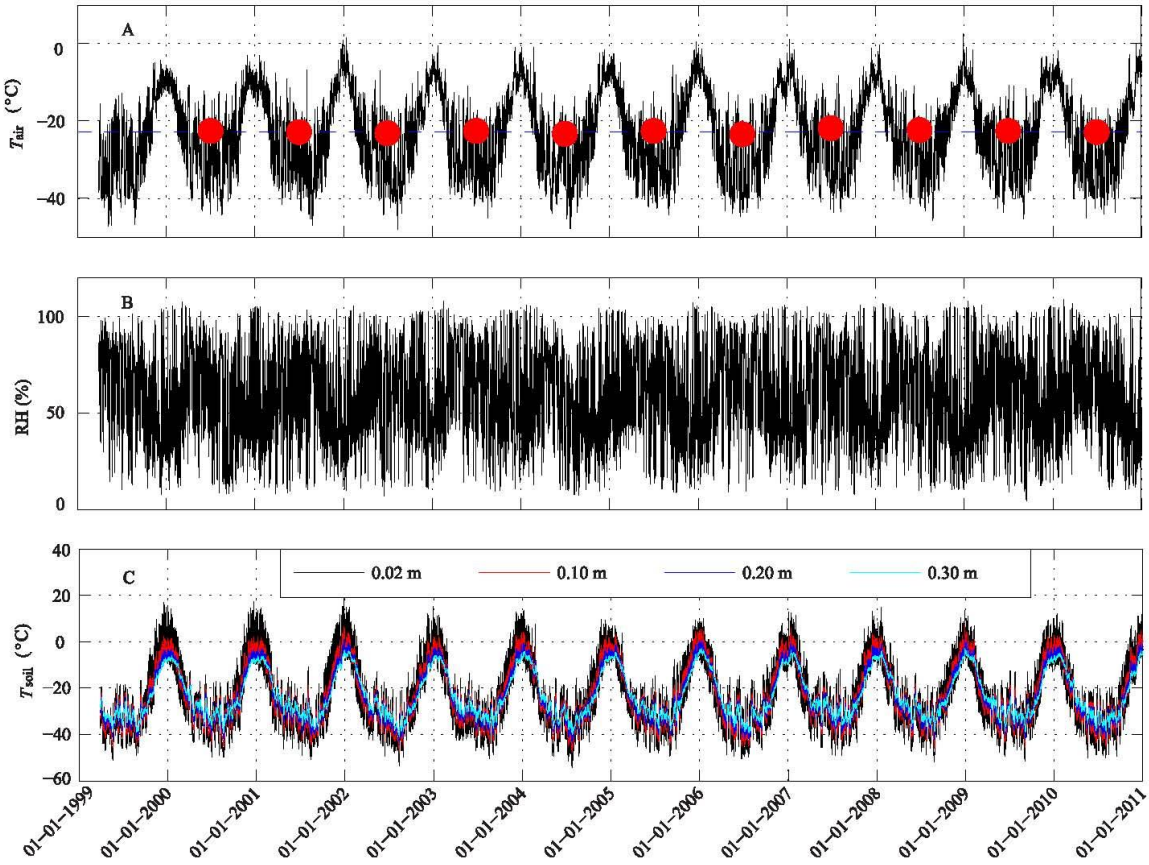

Figure 2.2. (a). Hourly measurements of atmospheric temperature (T_{air}). The dashed blue line delineates the average temperature during 12 year period; red filled circles are annual average temperatures. (b). Hourly measurements of relative humidity (RH). (c). Hourly measurements of soil temperatures (T_{soil}) at various depths for the 12 year period of this study.

2.4.2. Water Vapor Diffusion Model Results

The model results show that water vapor is generally lost from the soil-ice boundary throughout the year; the rate of loss is highest during the austral summer from December to January. During the winter, the water content in the atmosphere exceeds that in the dry soil above the massive subsurface ice (Figure 2.3a), resulting in a downward water vapor flux and ice condensation in the soil, with a maximum gain of 2.6×10^{-3} mm (Figure 2.3b). During the summer when sublimation rates exceed condensation rates, these transient accumulations of ice in the dry

soil are lost, and sublimation resumes at the boundary between the regolith and the massive ice. This leads to a net loss of massive subsurface ice during the summer (Figure 2.3c). The warming winds during the winter cause the air and soil temperature to temporarily increase to the point where net sublimation occurs. For the 12 year duration of the soil and meteorological data, the sublimation rate of the massive ground ice in Beacon Valley calculated by the water vapor diffusion model averages 0.17 mm a^{-1}.

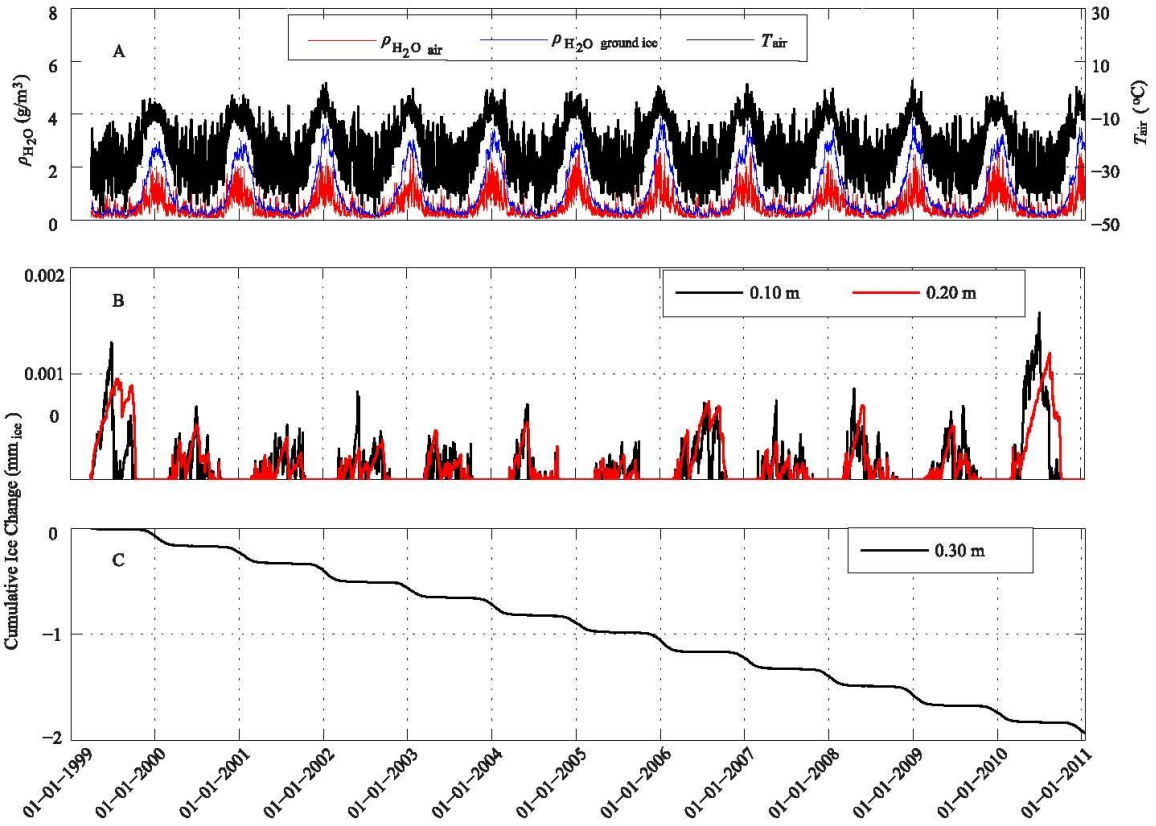

Figure 2.3. (a). Atmospheric temperature T_{air} (right axis) and water vapor concentration in atmosphere and at the ice boundary (left axis). (b). Cumulative ice formed in the dry soil due to water vapor condensation at 0.10 m and 0.20 m depth; all ice in the dry soil is lost during the following austral summer. (c). Cumulative change of the massive subsurface ice over the 12 year period.

2.4.3. Effect of Snow Cover Events

Hagedorn et al. [2007] modeled vapor transport assuming continuous annual snow cover that resulted in a net gain of 0.14 mm a^{-1} at the subsurface ice boundary suggesting that snow cover can potentially slow or reverse the sublimation rate. *McKay* [2009] suggested that snow cover is sufficient to stabilize subsurface ice at the high elevation site at University Valley under the conditions of a persistent annual snow cover for 1 year out of every 10 years. A 2-D model from *Kowalewski et al.* [2012] also suggested that snowfall in polygon troughs results in a net downward flux of water vapor that can condense and thereby decreases the sublimation rate.

While previous studies could only make assumptions about the timing and duration of snow cover, we documented snow cover from 2009 to 2011 using an automated camera. Figure 2.4 shows a typical snow event on 3 and 4 January in 2009. An extensive snow cover developed over a 6 h period (from 18:00 3 January to 00:00 4 January). By 18:00 h on 4 January, much of the snow had sublimated, exposing a portion of the soil surface. These snow cover events were incorporated into the vapor diffusion model by assuming that the air below the snow layer was saturated with water vapor when snow was present. Such a saturated water vapor layer on top of the soil temporarily reverses the vapor density gradient and thus the vapor flux. Incorporation of the snow cover events from January 2009 to January 2011 into the vapor diffusion model significantly slowed down the sublimation rates during the austral summer season with the most prominent effect in December and January, while snow cover during the rest of the year had a minimal effect on vapor transport. Over the 2 years of camera operation, the monitored snow cover reduced the ice sublimation rate to 0.15 mm a^{-1}.

If the snowfall conditions observed in 2009−2011 were representative of the past 12 years (additional images taken from 2011 to 2014 show near-identical trends in snow cover), surface snow would reduce the average modeled ice sublimation rate from 0.17 to 0.14 mm a^{-1}.

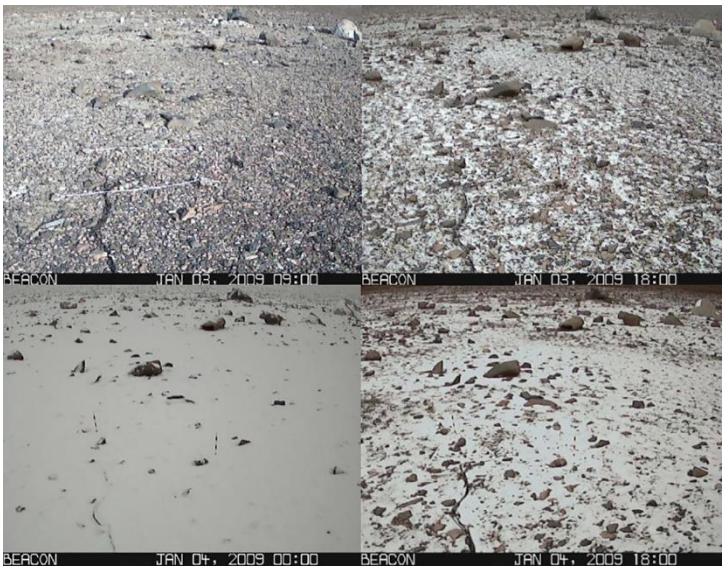

Figure 2.4. Examples of images at the ground surface in Beacon Valley during January 2009 that were used to document episodic snow events.

2.4.4. Effect of Snowmelt Events

During the summer, solar radiation can penetrate thin snow cover, and warming of the ground beneath the snow cover to a temperature above 0°C causes snow to melt. Although *Hagedorn et al.* [2010] determined a direct recharge of subsurface ice by snowmelt in Victoria Valley based on the stable isotope profile of the ice, it is unlikely that snowmelt infiltration will reach the ground ice table at 0.30 m in Beacon Valley due to generally lower soil temperatures. However, snowmelt water provides a buffer between the subsurface ice and the atmosphere because, like surface snow, it increases the water vapor concentration in the upper soil layer, thereby reducing the water vapor gradient and slowing the ice sublimation. Field measurements of EC at 0.05 m showed periodic spikes indicating that snowmelt had infiltrated into the soil. These

infiltration events occurred very consistently between 1 December and 31 January over the entire monitoring period from 1999 to 2011 (Figure 2.5).

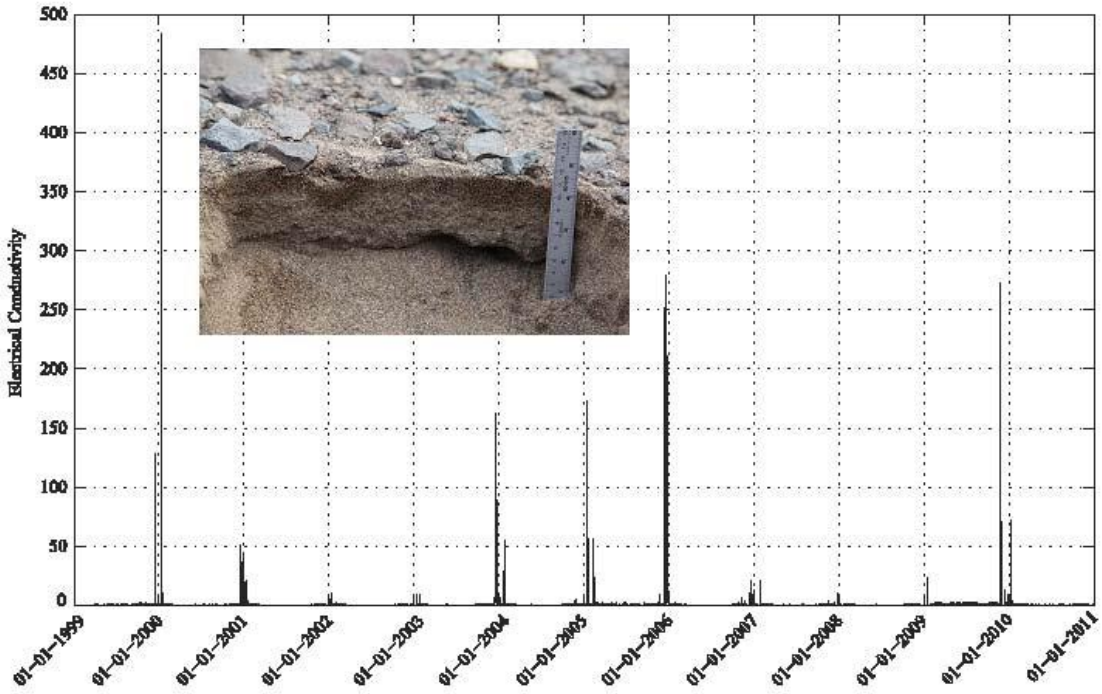

Figure 2.5. Electrical conductivity (EC) measurements with a relative scale: a spike in electroconductivity indicates a snowmelt event. Insert: snowmelt infiltration to several centimeters documented at 4 P.M. on 7 January, 2011 after an overnight snow event in Beacon Valley.

Snowmelt infiltration, at least to a depth of 0.05 m, can occur only under certain conditions of snow cover and solar radiation. Figure 2.6 compares the snow cover and snowmelt events along with the temperature profile at 0.02 m during the austral summer of 2009−2010. This comparison indicates that melting events generally occur near the end of the period of snow cover and that snow cover occurs more often and lasts longer than the snowmelt events throughout the year. This is based on several requirements to generate enough snowmelt infiltration to be recorded by the EC probe at 0.05 m: (1) ground surface temperature drops below 0°C for snow to persist; (2) solar radiation penetrating the snow cover is sufficient to warm the underlying soil above 0°C; otherwise,

the snow will sublimate directly back into the atmosphere without melting; and (3) the amount of snowmelt is sufficient to penetrate to a depth of 0.05 m.

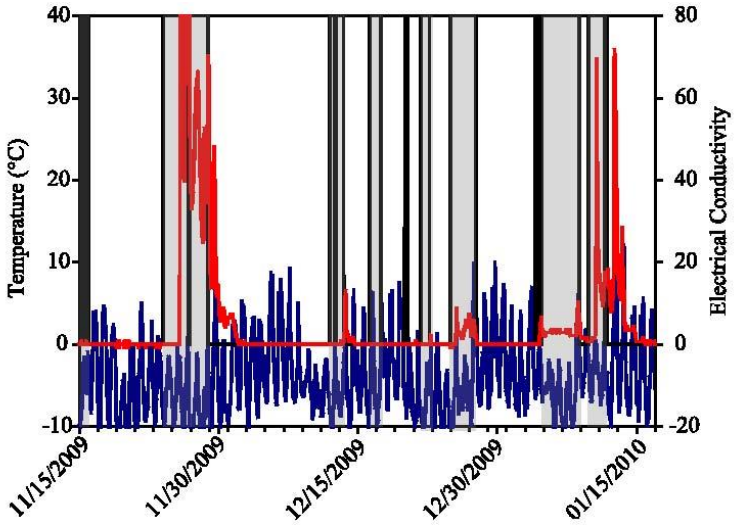

Figure 2.6. Measurements of ground surface temperature at 0.02 m, snow cover, and snowmelt (peak in electoral conductivity) for the austral summer 2009−2010. Temperature is plotted with the blue line, snow cover duration is represented by the grey shaded bars, and electrical conductivity by the red line for the period snow cover was documented.

The sublimation model was modified by incorporating these melt events. When the EC readings are above the detection limit, indicating that water is present in the soil, the RH of the surface layer was assumed to be 100% with respect to water. The presence of snow would lower or reverse the vapor density gradient in the dry soil and, as a consequence, decrease or stop the vapor flux out of the soil. The model results indicate that the saturated vapor pressure in the top soil layer exceeds the vapor pressure at the ice boundary from December to the end of January whenever there is a wetting event detected by the EC probe (Figure 2.5). As a result, a small amount of ice condenses in the dry soil and at the subsurface massive-ice boundary (Figure 2.7). With the incorporation of these summer wetting events, the sublimation rate at the soil-ice boundary decreases by 0.03 mm a^{-1} during the time of observation (1999 to 2011), and thus,

combined effect of the observed snow and snowmelt effects leads to a sublimation rate of 0.11 mm a^{-1}. The effect of snowmelt on water vapor transport as it is modeled here does not account for smaller snowmelt events or for liquid water infiltration and, therefore, may underestimate the slowing effect of snow on sublimation.

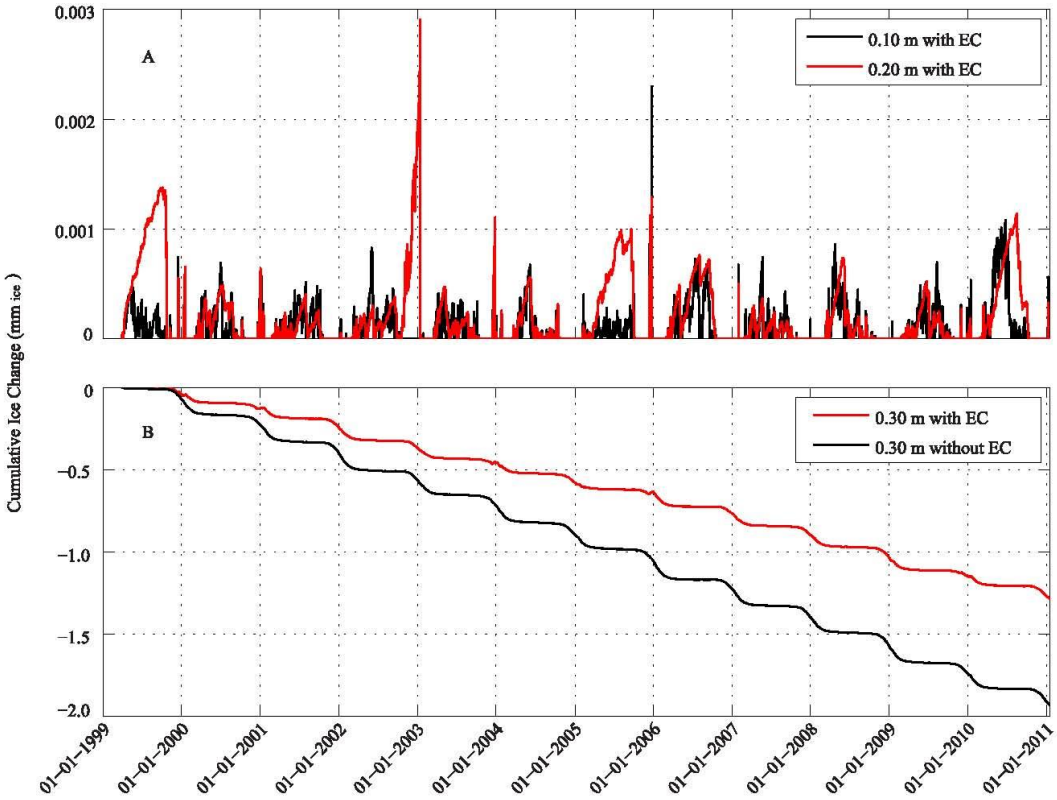

Figure 2.7. Water vapor diffusion model results including snow cover and wetting events as indicated by EC measurements for the dry regolith (a) and massive subsurface ice (b). The graphs are similar to Figure 2.3 with a reduced average sublimation rate to 0.11 mm_{ice} a^{-1}; the episodic snow cover wetting events lead to slight transient ice accumulation at the regolith-ice boundary (Figure 2.7b) as well as in the dry regolith (Figure 2.7a).

2.4.5. Modeling of the Long-Term Sublimation Rates

This sublimation rate of 0.11 mm a^{-1} for contemporary environmental conditions is significantly faster than the long-term rate estimated from cosmogenic isotopes in an ice core from

this study site (0.02−0.03 mm a^{-1}, *J. O. Stone et al.*, manuscript in preparation, 2015). The difference may well be due to the large glacial-interglacial climate variations in the recent geologic past.

The sublimation rate of subsurface ice is very sensitive to minor changes in temperature and also strongly depends on water vapor concentration in the atmosphere; therefore, it is important to examine the relationship between atmospheric temperature and RH, as presented in the next section. This correlation is then used, along with reconstructed paleotemperatures [*Steig et al.*, 2000], to investigate the long-term sublimation rates of the massive subsurface ice over the last 200 ka in Beacon Valley.

2.4.5.1. Covariance of Atmospheric Temperature and Humidity

Daily averages of the 12 year climate record of Beacon Valley were used to study the relationship between atmospheric temperature and humidity. RH shows a weak negative correlation with atmospheric temperature (Figure 2.8a), while the atmospheric water-vapor density ρ_v correlates positively with atmospheric temperature T_{air} (Figure 2.8b). The negative correlation between RH and T_{air} indicates that the amount of ρ_v increase with T_{air} is insufficient to maintain a constant RH. To visualize this, the blue line in Figure 2.8b delineates ρ_v calculated using a constant RH of 50% throughout the measured T_{air} range. It shows that water vapor density required to maintain a constant RH is larger than the measured ρ_v (red line in Figure 2.8b). Following *Gaffen et al.* [1992], the relationship between the daily averaged atmospheric water vapor density ρ_v and the daily averaged atmospheric temperature T_{air} (in K) in Beacon Valley is expressed as the natural logarithm of ρ_v versus the inverse of T_{air} with a correlation coefficient (r) of 0.933 ($r^2 = 0.8701$):

$$\ln(\rho_V) = 18.165 - \left(\frac{4.792\times10^3}{T_{air}}\right) \quad (2.8)$$

This relationship indicates that atmospheric vapor density decreases with the inverse of atmospheric temperature in a predictable manner: a decrease in temperature (that causes slower sublimation) leads to a lower atmospheric vapor density (that causes an opposite effect and results in faster sublimation). As stated above, however, the changes in ρ_v are not large enough to maintain a constant RH at different temperatures highlighting the importance to consider the covariance of temperature and RH when extending the sublimation model to longer time scales where detailed measurements of both parameters are absent. *Gaffen et al.* [1992] suggested that the relationship between the water vapor and temperature might slightly vary from month-to-month and year-to-year. With lack of long-term RH monitoring, our data provide our best estimate to adjust RH to changes in atmospheric temperature in Beacon Valley for the last 200 ka.

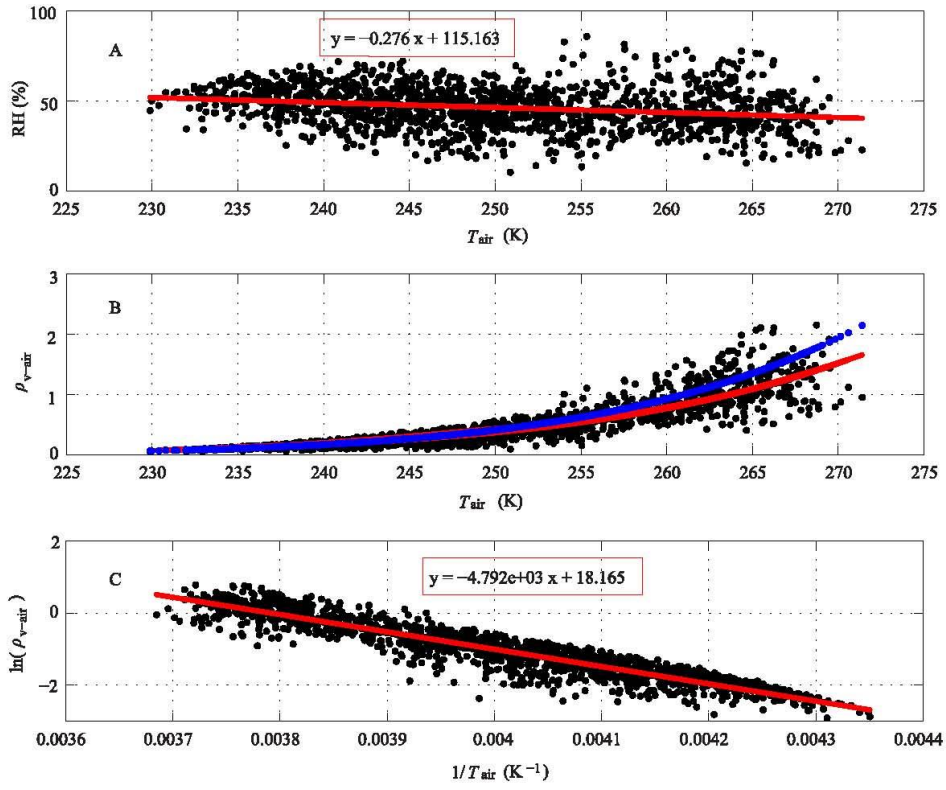

Figure 2.8. Relationships between daily averaged T_{air} and water vapor density. (a). RH versus T_{air}

with a weak negative correlation shown with the red line (b). Water vapor density versus T_{air} and its correlation shown with the red line. Blue line delineates the change of water vapor density with T_{air} given a constant RH of 50%. (c). Relationship between $1/T_{air}$ and water vapor density on a logarithmic scale.

2.4.5.2. Long-Term Sublimation Rate of the Massive Subsurface Ice

The long-term sublimation rate of the massive subsurface ice at Beacon Valley is investigated over the last 200 ka using temperature estimate reconstructed from the Taylor Dome ice core and assuming a constant temperature offset of 18.3ºC (Figure 2.9a). For each temperature, the concurrent atmospheric vapor density is calculated using the dependence of atmospheric vapor density on temperature (equation (2.8)). Other input parameters in the vapor diffusion model (i.e., depth of the soil-ice boundary, dry soil properties including porosity and tortuosity, and the frequency of the snow cover and snowmelt) are assumed to be the same as at the present time. The sublimation rate is then modeled using the vapor diffusion model for each available temperature (time steps dependent on the Taylor Dome ice core data). The modeled long-term sublimation rates of massive subsurface ice in Beacon Valley over the last 200 ka are plotted in Figure 2.9b.

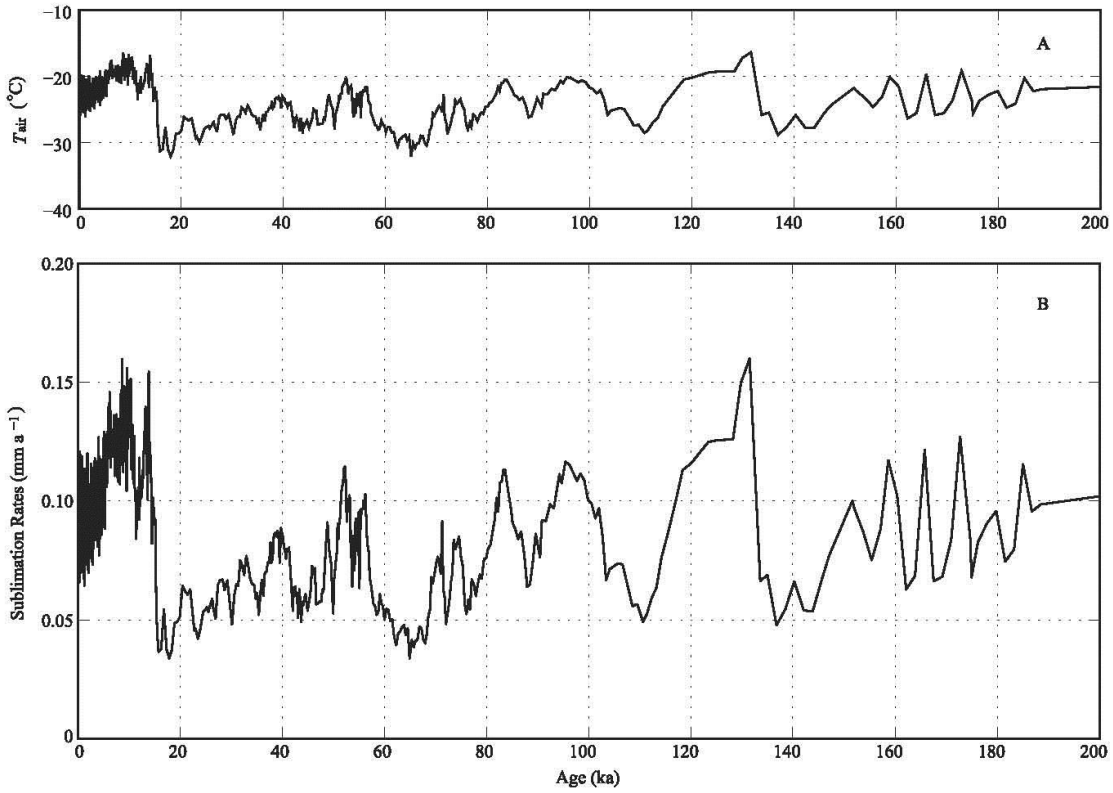

Figure 2.9. (a). Reconstructed T_{air} profile for Beacon Valley over the last 200 ka from Taylor Dome ice core records. (b). Modeled sublimation rates of massive subsurface ice in Beacon Valley for the last 200 ka.

Sublimation rates of the massive subsurface ice in Beacon Valley average 0.09 mm a^{-1} for the past 200 ka and vary from 0.04 to 0.17 mm a^{-1}, driven primarily by temperature variations of ~16.0°C. No stable condition for the massive subsurface ice existed at any time over the modeling period, but sublimation was slower, 0.04 mm a^{-1}, at approximately 18 ka and 65 ka, the coldest periods of the past 200 ka. The data presented here indicate that a decrease in temperature can slow sublimation; however, when coupled with concurrent changes in humidity, ice continues to sublimate.

Table 2.2 summarizes the modeled sublimation rates of the massive subsurface ice at Beacon Valley under different modeling scenarios. The average rate derived from the long-term model is more consistent with estimates of ice loss based on the abundance of cosmogenic nuclides in the Dry Valleys region (*J. O. Stone et al.*, manuscript in preparation, 2015). Furthermore, the dependence of the net sublimation rate on climate parameters, and the calculated sublimation history for the past 200 ka, will allow more realistic modeling of ^{10}Be accumulation in the ice. It is also possible that time-dependent calculation of the ^{10}Be buildup allowing for glacial-interglacial changes in the sublimation rate will provide a better fit to the ^{10}Be data than the simple, constant sublimation rate model used to interpret the data previously [*Stone et al.*, 2000].

Table 2.2. Modeled sublimation rates of the massive subsurface ice under various scenarios.

Modeling Scenarios	**Sublimation Rates (mm a^{-1})**
Vapor diffusion 1999-2011	0.17
Snow cover incorporated	0.14
Snowmelt and snow cover incorporated	0.11
Long-term rate over 200 ka	0.09

2.4.6. Potential Influences on the Long-Term Sublimation Rates

Perturbations in the key input parameters (temperature, RH, porosity, and EC detection) affect the long-term sublimation rates of the massive subsurface ice as illustrated in Figure 2.10. Other factors could also influence the estimated sublimation rates, i.e., depth of the subsurface ice table, soil texture, cloud cover, and variations in surface cover conditions. This study assumes that the thickness of the sublimation till was constant over the last 200 ka; however, it was shown that the sublimation rates decrease significantly with the thickness of the sublimation till above the massive ground ice [*Bryson et al.*, 2008; *Chevrier et al.*, 2008]. In addition, the sublimation rates of subsurface ice are not uniform throughout the polygons [*Kowalewski et al.*, 2012; *Mangold*,

2010; *Marchant et al.*, 2002; *Schäfer et al.*, 2000]. *Marchant et al.* [2002] suggested that the development of high centered polygons at the till surface exerts a strong control on ice sublimation; initially rates of sublimation are highest at immature polygon troughs, but as troughs deepen via sublimation, they become preferred sites for windblown snow, and this snow cover reduces underlying ice sublimation and may lead to the formation of secondary ice [*Kowalewski et al.*, 2012]. These observations indicate that sublimation rates vary with topography: maximum ice loss occurs along polygon trough walls; the lowest ice loss rates are at the base of the polygon trough; the polygon plateau has an ice loss rate in between [*Kowalewski et al.*, 2012]. The rates vary by a factor of 2.5. Both the temporal and spatial factors likely contribute to the differences between vapor diffusion models and cosmogenic isotope estimates.

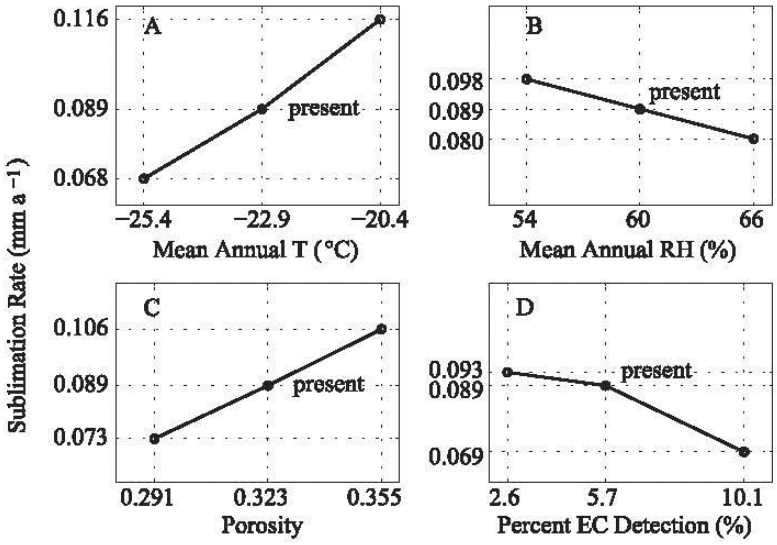

Figure 2.10. Sensitivity analysis on the effect of various parameters on sublimation rates: (a). mean annual temperature ± 2.5 °C; (b). mean annual RH ± 10% of the mean RH; (c). porosity ± 10%; (d). mean annual percentage of EC detection ± 50%.

In addition to the parameters discussed above, the presence of salts may play an important role in subsurface ice stability. The discovery of perchlorate in Beacon and University Valleys, albeit at low levels [*Kounaves et al.*, 2010b], indicates that salt with extremely low eutectic temperatures are present. In addition, *Chevrier et al.* [2008] and *Bryson et al.* [2008] have shown that slow adsorption kinetics of water vapor to grain surfaces can strongly affect the diffusion of water vapor through the regolith. Neither of these effects are included in our current model. *Kowalewski et al.* [2012] suggested that salt-rich horizons may reduce the porosity and thereby lower the sublimation rate. While it is evident that reduced porosity decreases the sublimation rate, there is no direct evidence to support the assertion that salts, which exist as part of the soil mineral assemblage, reduce porosity by filling in pore spaces.

The estimate of long-term sublimation rates in this study assumes continuous exposure of the ground surface; however, the valley floor may have been overridden by an expanded ice sheet during glacial periods in the Pleistocene or earlier [*Denton and Hughes*, 2002; *Denton et al.*, 1984]. This would stop subsurface ice sublimation and could potentially lead to subsurface ice recharge.

The longevity of the massive subsurface ice in Beacon Valley depends on the sublimation rate and the original thickness of the ice. The distribution of the buried Beacon ice is highly correlated with the granite drifts that are believed to have been deposited concurrently during a past advance of Taylor Glacier into Beacon Valley [*Sugden et al.*, 1995]. Based on the granite drifts, *Potter et al.* [2003] suggested that the ice surface in Beacon Valley may have been 350-450 m higher than where the ice remains now. Given that the bulk of this ice must have been clean, but overlaying dirty basal ice, as seen in numerous glaciers in the Dry Valleys [*Cuffey et al.*, 2000; *Fitzsimons et al.*, 2008], the most likely scenario is that the clean ice initially sublimated at much higher rates of thousands of meters per million years [*Bliss et al.*, 2011] and more slowly as a

sublimation till developed. In supporting this, *Ng et al.* [2005] found that the age of the sublimation till above the ice is on the order of several hundred thousand years. Furthermore, given the mineral content of the remaining ice, only a few tens of meters of the dirty ice sublimation would be required to produce the thickness of the sublimation till. It is unlikely that slow sublimation rates occurred for the entire downwasting history of the original ice body, but most likely have only occurred for the last tens of meters of basal ice.

2.5. Summary and Conclusions

In Beacon Valley, Antarctica, massive subsurface ice is unstable under current environmental conditions and yet it persists within 0.30 m of the surface. To determine the rate of water vapor exchange between the massive subsurface ice and the atmosphere in Beacon Valley more realistically, we developed an enhanced water vapor diffusion model that accounts for the effects of episodic snow cover and snowmelt events. This model is founded on 12 years of hourly data on air temperature, relative humidity, and soil temperature. The meteorological data show a consistent seasonal pattern with strong katabatic winds during the winter season that affect soil temperature profiles and, hence, water vapor gradients. The ice loss from the massive ice body based on a simple vapor-diffusion model averages 0.17 mm a^{-1} during 1999−2011 with most sublimation occurring during the summer season. Accounting for the episodic snow cover and snowmelt events reduces the ice sublimation rate by 30% to 0.11 mm a^{-1}. The modern sublimation rate estimated from our enhanced model is ~3 times greater than the long-term rate estimated from a cosmogenic isotope concentration profile in an ice core from the study site.

The difference between the contemporary and long-term rates is consistent with the large glacial-interglacial climate variations of the recent geologic past and is supported by the modeling

results defining the long-term sublimation rate over the past 200 ka. This model is based on the atmospheric temperature reconstructed from the ice core records from nearby Taylor Dome, and a detailed comparison between measured atmospheric temperature and relative humidity from 1999 to 2011 in Beacon Valley. The latter yielded a defined relationship between the atmospheric temperature and vapor density. The model produces an average sublimation rate of 0.09 mm a^{-1} for the past 200 ka. It is noted that the cosmogenic isotope record is sensitive to the sublimation rate during the last ~20 ka, which averaged 0.04 mm a^{-1} according to the model and this is comparable to the cosmogenic nuclide-based rate of 0.02−0.03 mm a^{-1}. This study indicates that ground surface conditions such as snow cover and snowmelt affect the sublimation rates of subsurface ice; however, under none of the scenarios is the massive subsurface ice in Beacon Valley stable during the past 200 ka. Even with the slowest loss rate, 40 meters of ice would be lost in 1 Ma. The model results suggest that the hypothesized age for buried glacier ice in the central Beacon Valley of 8.1 Ma to be unlikely. The sublimation rate and likely thickness of the dirty ice suggest that the massive subsurface ice may well be over 1 Ma old. This comprehensive vapor diffusion model also provides a valuable tool to study the long-term stability and prolonged persistence of subsurface ice on Earth, Mars, and other icy worlds, particularly where episodic surface frost/melt occurs.

Acknowledgements. This material is based upon work supported by the National Science Foundation under grants 0541054, 0636998, and 1341680 and NASA Mars Science Laboratory awarded via Malin Space Science Systems. Funding was also provided by Kenneth C. Robbins Graduate Fellowship, Joseph A. Endowed Vance Fellowship and the Dr. Howard A. Coombs Scholarship. Data supporting this paper are available at http://gcmd.nasa.gov/r/d/[GCMD]UW_Dry_Valley_Datalogging or by contacting the

corresponding author at liul99@uw.edu. We thank the Editors and reviewers for their comprehensive and insightful reviews. We are grateful to Antarctic Support Services, PHI, and our colleagues in Christchurch for superb logistical support in the Dry Valleys.

2.6. References

Anderson, D. M., L. W. Gatto, and F. C. Ugolini (1972), An Antarctic analog of Martian permafrost terrain, *Antarctic Journal of the U.S.*(7), 114-116.

Balme, M., and C. Gallagher (2009), An equatorial periglacial landscape on Mars, *Earth and Planetary Science Letters*, *285*(1), 1-15.

Black, R. F., and T. E. Berg (1963), Hydrothermal regimen of patterned ground, Victoria Land, Antarctica, *International Association of Science, Hydrology Commission of Snow and Ice*(61), 121-127.

Bliss, A. K., K. M. Cuffey, and J. L. Kavanaugh (2011), Sublimation and surface energy budget of Taylor Glacier, Antarctica, *Journal of Glaciology*, *57*(204), 684-696.

Bockheim, J. G. (2002), Landform and soil development in the McMurdo Dry Valleys, Antarctica: a regional synthesis, *Arctic Antarctic and Alpine Research*, *34*(3), 308-317.

Brown, J., O. Ferrians Jr, J. Heginbottom, and E. Melnikov (2002), Circum-Arctic Map of Permafrost and Ground-Ice Conditions, Version 2, *National Snow and Ice Data Center, Boulder, Colorado USA*.

Bryson, K. L., V. Chevrier, D. W. G. Sears, and R. Ulrich (2008), Stability of ice on Mars and the water vapor diurnal cycle: Experimental study of the sublimation of ice through a fine-grained basaltic regolith, *Icarus*, *196*(2), 446-458, doi:10.1016/j.icarus.2008.02.011.

Campbell, I. B., and G. G. C. Claridge (2006), Permafrost properties, patterns and processes in the transantarctic mountains region, *Permafrost and Periglacial Processes*, *17*(3), 215-232, doi:10.1002/Ppp.557.

Chevrier, V., D. R. Ostrowski, and D. W. G. Sears (2008), Experimental study of the sublimation of ice through an unconsolidated clay layer: Implications for the stability of ice on Mars and the possible diurnal variations in atmospheric water, *Icarus*, *196*(2), 459-476, doi:10.1016/j.icarus.2008.03.009.

Clifford, S. M., and D. Hillel (1983), The stability of ground ice in the equatorial region of Mars, *Journal of Geophysical Research*, *88*(B3), 2456-2474, doi:10.1029/JB088iB03p02456.

Clow, G. D., and E. D. Waddington (1996), Acquisition of borehole temperature measurements from Taylor Dome and the Dry Valleys for paleoclimate reconstruction, *Antarctic Journal of the United States*, *31*, 71-72.

Cuffey, K. M., H. Conway, A. M. Gades, B. Hallet, R. Lorrain, J. P. Severinghaus, E. J. Steig, B. Vaughn, and J. W. C. White (2000), Entrainment at cold glacier beds, *Geology*, *28*(4), 351-354, doi:10.1130/0091-7613(2000)028<0351:Eacgb>2.3.Co;2.

Denton, G. H., and T. J. Hughes (2002), Reconstructing the Antarctic Ice Sheet at the Last Glacial Maximum, *Quaternary Sci Rev*, *21*(1-3), 193-202, doi:10.1016/S0277-3791(01)00090-7.

Denton, G. H., M. L. Prentice, D. E. Kellogg, and T. B. Kellogg (1984), Late Tertiary history of the Antarctic ice-sheet - Evidence from the Dry Valleys, *Geology*, *12*(5), 263-267, doi:10.1130/0091-7613(1984)12<263:Lthota>2.0.Co;2.

Doran, P. T., C. P. McKay, G. D. Clow, G. L. Dana, A. G. Fountain, T. Nylen, and W. B. Lyons (2002), Valley floor climate observations from the McMurdo Dry Valleys, Antarctica, 1986-2000, *Journal of Geophysical Research-Atmospheres*, *107*(D24), 4772, doi:10.1029/2001jd002045.

Fitzsimons, S., N. Webb, S. Mager, S. MacDonell, R. Lorrain, and D. Samyn (2008), Mechanisms of basal ice formation in polar glaciers: An evaluation of the apron entrainment model, *Journal of Geophysical Research-Earth Surface*, *113*(F2), F02010, doi:10.1029/2006jf000698.

Fountain, A. G., T. H. Nylen, A. Monaghan, H. J. Basagic, and D. Bromwich (2010), Snow in the McMurdo Dry Valleys, Antarctica, *International Journal of Climatology*, *30*(5), 633-642, doi:Doi 10.1002/Joc.1933.

Fuller, E. N., Schettle.Pd, and J. C. Giddings (1966), A new method for prediction of binary gas-phase diffusion coefficients, *Ind Eng Chem*, *58*(5), 19-27.

Gaffen, D. J., W. P. Elliott, and A. Robock (1992), Relationships between tropospheric water vapor and surface temperature as oberseved by radiosondes, *Geophysical Research Letters*, *19*(18), 1839-1842.

Gleick, P. H. (1993), *Water in crisis: a guide to the world's fresh water resources*, Oxford University Press, Inc.

Gooseff, M. N., J. E. Barrett, P. T. Doran, A. G. Fountain, W. B. Lyons, A. N. Parsons, D. L. Porazinska, R. A. Virginia, and D. H. Wall (2003), Snow-patch influence on soil biogeochemical processes and invertebrate distribution in the McMurdo Dry Valleys, Antarctica, *Arctic Antarctic and Alpine Research*, *35*(1), 91-99.

Gruber, S. (2012), Derivation and analysis of a high-resolution estimate of global permafrost zonation, *The Cryosphere*, *6*(1), 221-233.

Hagedorn, B., R. S. Sletten, and B. Hallet (2007), Sublimation and ice condensation in hyperarid soils: Modeling results using field data from Victoria Valley, Antarctica, *Journal of Geophysical Research-Earth Surface*, *112*(F3), F03017, doi:10.1029/2006jf000580.

Hagedorn, B., R. S. Sletten, B. Hallet, D. F. McTigue, and E. J. Steig (2010), Ground ice recharge via brine transport in frozen soils of Victoria Valley, Antarctica: Insights from modeling delta O-18 and delta D profiles, *Geochimica Et Cosmochimica Acta*, *74*(2), 435-448, doi:10.1016/j.gca.2009.10.021.

Heldmann, J. L., W. Pollard, C. P. McKay, M. M. Marinova, A. Davila, K. E. Williams, D. Lacelle, and D. T. Andersen (2013), The high elevation Dry Valleys in Antarctica as analog sites for subsurface ice on Mars, *Planet Space Sci*, *85*, 53-58, doi:10.1016/j.pss.2013.05.019.

Hindmarsh, R. C. A., F. M. Van der Wateren, and A. L. L. M. Verbers (1998), Sublimation of ice through sediment in Beacon Valley, Antarctica, *Geografiska Annaler Series a-Physical Geography*, *80A*(3-4), 209-219.

Jakosky, B. M., and M. T. Mellon (2004), Water on Mars, *Physics Today*, *57*(4), 71-76.

Kounaves, S. P., et al. (2010), Discovery of natural perchlorate in the Antarctic Dry Valleys and its global implications, *Environ Sci Technol*, *44*(7), 2360-2364, doi:10.1021/Es9033606.

Kowalewski, D. E., D. R. Marchant, J. W. Head, and D. W. Jackson (2012), A 2D model for characterising first-order variability in sublimation of buried glacier ice, Antarctica: Assessing the influence of polygon troughs, desert pavements and shallow subsurface salts, *Permafrost and Periglacial Processes*, *23*(1), 1-14, doi:10.1002/Ppp.731.

Kowalewski, D. E., D. R. Marchant, J. S. Levy, and J. W. Head (2006), Quantifying low rates of summertime sublimation for buried glacier ice in Beacon Valley, Antarctica, *Antarctic Science, 18*(3), 421-428, doi:10.1017/S0954102006000460.

Lacelle, D., A. F. Davila, W. H. Pollard, D. Andersen, J. Heldmann, M. Marinova, and C. P. McKay (2011), Stability of massive ground ice bodies in University Valley, McMurdo Dry Valleys of Antarctica: Using stable O-H isotope as tracers of sublimation in hyper-arid regions, *Earth and Planetary Science Letters, 301*(1-2), 403-411, doi:10.1016/j.epsl.2010.11.028.

Lanagan, P. D., A. S. McEwen, L. P. Keszthelyi, and T. Thordarson (2001), Rootless cones on Mars indicating the presence of shallow equatorial ground ice in recent times, *Geophysical Research Letters, 28*(12), 2365-2367, doi:10.1029/2001gl012932.

Lowe, P. R. (1977), An approximating polynomial for the computation of saturated vapor pressure, *J. Appl. Meteorol., 16*, 100-103.

Mangold, N. (2010), Ice sublimation as a geomorphic process: A planetary perspective, *Geomorphology, 126*(1-2), 1-17.

Marchant, D. R., A. R. Lewis, W. M. Phillips, E. J. Moore, R. A. Souchez, G. H. Denton, D. E. Sugden, N. Potter, and G. P. Landis (2002), Formation of patterned ground and sublimation till over Miocene glacier ice in Beacon Valley, southern Victoria Land, Antarctica, *Geological Society of America Bulletin, 114*(6), 718-730.

McKay, C. P. (2009), Snow recurrence sets the depth of dry permafrost at high elevations in the McMurdo Dry Valleys of Antarctica, *Antarctic Science, 21*(1), 89-94, doi:10.1017/S0954102008001508.

McKay, C. P., M. T. Mellon, and E. I. Friedmann (1998), Soil temperatures and stability of ice-cemented ground in the McMurdo Dry Valleys, Antarctica, *Antarctic Science*, *10*(1), 31-38.

Mellon, M. T., R. E. Arvidson, J. J. Marlow, R. J. Phillips, and E. Asphaug (2008), Periglacial landforms at the Phoenix landing site and the northern plains of Mars, *Journal of Geophysical Research-Planets*, *113*, E00A23, doi:10.1029/2007je003039.

Mellon, M. T., W. C. Feldman, and T. H. Prettyman (2004), The presence and stability of ground ice in the southern hemisphere of Mars, *Icarus*, *169*(2), 324-340, doi:10.1016/J.Jicarus.10.022.

Morgan, D. J., J. Putkonen, G. Balco, and J. Stone (2011), Degradation of glacial deposits quantified with cosmogenic nuclides, Quartermain Mountains, Antarctica, *Earth Surface Processes and Landforms*, *36*(2), 217-228, doi:10.1002/Esp.2039.

Ng, F., B. Hallet, R. S. Sletten, and J. O. Stone (2005), Fast-growing till over ancient ice in Beacon Valley, Antarctica, *Geology*, *33*(2), 121-124, doi:10.1130/G21064.1.

Nylen, T. H., A. G. Fountain, and P. T. Doran (2004), Climatology of katabatic winds in the McMurdo Dry Valleys, southern Victoria Land, Antarctica, *Journal of Geophysical Research-Atmospheres*, *109*(D3), D03114, doi:10.1029/2003jd003937.

Oehler, D. Z. (2013), A periglacial analog for landforms in Gale Crater, Mars, in *44th Lunar and Planetary Science Conference*, edited.

Pewe, T. L. (1959), Sand-wedge polygons (tesselations) in the McMurdo Sound region, Antarctica - A progress report, *Am J Sci*, *257*(8), 545-552.

Potter JR, N., D. Marchant, and G. Denton (2003), Distribution of the granite-rich drift associated with old ice in Beacon Valley, Antarctica, paper presented at Geological Society of America, 2003 Annual Meeting.

Reiss, D., S. Gasselt, E. Hauber, G. Michael, R. Jaumann, and G. Neukum (2006), Ages of rampart craters in equatorial regions on Mars: Implications for the past and present distribution of ground ice, *Meteoritics & Planetary Science*, *41*(10), 1437-1452.

Schäfer, J. M., H. Baur, G. H. Denton, S. Ivy-Ochs, D. R. Marchant, C. Schluchter, and R. Wieler (2000), The oldest ice on Earth in Beacon Valley, Antarctica: New evidence from surface exposure dating, *Earth and Planetary Science Letters*, *179*(1), 91-99.

Schirrmeister, L., C. Siegert, T. Kuznetsova, S. Kuzmina, A. Andreev, F. Kienast, H. Meyer, and A. Bobrov (2002), Paleoenvironmental and paleoclimatic records from permafrost deposits in the Arctic region of Northern Siberia, *Quatern Int*, *89*, 97-118, doi:10.1016/S1040-6182(01)00083-0.

Schörghofer, N. (2005), A physical mechanism for long-term survival of ground ice in Beacon Valley, Antarctica, *Geophysical Research Letters*, *32*(19), L19503, doi:10.1029/2005gl023881.

Schörghofer, N. (2009), Buffering of sublimation loss of subsurface ice by percolating snowmelt: A theoretical analysis, *Permafrost and Periglacial Processes*, *20*(3), 309-313, doi:10.1002/Ppp.646.

Schörghofer, N., and O. Aharonson (2005), Stability and exchange of subsurface ice on Mars, *Journal of Geophysical Research-Planets*, *110*, E05003, doi:10.1029/2004je002350.

Sletten, R. S., B. Hallet, and R. C. Fletcher (2003), Resurfacing time of terrestrial surfaces by the formation and maturation of polygonal patterned ground, *Journal of Geophysical Research-Planets*, *108*(E4), 8044, doi:10.1029/2002je001914.

Speirs, J. C., D. F. Steinhoff, H. A. McGowan, D. H. Bromwich, and A. J. Monaghan (2010), Foehn winds in the McMurdo Dry Valleys, Antarctica: The origin of extreme warming events, *Journal of Climate*, *23*(13), 3577-3598, doi:10.1175/2010jcli3382.1.

Squyres, S. W., and M. H. Carr (1986), Geomorphic evidence for the distribution of ground ice on Mars, *Science*, *231*(4735), 249-252.

Steig, E. J., D. L. Morse, E. D. Waddington, M. Stuiver, P. M. Grootes, P. A. Mayewski, M. S. Twickler, and S. I. Whitlow (2000), Wisconsinan and Holocene climate history from an ice core at Taylor Dome, western Ross Embayment, Antarctica, *Geografiska Annaler: Series A, Physical Geography*, *82*(2-3), 213-235.

Stone, J. O., R. S. Sletten, and B. Hallet (2000), Old ice, going fast: Cosmogenic isotope measurements on ice beneath the floor of Beacon Valley, Antarctica *Eos Transactions, American Geophysical Union, Fall Meeting Supplement, Abstract H52C–21 81*(48).

Sugden, D. E., D. R. Marchant, N. Potter, R. A. Souchez, G. H. Denton, C. C. Swisher, and J. L. Tison (1995), Preservation of Miocene glacier ice in East Antarctica, *Nature*, *376*(6539), 412-414.

Vanderwateren, D., and R. Hindmarsh (1995), East Antarctic Ice-Sheet - Stabilists strike again, *Nature*, *376*(6539), 389-391.

Washburn, A. L. (1979), *Geocryology: A survey of periglacial processes and environments*, Wiley, New York.

Zalc, J. M., S. C. Reyes, and E. Iglesia (2004), The effects of diffusion mechanism and void structure on transport rates and tortuosity factors in complex porous structures, *Chemical Engineering Science, 59*(14), 2947-2960, doi:10.1016/j.ces.2004.04.028.

2.7. Supporting Information

Table S2.1 Annual and austral summer (December, January, and February) average, maximum, and minimum values of air temperature (Tair), RH, soil temperatures at depths, and annual degree days above freezing (DDAF) from 1999 to 2010.

		Annual			Summer (Dec, Jan, Feb)			Annual DDAF (℃·day)
		Average	Maximum	Minimum	Average	Maximum	Minimum	
1999	T_{air} (℃)	−25.7	−4.3	−47.2	−11.9	−4.3	−25.9	0.0
	RH (%)	61.4	100.0	7.7	45.8	100.0	7.7	–
	T at 0.02 m (℃)	−27.4	17.0	−51.1	−5.7	17.0	−27.7	68.5
	T at 0.10 m (℃)	−27.2	2.4	−45.7	−7.1	2.4	−21.1	0.0
	T at 0.20 m (℃)	−27.2	−3.5	−42.2	−8.4	−3.2	−18.4	0.0
	T at 0.30 m (℃)	−27.2	−7.1	−38.8	−9.7	−6.1	−16.6	0.0
2000	T_{air} (℃)	−22.5	−3.1	−44.3	−11.3	−3.0	−24.8	0.0
	RH (%)	56.7	100.0	8.2	53.4	100.0	11.6	–
	T at 0.02 m (℃)	−23.0	17.1	−49.7	−4.6	17.1	−27.4	102.4
	T at 0.10 m (℃)	−22.8	2.0	−45.2	−6.3	2.0	−20.5	1.1
	T at 0.20 m (℃)	−22.9	−3.2	−42.1	−7.7	−2.5	−17.2	0.0
	T at 0.30 m (℃)	−22.9	−6.1	−39.0	−9.1	−6.0	−15.2	0.0
2001	T_{air} (℃)	−22.9	0.9	−46.9	−9.9	1.6	−25.5	0.2
	RH (%)	56.8	100.0	8.5	46.6	100.0	10.0	–
	T at 0.02 m (℃)	−23.2	20.5	−50.8	−4.5	20.5	−28.0	155.5
	T at 0.10 m (℃)	−23.0	6.6	−44.3	−5.8	6.6	−21.3	12.9
	T at 0.20 m (℃)	−23.0	0.8	−40.3	−7.2	0.8	−18.4	0.2
	T at 0.30 m (℃)	−23.0	−3.7	−37.6	−8.6	−3.7	−16.4	0.0
2002	T_{air} (℃)	−23.2	1.6	−47.9	−10.4	−0.6	−22.2	0.1
	RH (%)	58.1	100.0	7.0	48.9	100.0	10.8	–
	T at 0.02 m (℃)	−24.2	15.2	−53.7	−5.2	15.2	−24.3	97.4

	T at 0.10 m (℃)	−23.6	3.7	−47.9	−6.4	2.2	−17.7	6.8
	T at 0.20 m (℃)	−23.6	−0.6	−44.5	−7.9	−2.4	−15.1	0.0
	T at 0.30 m (℃)	−23.5	−3.9	−41.2	−9.5	−5.8	−15.7	0.0
2003	T_{air} (℃)	−22.6	−0.6	−45.2	−10.2	−0.9	−23.5	0.0
	RH (%)	61.2	100.0	9.7	52.7	100.0	10.9	–
	T at 0.02 m (℃)	−23.0	12.7	−50.4	−4.9	13.4	−26.1	102.9
	T at 0.10 m (℃)	−22.6	3.7	−43.9	−5.6	4.1	−18.3	7.6
	T at 0.20 m (℃)	−22.7	−1.0	−40.1	−7.0	−0.7	−15.5	0.0
	T at 0.30 m (℃)	−22.7	−4.9	−37.1	−8.5	−4.4	−13.9	0.0
2004	T_{air} (℃)	−23.3	−0.9	−47.8	−10.3	−1.7	−27.8	0.0
	RH (%)	55.6	100.0	7.4	56.1	100.0	11.6	–
	T at 0.02 m (℃)	−23.9	13.4	−54.2	−6.7	9.1	−24.0	80.8
	T at 0.10 m (℃)	−23.4	4.1	−47.6	−6.2	2.9	−19.1	7.8
	T at 0.20 m (℃)	−23.4	−0.7	−43.8	−7.4	−1.4	−17.4	0.0
	T at 0.30 m (℃)	−23.3	−4.4	−40.1	−8.7	−4.6	−15.9	0.0
2005	T_{air} (℃)	−22.5	0.4	−44.3	−9.4	0.4	−24.8	0.0
	RH (%)	58.7	100.0	8.8	49.4	100.0	10.8	–
	T at 0.02 m (℃)	−23.1	9.2	−49.4	−5.8	9.9	−25.1	46.8
	T at 0.10 m (℃)	−22.7	4.8	−43.8	−5.0	5.2	−18.3	17.3
	T at 0.20 m (℃)	−22.7	0.2	−40.4	−6.3	0.6	−16.0	0.0
	T at 0.30 m (℃)	−22.7	−3.5	−37.7	−7.8	−3.0	−14.3	0.0
2006	T_{air} (℃)	−23.4	−1.1	−44.8	−10.8	1.2	−29.0	0.0
	RH (%)	62.9	100.0	9.2	51.8	100.0	13.0	–
	T at 0.02 m (℃)	−24.3	9.9	−50.6	−6.8	12.8	−29.8	35.3
	T at 0.10 m (℃)	−23.6	5.2	−45.0	−6.3	5.7	−22.8	14.5
	T at 0.20 m (℃)	−23.5	0.6	−42.0	−7.5	0.5	−19.9	0.3
	T at 0.30 m (℃)	−23.4	−3.0	−39.4	−8.8	−3.7	−17.5	0.0
2007	T_{air} (℃)	−21.8	1.2	−43.8	−11.7	−0.4	−25.4	0.3
	RH (%)	57.9	100.0	7.7	48.5	100.0	11.8	–

	T at 0.02 m (℃)	−22.5	13.2	−49.0	−7.2	15.0	−27.6	75.1
	T at 0.10 m (℃)	−22.2	5.7	−43.3	−7.0	3.5	−20.5	14.2
	T at 0.20 m (℃)	−22.3	0.5	−39.9	−8.2	−1.2	−17.6	0.2
	T at 0.30 m (℃)	−22.3	−3.7	−36.6	−9.4	−4.1	−15.7	0.0
2008	T_{air} (℃)	−22.3	2.6	−45.8	−11.1	2.6	−28.6	1.2
	RH (%)	55.6	100.0	9.1	46.3	100.0	10.3	–
	T at 0.02 m (℃)	−22.9	15.0	−51.7	−6.8	13.6	−30.6	63.2
	T at 0.10 m (℃)	−22.5	7.5	−45.9	−6.4	7.5	−23.5	13.5
	T at 0.20 m (℃)	−22.6	1.9	−42.2	−7.6	1.9	−20.3	0.9
	T at 0.30 m (℃)	−22.5	−3.0	−38.8	−8.8	−3.0	−17.9	0.0
2009	T_{air} (℃)	−22.6	−0.9	−45.2	−10.6	−1.8	−26.9	0.0
	RH (%)	59.0	100.0	4.6	56.4	100.0	13.7	–
	T at 0.02 m (℃)	−23.5	11.0	−51.4	−6.5	12.0	−26.8	49.6
	T at 0.10 m (℃)	−23.0	4.2	−45.7	−6.2	2.8	−20.5	5.2
	T at 0.20 m (℃)	−23.0	−0.3	−42.2	−7.4	−2.0	−17.9	0.0
	T at 0.30 m (℃)	−22.9	−3.9	−38.9	−8.7	−5.0	−16.1	0.0
2010	T_{air} (℃)	−22.9	0.1	−45.0	–	–	–	0.0
	RH (%)	59.3	100.0	10.5	–	–	–	–
	T at 0.02 m (℃)	−23.6	12.0	−50.2	–	–	–	76.8
	T at 0.10 m (℃)	−23.1	4.6	−45.0	–	–	–	15.5
	T at 0.20 m (℃)	−23.1	0.0	−41.7	–	–	–	0.0
	T at 0.30 m (℃)	−23.0	−4.1	−38.7	–	–	–	0.0

Chapter 3. Soil thermal properties and ground thermal regime above an ancient ground ice body in Beacon Valley, Antarctica

The content of this chapter is currently in preparation for publication as:

Liu, L., R. S. Sletten, B. Hallet, E. D. Waddington, and S. E. Wood (in prep), Soil properties and ground thermal regime above an ancient ground ice body in Beacon Valley, Antarctica, *Journal of Geophysical Research: Earth Surface*.

3.1. Abstract

Subsurface temperatures in polar environments are important for understanding periglacial processes and ground ice stability. Most models of the ground thermal regime in permafrost areas have been developed for the Arctic; there are few detailed studies in Antarctica where soils are subjected to much colder and dryer conditions. Here, we present a study on the soil thermal properties and the subsurface temperatures in Beacon Valley, one of the McMurdo Dry Valleys of Antarctica, where the stability and long-term persistence of ground ice are of great interest. For the temperature range of −47.9 to 7.5 ℃ at our study site, the heat capacity of the dry soil is 589 to 687 J kg^{-1} K^{-1}, thermal conductivity is 0.29 to 0.32 W m^{-1} K^{-1}, and the calculated thermal diffusivity is 0.30 to 0.32 mm^2 s^{-1}. Both the finite difference method (FDM) and the finite volume method (FVM) were used to solve the 1-D heat diffusion equation. Utilizing the temperature-dependent thermal properties, the FVM modeled temperature most closely approximates the measured temperature at all depths with average differences ranging from 0.01 ℃ to 0.03 ℃. There was a negligible effect on the temperature profile due to the latent heat from documented episodic snowmelt events or modeled changes in ice content due to condensation or

sublimation. This study is applicable to systems where subsurface temperature measurements are not available such as the frigid, hyperarid environment on Mars.

3.2. Introduction

Modeling subsurface temperature is of particular interest for permafrost-affected soils in the Arctic and Antarctica because it helps predict the active layer thickness, latent heat effect of water phase changes, soil moisture content, and ground (ice) stability [*Boike et al.*, 1998; *Hagedorn et al.*, 2007; *Ikard et al.*, 2009; *Lachenbruch et al.*, 1962; *Liu et al.*, 2015; *Putkonen*, 1998; *Romanovsky and Osterkamp*, 1997; 2000; *Roth and Boike*, 2001]. A number of factors, including meteorology, terrain, soil properties and snow, influence the subsurface temperature by affecting the energy flow between the atmosphere and the ground [*Gold and Lachenbruch*, 1973]. A key property of the ground that determines its response to temperature changes at the surface is the thermal diffusivity, which is a measure of the ability of a material to conduct thermal energy relative to its ability to store thermal energy. Thermal diffusivity (α) includes the components of thermal conductivity (k) and volumetric heat capacity (ρC), soil latent heat, and water content and is defined as:

$$\alpha = \frac{k}{\rho C} \tag{3.1}$$

A quantitative understanding of the processes controlling the thermal behavior of permafrost is paramount to study its response to a changing climate and to improve current climate models [*Kane et al.*, 1991].

While both the Arctic and Antarctica have permafrost, they possess distinct environments: most soils in continental Antarctica have a mean annual temperature below the freezing point of water [*Bockheim and Hall*, 2002]. In contrast, the arctic soils typically experience thawing conditions during the summer and have free liquid water in the active layer [*Brown et al.*, 2002; *Lachenbruch et al.*, 1962]. Arctic thermal studies are primarily based on 1-D thermal diffusion

models for soils that are often water saturated above the permanently frozen zone and are solved by a finite difference scheme; these studies show the importance of non-conductive heat transfer processes, e.g. energy consumed from rapid snowmelt leads to more rapid warming of the soil in the late spring, and latent heat released due to ice growth slows freezing in the autumn (known as the zero degree curtain) [*Hinkel and Outcalt*, 1994; *Putkonen*, 1998; *Romanovsky and Osterkamp*, 2000; *Roth and Boike*, 2001]. In general, heat is transferred primarily via conduction in the Arctic soils, and the water-rich soils are highly conductive thermally. Moreover, latent heat and vapor migration are also important processes affecting the thermal dynamics. Due to the lack of liquid water, latent heat effects are generally less important in Antarctic soils; these effects will be assessed here.

The current study focuses on soils in the McMurdo Dry Valleys (MDV) of Antarctica, which is the largest ice free area on the continent [*Priscu*, 1998]. The environment is frigid and hyper-arid, with mean air temperatures of approximately −20.0 ℃ and less than 100 mm annual precipitation [*Bromwich*, 1988; *Clow et al.*, 1988; *Fountain et al.*, 2010]. Due to the frigid conditions, liquid water is rare; however, near surface ground ice is pervasive in the MDV. *Bockheim et al*. [2007] estimated that, within the top meter, 53% of the MDV is comprised of ice-cemented permafrost and 43% is "dry permafrost", ground that remains permanently below 0 ℃ but lacks ice. There is additional interest in the MDV since they are considered to be the best terrestrial analog for Mars with regard to research involving periglacial processes, geomorphic features, and as indicators of ground ice [*Heldmann et al.*, 2013]. As is common in the MDV, ground ice beneath a dry layer (<0.1 m) of soil was discovered by the Phoenix lander [*Mellon et al.*, 2009].

Previous studies in the MDV have focused on the stability of subsurface ice using vapor diffusion models [*Hagedorn et al.*, 2007; *Hindmarsh et al.*, 1998; *Kowalewski et al.*, 2006; *Liu et al.*, 2015; *McKay*, 2009; *McKay et al.*, 1998; *Mellon et al.*, 2009; *Paige*, 1992; *Rossbacher and Judson*, 1981; *Schörghofer and Aharonson*, 2005]. Modeling studies of the ground thermal regime and thermal properties are rare in Antarctic soils. Heat transfer in the MDV can be treated as purely conductive; latent heat contributions can be ignored due to the very dry conditions and dearth of liquid water. *Putkonen et al.* [2003] modeled the ground temperatures at Beacon Valley using a standard 1-D thermal conduction model with 2 layers (dry soil and ice) to evaluate the internal consistency of the measured and assumed thermal conductivities. *Hunt et al.* [2010] developed an energy model that incorporated sensible heat exchange between the atmosphere and ground surface, inter- and intra-layer heat conduction by rock and soil, and shortwave and longwave radiation in Taylor Valley. Their model accounted for 96−99% of the observed variation in soil surface temperature but overestimated surface temperatures in winter by a few degrees.

Our modeling study focuses on the subsurface thermal regime at Beacon Valley, Antarctica. We model conductive heat transfer constrained by hourly temperature measurements at the ground surface. Both the finite difference method (FDM) and the finite volume method (FVM) are used to numerically solve the heat diffusion equation. The model's ability to reproduce the temperature profile is evaluated by comparing modeled temperatures to our in situ hourly temperature measurements made at various depths below the surface for over a decade. A sensitivity analysis of the soil thermal parameters on the modeled temperatures is also presented. The contribution of latent heat due to documented snowmelt and due to ice condensation or sublimation, both estimated by a physical vapor transport model [*Liu et al.*, 2015], was also assessed. This detailed study provides a comprehensive test of a current thermal model, which can be used in other

systems including those where subsurface temperature measurements are not available, such as on Mars.

3.3. Geologic Setting at Beacon Valley, Antarctica

The present day environment of the MDV is a frigid, polar desert exhibiting a hyperarid precipitation regime with mean air temperatures of approximately −20.0 ℃ and less than 100 mm annual precipitation [*Bromwich*, 1988; *Clow et al.*, 1988; *Fountain et al.*, 2009]. Sublimation in the MDV exceeds precipitation at all localities, except where wind-blown snow accumulates [*Fountain et al.*, 2009; *Gooseff et al.*, 2003]. Sublimation is largely responsible for glacier ablation in the MDV [*Chinn*, 1980; *Fountain et al.*, 1998]. Beacon Valley is the largest ice free valley in the Quartermain Mountains, and is approximately 3 km wide and 12 km long (Figure 3.1). It is one of the higher elevation valleys with the main valley floor in central Beacon Valley at approximately 1350 m above sea level. The mean annual temperature is −22.9 ℃ based on our field measurements [*Liu et al.*, 2015] and the estimated mean annual water-equivalent precipitation is less than 10 mm a^{-1} [*Bromwich et al.*, 2005; *Fountain et al.*, 2009]. Polygonal patterned ground covers the floor of Beacon Valley; the 10−20 m polygons are equidimensional, have straight sides that intersect at triple junctions at similar angles, and are delimited by with deep troughs [*Marchant et al.*, 2002; *Sletten et al.*, 2003].

At our study site (77 °49′S and 160 °39′E) in central Beacon Valley, massive ground ice is 30−50 cm below the surface (Figure 3.1 insert). The ice contains approximately 3 wt% mineral debris, and has been sublimating for at least the past 200 ka [*Liu et al.*, 2015]. Sublimation of the ice leaves behind the debris producing a thin protective cap of sublimation till. This ice has received much attention initially spurred by the report by *Sugden et al.* [1995] that it was over 8.1 Ma old based on the age of tephra found in a sand wedge above the ice. The age of this buried ice

was questioned on theoretical grounds based on models of sublimation [*Vanderwateren and Hindmarsh*, 1995]. In addition, reanalysis of cosmogenically dated cobbles [*Marchant et al.*, 2002; *Schäfer et al.*, 2000] that are deposited from the ice body as it sublimates indicates that the sublimation till overlying the ice is only several hundred thousand years old [*Ng et al.*, 2005]. This discrepancy has raised much interest in studying the ground ice stability in the MDV [*Hagedorn et al.*, 2007; *Hindmarsh et al.*, 1998; *Kowalewski et al.*, 2012; *Kowalewski et al.*, 2006; *Liu et al.*, in review; *McKay*, 2009; *McKay et al.*, 1998; *Mellon et al.*, 2009; *Paige*, 1992; *Rossbacher and Judson*, 1981; *Schörghofer*, 2005; *Schörghofer and Aharonson*, 2005].

Our analysis uses more than a decade of continuous temperature measurements from the relatively stable central portion of a polygon, approximately midway between its center and the trough 5.9 m away, with a total thickness of the sublimation till above the ice of 0.30 m. Ground temperature was recorded hourly using a Campbell CR10X data logger with thermistors calibrated at the University of Washington to within ±0.02 ℃. The thermistors were installed in the ice-free soil at depths of 0.02 m, 0.10 m, 0.20 m, and 0.30 m (the regolith-ice boundary), and in the ice at depths of 0.45 m, and 0.60 m. Small holes were drilled into the ice to install the thermistors. Temperatures were also measured deeper in the ice, 4 m, 9 m, 14 m, and 19.6 m below the surface in a borehole in an adjacent polygon.

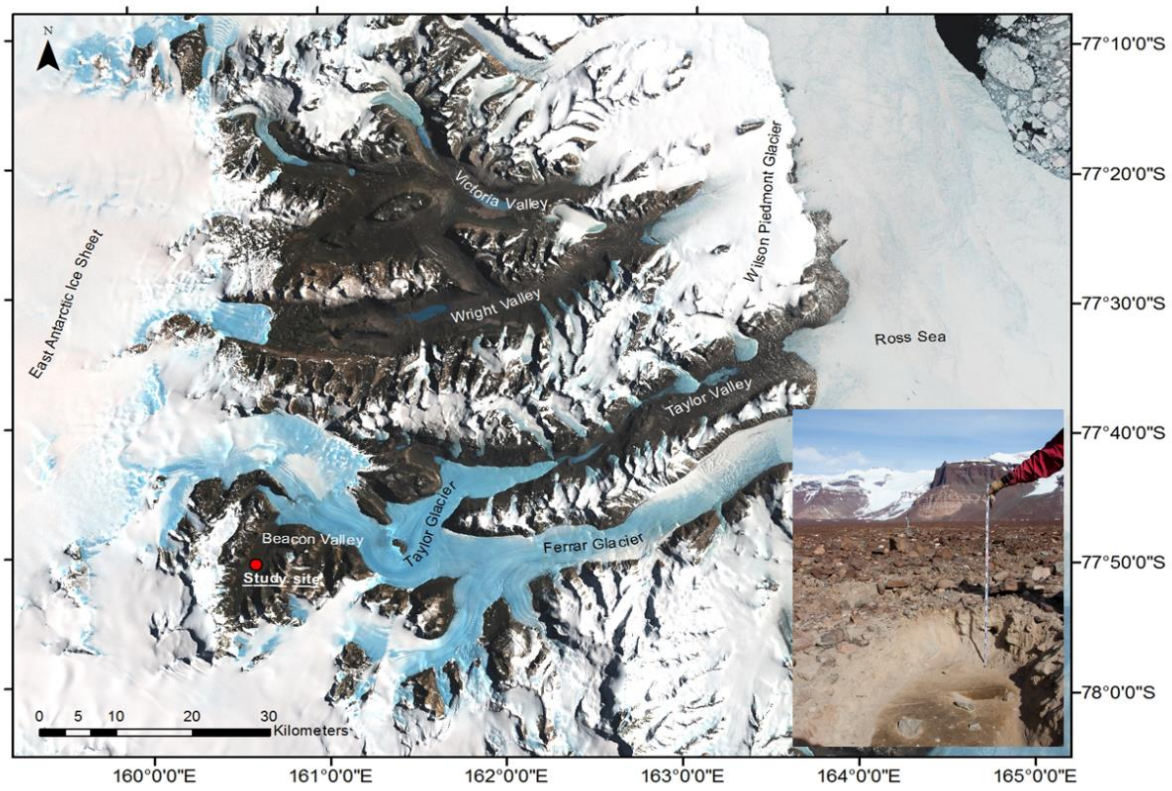

Figure 3.1. The McMurdo Dry Valleys (MDV) lie between the McMurdo Sound region of the Ross Sea and the East Antarctic Ice Sheet. Insert: buried massive ice lies beneath several decimeters of the regolith in Beacon Valley, Antarctica.

3.4. Soil and Ice Thermo-Physical Properties

3.4.1. Soil Bulk Density

The bulk density of the dry soil (ρ_s) was determined by pouring soils freely into a chamber of known volume and tapping and shaking the soil chamber gently between additions of small volumes of soil. This procedure was carried out in triplicate, and the average bulk density of soil from our study site is 1640 kg m^{-3}.

3.4.2. Soil Heat Capacity

The heat capacity (C_s) of the dry soil was measured using a Q2000 heat-flux Differential Scanning Calorimeter (DSC by TA Instruments). The DSC measures specific heat capacity by

heating a sample and measuring the temperature difference between the sample and a standard. In order to obtain reliable results, three measurements are usually carried out [*Thomas*, 2003]. First, a baseline is recorded with both sample pans empty, yielding a signal bias inherent in the system. Next is a reference test, in which a sample with a well-defined specific heat is tested for comparison to an experimental sample. Finally, an experimental sample is tested. The baseline allows removal of system bias from the data, while the reference test allows calculation of the specific heat of the experimental sample as a ratio of the reference material specific heat. For heat flux standards, synthetic sapphire supplied by TA Instruments was used. The sample pans used for the DSC analysis were Tzero^{TM} aluminum sample pans. The DSC is cooled by liquid nitrogen and uses nitrogen as a purge gas at a flow rate of 50 ml min^{-1}.

Calibration of the DSC for heat-capacity measurements requires both a temperature calibration and a heat flux calibration [*Della Gatta et al.*, 2006; *Höhne et al.*, 2003; *Price*, 1995]. Because the calibration factor is known to be sensitive to many different experimental factors, including scanning rate, sample size, sample geometry, etc. [*Höhne et al.*, 2003], we kept the protocol for both calibration and sample analysis identical over all runs: (1) heating at 80.0 ℃ to drive off soil moisture, (2) a 5 min isothermal period at –100.0 ℃, and (3) a 20.0 ℃ min^{-1} cooling scan to 25.0 ℃. Heat capacity is determined from the measured heat flux and the heating rate.

The measured heat capacity of the dry soil from our study site in Beacon Valley shows a strong temperature dependence, ranging from 585 to 691 J kg^{-1} K^{-1} from −50.0 to +10.0 ℃ (Figure 3.2a); this dependence is similar to previous studies on silicate minerals [*Robinson and Haas*, 1983; *Winter and Saari*, 1969]. The measured heat capacity values are smaller than the typical values used for the Antarctica dry soils of ~800 J kg^{-1} K^{-1} [*Putkonen et al.*, 2003; *Sizemore and Mellon*, 2006; *Swanger and Marchant*, 2007] and lower than the values for the planetary soils [*Winter and*

Saari, 1969]. This may be due to the different mineralogical compositions at different locations [*Alnefaie and Abu-Hamdeh*, 2013] including the presence of secondary minerals from weathering of these old soils. There is no significant variation in measured heat capacity with depth.

3.4.3. Soil Thermal Conductivity

The thermal conductivity of the dry permafrost (k_s) was estimated using the Johansen's method [*Farouki*, 1981a; *Farouki*, 1981b; *Johansen*, 1975]. Considering the experimental data, *Johansen* [1975] noted that the thermal conductivity of the dry natural soils is mainly determined by dry density or porosity; the conductivity of the mineral grains had relatively little effect. Setting the conductivity ratio (solids to air) to 125, *Johansen* [1975] developed a semi-empirical equation that is based on the Maxwell-Fricke′s equation:

$$k_s = \frac{\varepsilon+(1-\varepsilon)\times 6.65}{\varepsilon+(1-\varepsilon)\times 0.053} \tag{3.2}$$

where ε is porosity that can be estimated based on intrinsic density ρ_i (kg m^{-3}) and the dry bulk density ρ_b (kg m^{-3}) of the soil $\varepsilon = 1 - \rho_b/\rho_i$. Equation (3.2) will then be of the form:

$$k_s = \frac{0.024\rho_i + 0.1356\,\rho_b}{\rho_i - 0.0.947\,\rho_b} \tag{3.3}$$

The calculated thermal conductivity of the dry soil k_s is approximately 0.31 W m^{-1} K^{-1} at our study site. It has been shown that thermal conductivity also varies with temperature and this has been modeled using *Wood*'s model [*Wood*, 2011]. This model estimates the bulk thermal conductivity of the dry soil given the environment properties (i.e., temperature, gravity, and depth), the gas properties (i.e., atmospheric gas composition and atmospheric pressure), and the soil composition and particle properties (i.e., the soil composition, particle size, and porosity). The conductivity increases with temperature (Figure 3.2b) due to the combined effects of the

temperature on the thermal conductivities of the pore-filling gas, mineral grains, and the radiative component [*Piqueux and Christensen*, 2009; *Wood*, 2011].

The thermal conductivity values presented in this study compare favorably to other reported values elsewhere in the MDV. *McKay et al.* [1998] found the thermal conductivity of the ice-free soil to be 0.6 ± 0.1 W m^{-1} K^{-1} at Linnaeus Terrace (77°36'S, 161°05'E) based on the attenuation and phase of the measured temperature variation with depth. *Putkonen et al.* [2003] found values for thermal conductivity based on their model to be 0.4 W m^{-1} K^{-1} in dry debris at Beacon Valley, larger than the in-situ measurement of 0.2 W m^{-1} K^{-1} and laboratory measurements of 0.3 W m^{-1} K^{-1}. The thermal conductivity values of the dry soil in the MDV are one fourth to one fifth of those of the arctic soils [*Putkonen*, 1998; *Romanovsky and Osterkamp*, 1995] due to the lack of ice/water, and are ~10 times larger than the values suggested for Martian soils [*Clifford*, 1993a; *Martínez et al.*, 2014; *Mellon and Jakosky*, 1993]. The relative low thermal conductivity of the dry soil makes it an effective insulator that limits the penetration of the heat wave in the summer; therefore, the underlying massive ice is relatively insensitive to the annual temperature extremes.

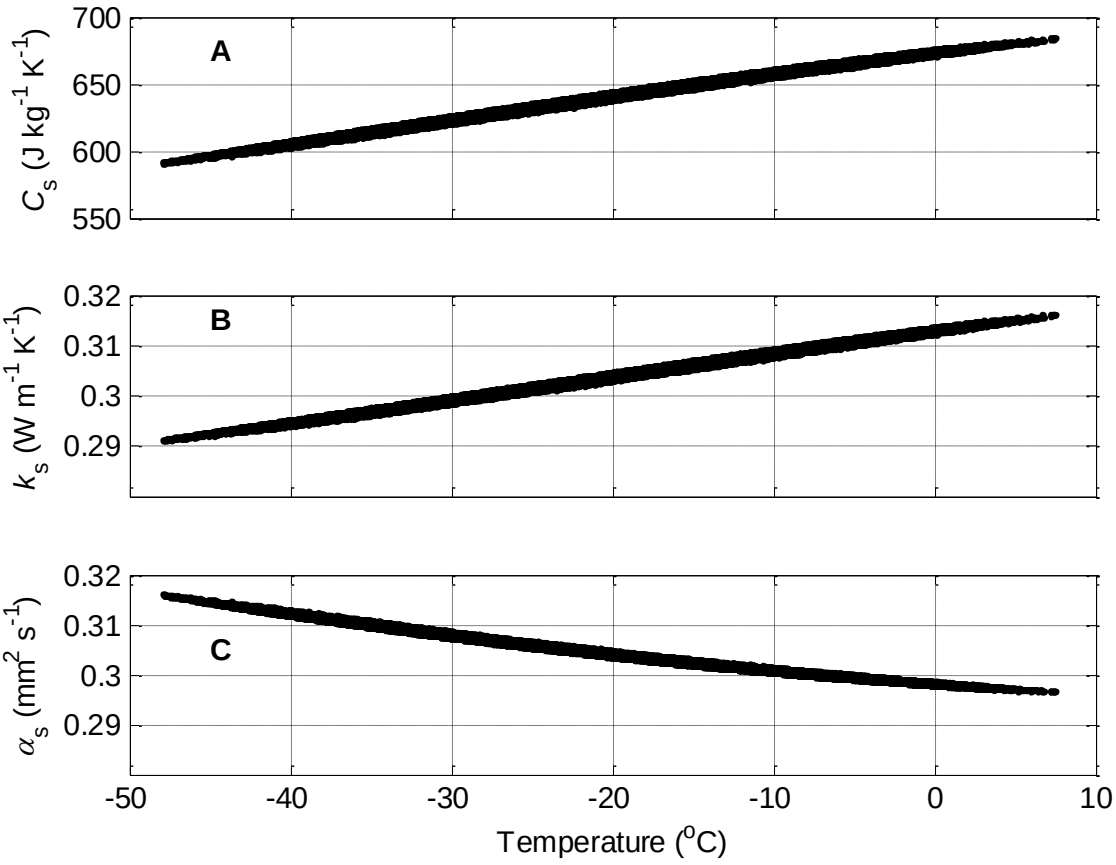

Figure 3.2. Thermal properties of the dry soil at 0.10 m from our study site in Beacon Valley: (a) measured heat capacity in J kg^{-1} $K^{-1}$and (b) calculated thermal diffusivity in mm^2 s^{-1}.

3.4.4. Soil Thermal Diffusivity

The calculated thermal diffusivity of the dry soil at our study site using equation (3.1) is shown in Figure 3.2c; it ranges from 0.30 to 0.32 mm^2 s^{-1} for the temperature range of −47.9 ℃ to 7.5 ℃. There is a negative correlation with temperature, opposite to the temperature dependence of the heat capacity and thermal conductivity because of the stronger temperature dependence of the heat capacity than that of the thermal conductivity. Several studies have assessed the thermal diffusivity of soils from continental Antarctica. *Campbell et al.* [1997] reported thermal diffusivity values of 0.124 to 0.138 mm^2 s^{-1} for soils located near Scott Base (on Ross Island, across McMurdo

Sound from MDV) and two locations ~70 km north of Taylor Valley. *Ikard et al.* [2009] characterized soil thermal properties along a soil-moisture gradient adjacent to Lake Fryxell in Taylor Valley, Antarctica, and they found diffusivity values tended to decrease with decreasing soil moisture; the reported thermal diffusivity range from 0.0029 to 0.116 $mm^2\ s^{-1}$. Variations in thermal diffusivity values are likely because of different moisture content and bulk density at each site.

3.4.5. Massive Ground Ice Thermal Diffusivity

The thermo-physical properties of ice: density ρ_i, heat capacity C_i, and thermal conductivity k_i, also vary with temperature (Table 3.1, data from the CRC Handbook of Chemistry and Physics, 89th Edition, [2008-2009]). The thermal conductivity and density of ice decrease with temperature while the heat capacity increases. The thermal diffusivity of ice calculated using equation (3.1) averages approximately 1.3 $mm^2\ s^{-1}$ and decreases with temperature.

Table 3.1. Calculated thermal diffusivity of ice using ice density, heat capacity, and thermal conductivity values for the range of temperature in this study from the CRC Handbook of Chemistry and Physics, 89th Edition, [2008-2009].

Temperature T (℃)	Density ρ_i (kg m^{-3})	Heat Capacity C_i (kJ $kg^{-1}\ K^{-1}$)	Thermal Conductivity k_i (W $m^{-1}\ K^{-1}$)	Thermal Diffusivity α_i ($mm^2\ s^{-1}$)
0	916.7	2.10	2.16	1.12
−10.0	918.2	2.02	2.26	1.22
−20.0	919.6	1.95	2.38	1.33
−30.0	920.9	1.88	2.50	1.44
−40.0	922.2	1.80	2.63	1.58
−50.0	923.5	1.73	2.77	1.73

The thermal diffusivity of ice is approximately four times higher than the thermal diffusivity values of the dry soil. The sharp compositional interface between the overlying dry soil

and the massive ice underneath leads to an abrupt change in thermal diffusivity across the soil-ice boundary, which requires special attention in the numerical modeling as discussed below.

3.5. Ground Thermal Regime

3.5.1. Model Description

This section describes the governing equation of the 1-D thermal model, the numerical approaches adopted, and the initial and boundary conditions used to in the model.

3.5.1.1. Heat Diffusion Equation

For a relatively uniform surface with little relief in cold and hyper-arid environments, the subsurface thermal regime can be described using the general 1-D thermal diffusion equation without phase changes, or other heat sources or sinks:

$$\rho_m C(T)_m \frac{\partial T}{\partial t} = \frac{\partial}{\partial z}\left(k_m(T)\frac{\partial T}{\partial z}\right) \tag{3.4}$$

where T is temperature (℃), t is time (s), k is the thermal conductivity (W m^{-1} K^{-1}), ρ is the density (kg m^{-3}), C is the heat capacity (J K^{-1} kg^{-1}), z is depth (m), and m refers to the different media through which heat is conducting (s for the dry soil and i for the massive ground ice). Accordingly, the rate of temperature change is related to the vertical gradients in thermal conductivity and temperature gradient at various depths, as well as the other relevant material properties.

Simplifying assumptions have been made to model the subsurface thermal regime. For example, the surface energy flux, largely driven by solar radiation, is assumed to propagate vertically downwards in a laterally uniform soil by heat conduction; convective processes are neglected due to the lack of vertical bulk motion in the ground. Therefore, annual and higher frequency fluctuations in soil temperature at depth are assumed to be driven by atmospheric

forcing, primarily through surface temperature fluctuations. The heat release/consumption associated with water phase changes is omitted here; it is negligible because of the extremely dry conditions and absence of liquid water in Beacon Valley. The 1-D thermal diffusion equation applies only when the temperature and elevation of the surface can be considered uniform for lateral distances equal to several times the depth of interest [*Gold and Lachenbruch*, 1973].

3.5.1.2. Numerical Methods for Heat Diffusion Equation

Equation (3.4) is numerically evaluated by stepping through time and space in discrete steps. In this study, a fully implicit scheme was used, where it finds a solution by simultaneously solving the time and spatial derivatives involving both the current state of the system and the future state. It allows for a large time step and simplifies the resulting equations while accurately representing the heat diffusion equation [*Botte et al.*, 2000; *Patankar*, 1980].

The finite difference method (FDM) is a popular numerical technique for solving systems of differential equations that describe mass, momentum, and energy balances. Take heat diffusion for example, in the FDM, the heat equation is approximated by a set of algebraic equations using a Taylor Series expansion, and the accuracy is improved by using more terms in the series and using smaller grid spacing sizes. This method is very useful in various studies due to its simplicity; however, the FDM sometimes yields unrealistic behavior and the energy is rigorously conserved only in the limit when the grid spacing approaches zero [*Patankar*, 1980; *West and Fuller*, 1996]. To circumvent this situation, the finite volume method (FVM) was developed, where the heat equation is integrated over a finite volume. Energy is rigorously conserved because the FVM integrates over small control volumes and the flux of energy at the common interface between two adjacent control volumes is represented consistently by the same expression. Thermal conductivities at the interfaces of adjacent control volume interfaces (i.e. interfaces of *w* and *e* in

Figure 3.A.2. in Appendix 3.A) are expressed using the geometric mean (see equations (3.A.11) and (3.A.12) in Appendix 3.A), which allows for accurate representation of identical heat flux across the interfaces of two adjacent volumes. Details of the discretization process and the numerical representation for both the FDM and the FVM are presented in Appendix 3.A.

3.5.1.3. Boundary Conditions

Boundary conditions as well as an initial condition are needed to solve the 1-D transient heat diffusion equation numerically. At Beacon Valley, the top boundary is set by hourly near-surface ground temperature measurements at 0.02 m depth at the study site over a 12 year period [*Liu et al.*, 2015]. This depth is a minimum depth for inserting a thermistor without altering the surface characteristics of this soil, as has been found in other studies [*Guglielmin*, 2006; *Guglielmin et al.*, 2003; *Osterkamp*, 2003]. The average annual near-surface ground temperature is −23.6 ℃, with a maximum and minimum temperature of 20.5 ℃ and −54.2 ℃. The surface temperature is more variable during the winter than the summer due to warm katabatic winds that can warm the air by several tens of degrees Celsius in a short period of time [*Hagedorn et al.*, 2007; *Nylen et al.*, 2004]. The bottom boundary is measured borehole temperature at 30 m in lower Beacon Valley. At this depth, seasonal variations are less than one hundredth of a degree and the temperature converges to the mean annual temperature of −23.0 ℃. The initial condition was assumed to be −20.0 ℃ at all depths.

3.5.2. Model Results

As described earlier, the thermal model is driven by observed near-surface ground temperature. Soil and ice thermal diffusivities are functions of temperature at corresponding depths, and they are updated at every iteration. Figure 3.3 summarizes the modeled ground temperature profile over the 12 year period. The upper graph shows the modeled results from 0−1 m. At the

ground surface, seasonal temperature variations are prominent, and propagate into the permafrost. The maximum depth to which the soil temperatures rise above zero (the active layer) during the austral summer is ~0.15 m (Figure 3.3). The diurnal skin depth is approximately 0.12 m. The buried ice is relatively insensitive to short-lived temperature extremes due to the insulating effect of the overlying dry soil layer and essentially integrates the long-term mean soil surface temperature.

In addition to the prominent seasonal temperature variations, on multiple occasions during the winter the surface suddenly warms several tens of degrees Celsius due to the increased air temperature from foehn winds [*Nylen et al.*, 2004; *Speirs et al.*, 2010]. These warming events can affect the temperature to several meters, as reflected in the model results. The lower graph in Figure 3.3 shows the modeled thermal profile from 0−30 m. As indicated by that white dashed line, seasonal temperature fluctuations attenuate to less than 0.5 ℃ at 21 m, which is consistent with other studies elsewhere in the MDV [*Campbell*, 1997; *Guglielmin et al.*, 2011; *Putkonen et al.*, 2003] .

The soil temperature gradient is the principle variable in studies of vapor transport and ground ice sublimation [*Hagedorn et al.*, 2007; *Liu et al.*, 2015]. The soil temperature decreases with depth during the austral summer; when solar radiation is weak or absent during austral winter, the soil is colder at the surface and the temperature gradient reverses (Figure 3.3). However, katabatic during the winter can warm the soil considerably to a depth of 1.5 m and temporarily invert the temperature profile. These large soil temperature fluctuations in the winter are consistent with studies in Victoria Valley [*Hagedorn et al.*, 2007].

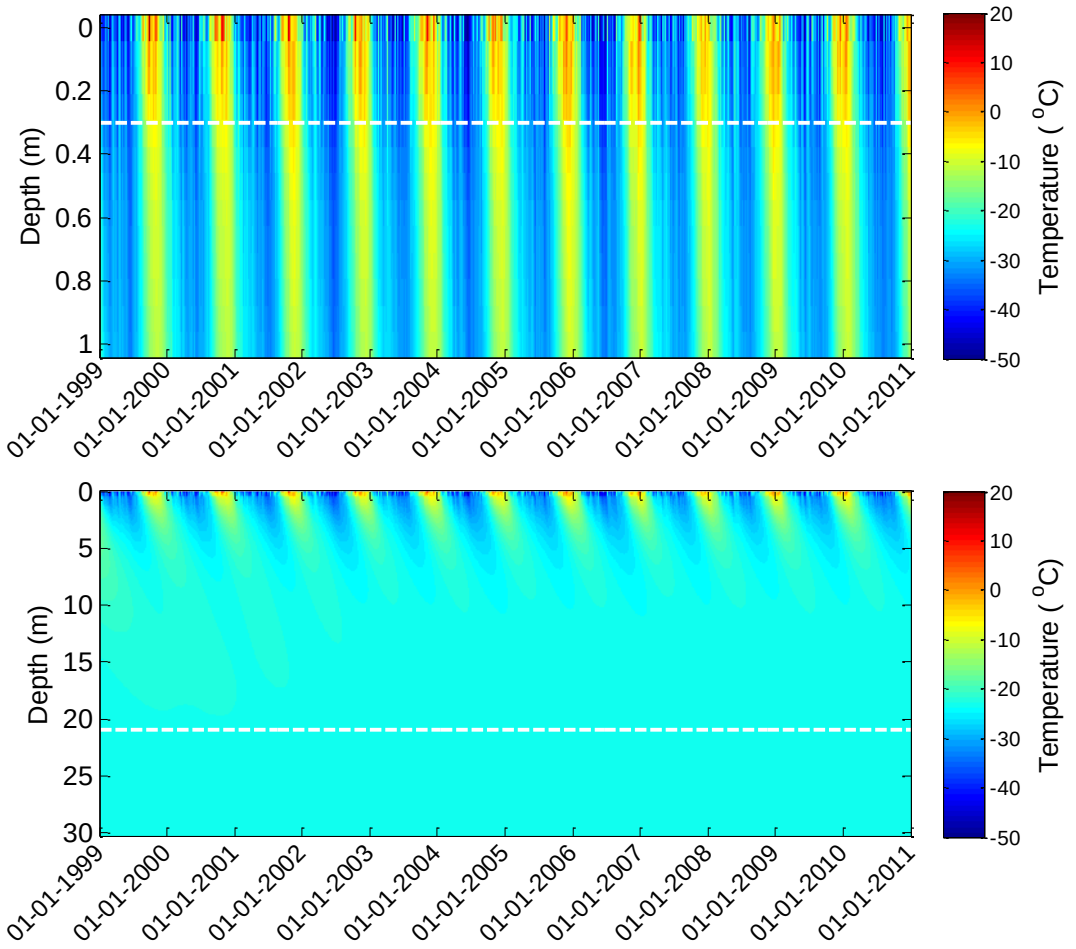

Figure 3.3. Modeled temperature profile over the 12 year period at study site. Upper graph: 0−1 m. The white dashed line represents the soil-ice boundary at 0.3 m. Lower graph: 0−30 m. The white dashed lines represent the 21 m depth where temperature variations are less than 0.5°C.

3.5.3. Model Validation against Measured Temperatures

The modeled temperatures are compared for both the FDM and the FVM to the field measurements made at four depths (Figure 3.4, see Appendix 3.B for complete comparison). In general, the modeled temperatures agree well with field measurements. The differences between measured and modeled temperatures are shown on the right side of the panel on each figure (Figure 3.4, Figure 3.B.1−3.B.3). Using the FDM, there is a systematic offset with modeled temperature being higher in the summer and lower in the winter compared to measured temperature (Figure

3.4 and Figure 3.B.1). The average differences at various depths vary from −0.5 ℃ to 0.5 ℃ with actual differences reaching ±4.0 ℃. This results from the abrupt change in temperature gradient across the soil-ice boundary caused by significant difference of thermal diffusivity between soil and ice; the FDM does not represent the heat flux accurately across this boundary considering the grid spacing used in this study [*Patankar*, 1980].

In contrast, modeled temperatures using FVM are close to measured temperatures. The FVM model was run using both temperature-independent and temperature-dependent thermal parameters, and they both yield realistic temperatures based on the in situ measurements (Figure 3.4 and Figure 3.B.2−3.B.3). Using the temperature-dependent parameters, the average differences between the FVM modeled temperatures and those measured at various depths range from 0.01 ℃ to 0.03 ℃; individual differences at any particular time range from −0.6 ℃ to 0.6 ℃ (Figure 3.4 and Figure 3.B.2−3.B.3). The temperature-dependent thermal properties not only help reduce the model′s error by ~40%, but also provide more realistic estimates when modeling the subsurface thermal regime.

The FVM modeled temperatures were also compared to measured borehole temperatures in Beacon Valley at a range of depths (Figure 3.B.4), and there is a remarkably close agreement between the modeled and measured temperatures. For example, modeled and measured temperatures agree well at 0.3 m, the depth of soil-ice boundary; respectively, they average −23.2 ℃ and −23.1 ℃ over the 12 year length of the record, and reach a maxima of −3.0 ℃ and −2.9 ℃ in December and a minima of −41.3 ℃ and −41.2 ℃ in August. The fraction of variation in the dependent variable accounted for by the model (coefficient of determination r^2) ranges from 0.9992 to 0.9996 at different depths, and the root mean squared error (RMSE) ranges from 0.2 ℃ to 0.3 ℃ (Table 3.2). Overall, the FVM is a more appropriate and accurate approach when

modeling subsurface temperature in systems with abrupt changes in thermal properties. Notably, these include soils in the MDV and the Martian subsurface where massive ground ice underlies a layer of dry soil.

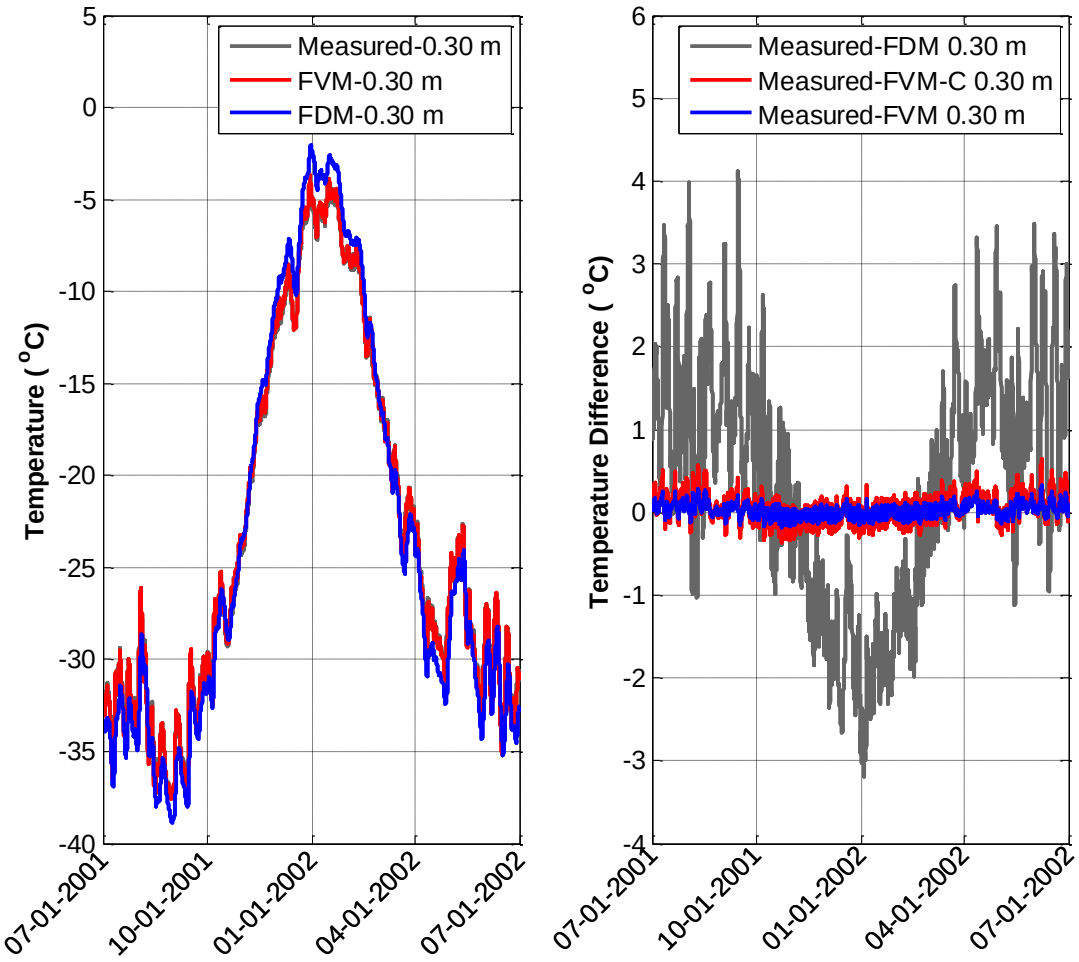

Figure 3.4. Measured temperatures and modeled temperature using the FDM and the FVM and the differences between them at 0.30 m in Beacon Valley during the period of 07/01/2001 to 07/01/2002 (see Appendix 3.B for more complete comparisons). On the right plot, the red line shows the temperature difference using temperature-independent thermal parameters in the FVM.

There still is, however, a small temporal variation in the differences between measured and the FVM modeled temperatures (Figure 3.4 and Figure 3.B.2−3.B.3). At a depth of 21 m, seasonal temperature variations are significantly attenuated and the temperature averages −23.0 ℃. This

slight difference from the mean annual near surface temperature (−23.6 ℃) may be due to geothermal gradient and is consistent with the gradients measured for this region; they range from 30 to 33 ℃/km [*Decker*, 1974]. At shallow depths where temperature variations are significant, thermal diffusivity values used in the model directly affect the calculated temperature. Therefore, inaccurate values of local thermal diffusivity could degrade the accuracy the model, and may account for the small residual differences between the measured and modeled temperatures.

3.6. Discussion

The sensitivity of the model has been analyzed with regard to the thermal conductivity *k* and to the latent-heat effects of the episodic snowmelt and of the ice sublimation and/or condensation. The following discussion is based on our FVM model constrained by the temperature-dependent thermal parameters.

3.6.1. Sensitivity of the Model to Thermal Conductivity

The sensitivity of the model to thermal conductivity is tested for the 12 year period that was used to assess the fit of the modeled temperature to actual temperature measurements. This study explores the effect of changing the thermal conductivity of the upper dry soil layer and of the lower ground ice layer by ±20%, both separately and together. Table 3.2 lists the results of the sensitivity tests at depths of 0.20 m, 0.30 m, 0.45 m, and 0.60 m for the various scenarios, where RMSE and r^2 are all calculated relative to measured temperature at corresponding depths. The results show that increasing the thermal conductivity of either the dry soil layer, the ice layer, or both increases RMSE and reduces r^2 values substantially at all depths. Decreasing the thermal conductivity by 20% also results in an even worse fit between modeled and measured temperatures, and higher RMSE values, than increasing thermal conductivity.

As can be seen in Table 3.2, the model is more sensitive to the thermal conductivity of the dry soil layer than that of the ice at all depths. The model's sensitivity to the change in the thermal conductivity of both dry soil layer and ground ice layer is intermediate. The high relative sensitivity to k_s of the dry soil layer is expected because the 1-D thermal model is driven by the near-surface ground temperature, and temperature variations attenuate quickly with depth, hence the thermal properties of the near-surface material have the greatest impact on the calculated variations in ground temperatures.

Table 3.2. Results of the model's sensitivity analysis of thermal conductivity at various depths.

		K_{soil}&K_{ice}		K_{soil} + 20%		K_{ice} + 20%		K_{soil}&K_{ice} + 20%	
Increased α	Depth (m)	RMSE (℃)	R^2	RMSE (℃)	R^2	RMSE (℃)	R^2	RMSE (℃)	R^2
	0.20	0.3	0.9992	0.3	0.9993	0.3	0.9992	0.2	0.9995
	0.30	0.2	0.9996	0.5	0.9975	0.2	0.9996	0.3	0.9988
	0.45	0.2	0.9996	0.4	0.9980	0.4	0.9982	0.2	0.9995
	0.60	0.2	0.9996	0.3	0.9984	0.5	0.9968	0.2	0.9996
		K_{soil}&K_{ice}		K_{soil} − 20%		K_{ice} − 20%		K_{soil}&K_{ice} − 20%	
Decreased α	Depth (m)	RMSE (℃)	R^2	RMSE (℃)	R^2	RMSE (℃)	R^2	RMSE (℃)	R^2
	0.20	0.3	0.9992	0.5	0.9993	0.3	0.9991	0.4	0.9983
	0.30	0.2	0.9996	0.5	0.9975	0.3	0.9988	0.3	0.9991
	0.45	0.2	0.9996	0.8	0.9923	0.2	0.9994	0.5	0.9969
	0.60	0.2	0.9996	0.9	0.9884	0.2	0.9996	0.6	0.9945

3.6.2. Latent Heat Effect of Episodic Snowmelt

Conductive heat transport governs the ground thermal regime; temperature variations attenuate and lag with depth. Based on our model results that are generated assuming latent heat effects are negligible, the temperatures showed no signs of phase change of soil ice or water, in contrast with most arctic or alpine soils in which latent heat plays an important role [*Hinkel and Outcalt*, 1994; *Putkonen*, 1998; *Romanovsky and Osterkamp*, 2000; *Roth and Boike*, 2001]; however, as can be seen in Figure 3.4 and Figure 3.B.3, there is still a slight mismatch between

the measured and modeled temperatures, which might be caused by non-conductive heat transport due to episodic snowmelt events in the MDV. As shown in *Liu et al.*[2015], snowmelt infiltration events, indicated by electric conductivity (EC) measurements in the soil at 0.05 m depth (Figure 3.5a), consistently occurred between 1999 and 2011 based on our field measurements in Beacon Valley.

Because the amount of snowmelt that infiltrated and the infiltration depth were not known, the hourly temperature change at each depth was calculated to study the potential impact of vertical water advection or latent heat release. This approach is possible given the high data collection frequency. For one of the biggest snowmelt events during the measurement period, at the beginning of January 2006, the measured hourly temperature change is shown in Figure 3.5. Note the decrease in hourly temperature change with depth, as expected in a system dominated by heat conduction. There are no obvious deviations in the hourly changes in temperature at depths during the corresponding time period, beginning of January 2006; therefore, the latent heat effect of the snowmelt event recorded during the period of observation appears negligible at the study site.

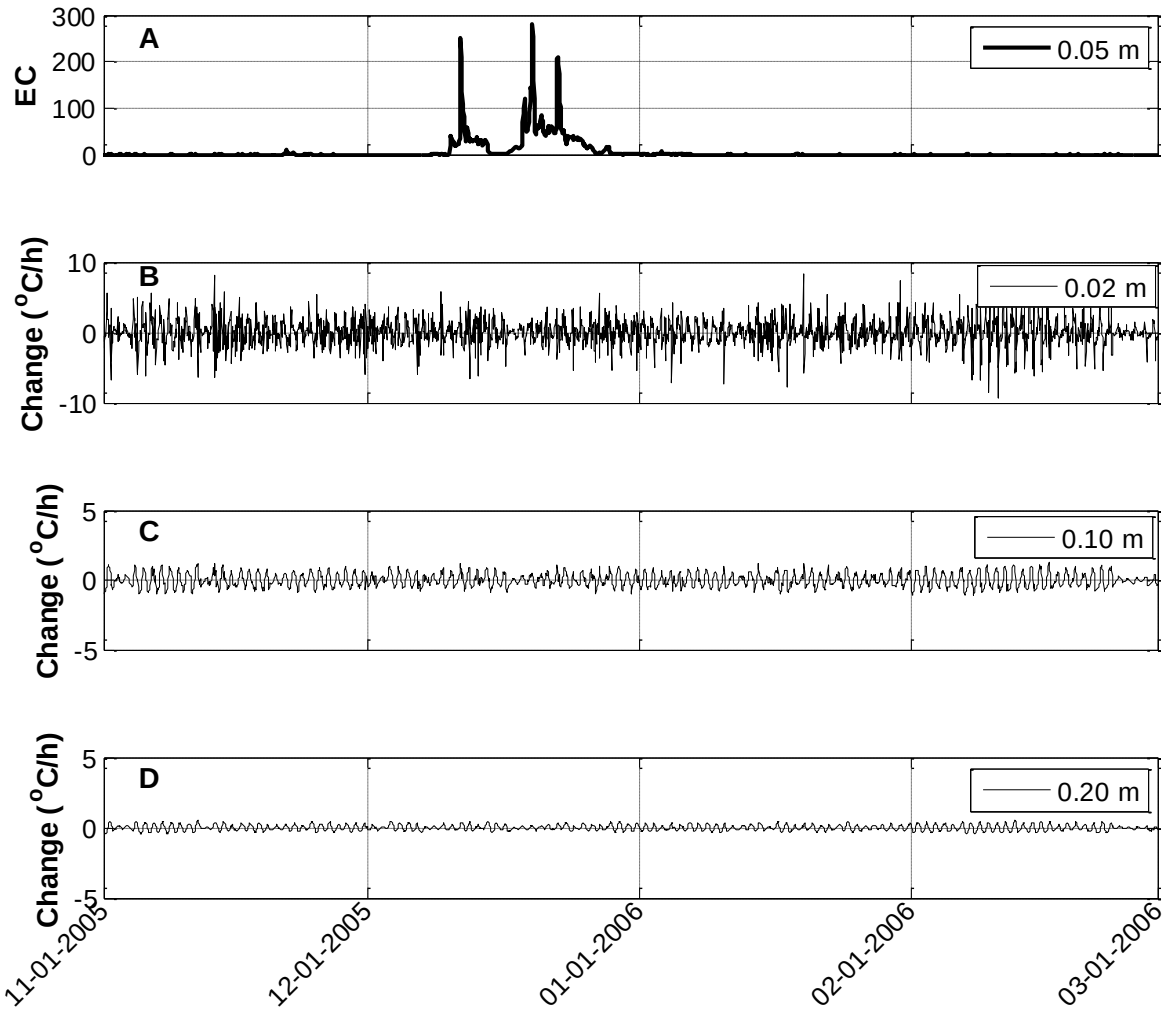

Figure 3.5. (a) Hourly EC measurements at 0.05 m as an indication for episodic snowmelt events for the period of 11/01/2005–03/01/2006; (b), (c), and (d) Measured hourly temperature change in the dry soil for the period of 11/01/2005–03/01/2006 at depths of 0.02 m, 0.10 m, and 0.20 m, respectively.

3.6.3. Latent Heat Effect of Ice Sublimation/Condensation

Another physical process that could potentially account for the difference between the modeled and measured temperature is the latent heat effect of ice condensation/sublimation. When ice condenses, it releases heat and when it sublimates, it consumes heat. These processes can be represented as a source/sink term in the heat diffusion equation (equation (3.4)) modified from *Putkonen* [1998]:

$$\rho_m C(T)_m \frac{\partial T}{\partial t} = \frac{\partial}{\partial z}\left(k_m(T)\frac{\partial T}{\partial z}\right) + \frac{L_V \rho_i}{V_u}\frac{\partial V}{\partial t} \quad (3.5)$$

where L_v is the latent heat of vaporization of ice (J kg^{-1}), ρ_i is density of ice (kg m^{-3}), V_u is unit volume (1 m^3), V is volume of ice (m^3). The amount of ice change in the dry soil layer, as well as the ice boundary, is estimated based on vapor diffusion model results at the study site [*Liu et al*., 2015].

In general, the rate of ice loss or gain is on the order of 10^{-8} m^3 h^{-1}. This gives the third term in equation (3.5) ($\frac{L_V \rho_i}{V_u}\frac{\partial V}{\partial t}$) on the order of 10^{-2} J m^{-3} h^{-1}, which is several orders of magnitude smaller than the first and second term ($10^6 - 10^7$ J m^{-3} h^{-1}). The latent heat effect can be examined in greater detail by incorporating it (the third term in equation (3.5)) into the heat diffusion model; the results are shown in Figure 3.6. This latent heat does affect the modeled temperature results, but only slightly, at most 10^{-3} °C. The intrinsic latent heat of vaporization of ice is a large term; however, the actual latent heat produced/consumed by ice condensation/sublimation is very small due to the small amount of ice forming or sublimating.

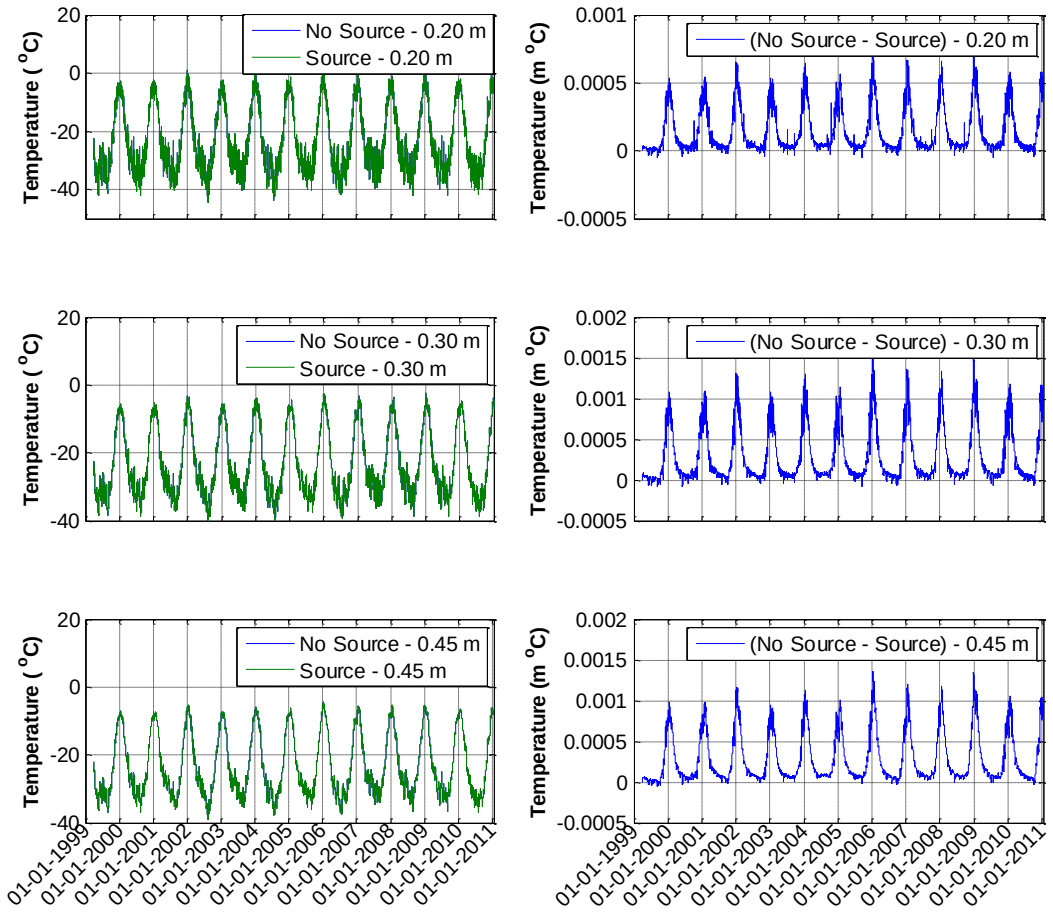

Figure 3.6. Comparison of modeled temperature results with and without source term from ice condensation/sublimation at 0.20 m, 0.30 m, and 0.45 m, respectively.

3.6.4. Polygon Trough Effects

To date, analyses of the thermal regime in the MDV utilize 1-D models of heat conduction suitable for infinite half-spaces or planar layers of laterally homogeneous medium (i.e. only vertical conductive heat transfer). The effects of significant local relief would complicate or obscure the regional subsurface thermal regime [*Lachenbruch et al.*, 1962]. Because the nearest polygon trough is ~5 m from the borehole with thermistors, lateral heat flow to and from polygon troughs is likely to contribute negligibly to the temperature at shallow depths (< 1 m). However,

at greater depth, the cold polygon troughs and lateral heat flow may have some influence, and a two- or three-dimensional model may provide a more exact solution. This could explain some of the offsets among the borehole temperature comparisons (Figure 3.B.4).

3.7. Summary and Conclusions

This study characterized the soil thermal properties and developed numerical models of the ground thermal regime in Beacon Valley in the MDV of Antarctica using a 1-D heat diffusion equation. Both heat capacity and thermal conductivity have a positive temperature dependence. For the temperature range of −47.9 to 7.5°C at our study site, the heat capacity of the dry soil ranges from 589 to 687 J kg^{-1} K^{-1} and thermal conductivity ranges from 0.29 to 0.33 W m^{-1} K^{-1}; thermal diffusivity ranges from 0.30 to 0.32 mm^2 s^{-1} with a negative temperature dependence. For the massive ground ice, heat capacity ranges from 1800 to 2060 J kg^{-1} K^{-1}, thermal conductivity from 2.20 to 2.63 W m^{-1} K^{-1}, and thermal diffusivity from 1.17 to 1.58 mm^2 s^{-1}.

According to the thermal model, soil temperature at depth is driven primarily by the surface temperature measurements. Both the FDM and the FVM were employed to numerically evaluate the temperature profile and its evolution; the modeled temperatures agree well with *in situ* temperature measurements for both methods. Nevertheless, the FVM results more closely match measured temperature with average differences ranging from 0.01 ℃ to 0.03 ℃ at various depths. Seasonal as well as shorter-term fluctuations are reflected well in the model results; these include foehn winds that warm up the surface temperature by several tens of degrees during the winter. A realistic thermal model is essential for modeling vapor diffusion to investigate the stability of ground ice in the absence of in situ temperature measurements. In addition to more accurately modeling the subsurface temperature, using temperature-dependent thermal parameters for the dry soil and the massive ground ice provides more realistic constraints. The model is sensitive to

changes in the thermal conductivity of either the dry soil layer or ground ice layer, or both. Latent heat from episodic snowmelt and ice sublimation/condensation could alter the temperature up to 10^{-3} ℃, which is insufficient to impact the temperature observations.

Overall, the FVM handles this system better than the FDM by conserving heat flux using the geometric mean of thermal conductivities at the control volume interfaces, and this is critical when dealing with multi-layer systems with abrupt change in thermal diffusivity. This approach can be widely applied to the cold, dry environments, including other regions in Antarctica, high mountain ranges in the central Asian and South America, and on Mars.

Acknowledgements. This material is based upon work supported by the National Science Foundation under grants 0541054, 0636998, and 1341680 and NASA Mars Science Laboratory awarded via Malin Space Science Systems. Funding was also provided by Kenneth C. Robbins Graduate Fellowship, Joseph A. Endowed Vance Fellowship and the Dr. Howard A. Coombs Scholarship. Data supporting this study are available at http://gcmd.nasa.gov/r/d/[GCMD]UW_Dry_Valley_Datalogging or upon request from the corresponding author (liul99@uw.edu). The authors like to thank Jonathan Toner for his help with the DSC measurements. We are also grateful to Antarctic Support Services, PHI, and our colleagues in Christchurch for superb logistical support in the Dry Valleys.

3.8. References

Alnefaie, K. A., and N. H. Abu-Hamdeh (2013), Specific Heat and Volumetric Heat Capacity of Some Saudian Soils as affected by Moisture and Density, paper presented at International Conference on Mechanics, Fluids, Heat, Elasticity and Electromagnetic Fields.

Bockheim, J. G., I. B. Campbell, and M. McLeod (2007), Permafrost distribution and active-layer depths in the McMurdo dry valleys, Antarctica, *Permafrost and Periglacial Processes*, *18*(3), 217-227, doi:10.1002/Ppp.588.

Bockheim, J. G., and K. J. Hall (2002), Permafrost, active-layer dynamics and periglacial environments of continental Antarctica, *South African Journal of Science*, *98*(1-2), 82-90.

Boike, J., K. Roth, and P. P. Overduin (1998), Thermal and hydrologic dynamics of the active layer at a continuous permafrost site (Taymyr Peninsula, Siberia), *Water Resources Research*, *34*(3), 355-363.

Botte, G. G., J. A. Ritter, and R. E. White (2000), Comparison of finite difference and control volume methods for solving differential equations, *Comput Chem Eng*, *24*(12), 2633-2654, doi:10.1016/S0098-1354(00)00619-0.

Bromwich, D. H. (1988), Snowfall in High Southern Latitudes, *Reviews of Geophysics*, *26*(1), 149-168, doi:10.1029/Rg026i001p00149.

Bromwich, D. H., A. J. Monaghan, K. W. Manning, and J. G. Powers (2005), Real-time forecasting for the Antarctic: An evaluation of the Antarctic Mesoscale Prediction System (AMPS), *Mon Weather Rev*, *133*(3), 579-603, doi:10.1175/Mwr-2881.1.

Brown, J., O. Ferrians Jr, J. Heginbottom, and E. Melnikov (2002), Circum-Arctic Map of Permafrost and Ground-Ice Conditions, Version 2, *National Snow and Ice Data Center, Boulder, Colorado USA.*

Campbell, D. I., Macculloch, R.J.L. & Campbell, I.B. (1997), Thermal regimes of some soils in the McMurdo Sound region, Antarctica., *In LYONS, W.B., HOWARD-WILLIAMS,C.&HAWES, I., eds. Ecosystem processes in Antarctic ice-free landscapes., Rotterdam: Balkema*, 45-55.

Chinn, T. (1980), Glacier balances in the dry valleys area, Victoria Land, Antarctica, 237-247.

Clifford, S. M. (1993), A model for the hydrologic and climatic behavior of water on Mars, *Journal of Geophysical Research: Planets (1991–2012)*, *98*(E6), 10973-11016.

Clow, G. D., C. P. McKay, G. M. Simmons, and R. A. Wharton (1988), Climatological Observations and Predicted Sublimation Rates at Lake Hoare, Antarctica, *Journal of Climate*, *1*(7), 715-728, doi:10.1175/1520-0442(1988)001<0715:Coapsr>2.0.Co;2.

Decker, E. (1974), Preliminary geothermal studies of the Dry Valley Drilling Project holes at McMurdo Station, Lake Vanda, Lake Vida, and New Harbour, Antarctica, *Dry Valley Drilling Project Bulletin*, *4*, 22-23.

Della Gatta, G., M. J. Richardson, S. M. Sarge, and S. Stolen (2006), Standards, calibration, and guidelines in microcalorimetry - Part 2. Calibration standards for differential scanning calorimetry - (IUPAC Technical Report), *Pure Appl Chem*, *78*(7), 1455-1476, doi:DOI 10.1351/pac200678071455.

Farouki, O. T. (1981a), The Thermal-Properties of Soils in Cold Regions, *Cold Regions Science and Technology*, *5*(1), 67-75, doi:10.1016/0165-232x(81)90041-0.

Farouki, O. T. (1981b), Thermal properties of soils, DTIC Document, U.S. Army Cold Regions Research and Engineering Laboratory, pp.

Fountain, A. G., G. L. Dana, K. J. Lewis, B. H. Vaughn, and D. H. McKnight (1998), *Glaciers of the McMurdo Dry Valleys, southern Victoria Land, Antarctica*, American Geophysical Union.

Fountain, A. G., T. H. Nylen, A. Monaghan, H. J. Basagic, and D. Bromwich (2009), Snow in the McMurdo Dry Valleys, Antarctica, *International Journal of Climatology*, *30*(5), 633-642, doi:10.1002/Joc.1933.

Fountain, A. G., T. H. Nylen, A. Monaghan, H. J. Basagic, and D. Bromwich (2010), Snow in the McMurdo Dry Valleys, Antarctica, *International Journal of Climatology*, *30*(5), 633-642, doi:Doi 10.1002/Joc.1933.

Gold, L. W., and A. H. Lachenbruch (1973), *Thermal conditions in permafrost: a review of North American literature*.

Gooseff, M. N., J. E. Barrett, P. T. Doran, A. G. Fountain, W. B. Lyons, A. N. Parsons, D. L. Porazinska, R. A. Virginia, and D. H. Wall (2003), Snow-patch influence on soil biogeochemical processes and invertebrate distribution in the McMurdo Dry Valleys, Antarctica, *Arctic Antarctic and Alpine Research*, *35*(1), 91-99.

Guglielmin, M. (2006), Ground surface temperature (GST), active layer and permafrost monitoring in continental Antarctica, *Permafrost and Periglacial Processes*, *17*(2), 133-143, doi:10.1002/Ppp.553.

Guglielmin, M., M. Balks, and R. Paetzold (2003), Towards an Antarctic active layer and permafrost monitoring network, paper presented at Proceedings of the Eighth International Conference on Permafrost.

Guglielmin, M., M. R. Balks, L. S. Adlam, and F. Baio (2011), Permafrost Thermal Regime from Two 30-m Deep Boreholes in Southern Victoria Land, Antarctica, *Permafrost and Periglacial Processes*, *22*(2), 129-139, doi:10.1002/Ppp.715.

Hagedorn, B., R. S. Sletten, and B. Hallet (2007), Sublimation and ice condensation in hyperarid soils: Modeling results using field data from Victoria Valley, Antarctica, *Journal of Geophysical Research-Earth Surface*, *112*(F3), F03017, doi:10.1029/2006jf000580.

Heldmann, J. L., W. Pollard, C. P. McKay, M. M. Marinova, A. Davila, K. E. Williams, D. Lacelle, and D. T. Andersen (2013), The high elevation Dry Valleys in Antarctica as analog sites for subsurface ice on Mars, *Planet Space Sci*, *85*, 53-58, doi:10.1016/j.pss.2013.05.019.

Hindmarsh, R. C. A., F. M. Van der Wateren, and A. L. L. M. Verbers (1998), Sublimation of ice through sediment in Beacon Valley, Antarctica, *Geografiska Annaler Series a-Physical Geography*, *80A*(3-4), 209-219.

Hinkel, K. M., and S. I. Outcalt (1994), Identification of heat-transfer processes during soil cooling, freezing, and thaw in central alaska, *Permafrost and Periglacial Processes*, *5*(4), 217-235.

Höhne, G., W. Hemminger, and H.-J. Flammersheim (2003), *Differential scanning calorimetry*, Springer Science & Business Media.

Hunt, H. W., A. G. Fountain, P. T. Doran, and H. Basagic (2010), A dynamic physical model for soil temperature and water in Taylor Valley, Antarctica, *Antarctic Science*, *22*(4), 419-434, doi:10.1017/S0954102010000234.

Ikard, S. J., M. N. Gooseff, J. E. Barrett, and C. Takacs-Vesbach (2009), Thermal Characterisation of Active Layer Across a Soil Moisture Gradient in the McMurdo Dry Valleys, Antarctica, *Permafrost and Periglacial Processes*, *20*(1), 27-39, doi:10.1002/Ppp.634.

Johansen, O. (1975), Thermal conductivity of soils, Ph.D. thesis, University of Trondheim, Norway, ADA044002.

Kane, D. L., L. D. Hinzman, and J. P. Zarling (1991), Thermal Response of the Active Layer to Climatic Warming in a Permafrost Environment, *Cold Regions Science and Technology*, *19*(2), 111-122.

Kowalewski, D. E., D. R. Marchant, J. W. Head, and D. W. Jackson (2012), A 2D model for characterising first-order variability in sublimation of buried glacier ice, Antarctica: Assessing the influence of polygon troughs, desert pavements and shallow subsurface salts, *Permafrost and Periglacial Processes*, *23*(1), 1-14, doi:10.1002/Ppp.731.

Kowalewski, D. E., D. R. Marchant, J. S. Levy, and J. W. Head (2006), Quantifying low rates of summertime sublimation for buried glacier ice in Beacon Valley, Antarctica, *Antarctic Science*, *18*(3), 421-428, doi:10.1017/S0954102006000460.

Lachenbruch, A. H., M. C. Brewer, G. W. Greene, and B. Vaughn Marshall (1962), Temperatures in permafrost, paper presented at Temperature; Its Measurement and Control in Science and Industry, Volume 1.

Lide, D. R. (2008-2009), *Handbook of Chemistry and Physics*, 89th ed., CRC.

Liu, L., R. S. Sletten, B. Hagedorn, B. Hallet, C. P. McKay, and J. O. Stone (2015), An enhanced model of the contemporary and long-term (200 ka) sublimation of the massive subsurface ice in Beacon Valley, Antarctica, *Journal of Geophysical Research: Earth Surface*, 120, doi:10.1002/2014JF003415.

Marchant, D. R., A. R. Lewis, W. M. Phillips, E. J. Moore, R. A. Souchez, G. H. Denton, D. E. Sugden, N. Potter, and G. P. Landis (2002), Formation of patterned ground and sublimation

till over Miocene glacier ice in Beacon Valley, southern Victoria Land, Antarctica, *Geological Society of America Bulletin*, *114*(6), 718-730.

Martínez, G., N. Renno, E. Fischer, C. Borlina, B. Hallet, M. Torre Juárez, A. Vasavada, M. Ramos, V. Hamilton, and J. Gomez-Elvira (2014), Surface energy budget and thermal inertia at Gale Crater: Calculations from ground-based measurements, *Journal of Geophysical Research: Planets*, *119*(8), 1822-1838.

McKay, C. P. (2009), Snow recurrence sets the depth of dry permafrost at high elevations in the McMurdo Dry Valleys of Antarctica, *Antarctic Science*, *21*(1), 89-94, doi:10.1017/S0954102008001508.

McKay, C. P., M. T. Mellon, and E. I. Friedmann (1998), Soil temperatures and stability of ice-cemented ground in the McMurdo Dry Valleys, Antarctica, *Antarctic Science*, *10*(1), 31-38.

Mellon, M. T., et al. (2009), Ground ice at the Phoenix Landing Site: Stability state and origin, *Journal of Geophysical Research*, *114*, E00E07, doi:10.1029/2009je003417.

Mellon, M. T., and B. M. Jakosky (1993), Geographic Variations in the Thermal and Diffusive Stability of Ground Ice on Mars, *Journal of Geophysical Research-Planets*, *98*(E2), 3345-3364.

Ng, F., B. Hallet, R. S. Sletten, and J. O. Stone (2005), Fast-growing till over ancient ice in Beacon Valley, Antarctica, *Geology*, *33*(2), 121-124, doi:10.1130/G21064.1.

Nylen, T. H., A. G. Fountain, and P. T. Doran (2004), Climatology of katabatic winds in the McMurdo Dry Valleys, southern Victoria Land, Antarctica, *Journal of Geophysical Research-Atmospheres*, *109*(D3), D03114, doi:10.1029/2003jd003937.

Osterkamp, T. E. (2003), Establishing long-term permafrost observatories for active-layer and permafrost investigations in Alaska: 1977-2002, *Permafrost and Periglacial Processes, 14*(4), 331-342, doi:DOI 10.1002/ppp.464.

Paige, D. A. (1992), The thermal stability of near-surface ground ice on Mars, *Nature, 356*(6364), 43-45.

Patankar, S. V. (1980), *Numerical Heat Transfer and Fluid Flow*, New York: Hemisphere Publishing.

Piqueux, S., and P. R. Christensen (2009), A model of thermal conductivity for planetary soils: 1. Theory for unconsolidated soils, *Journal of Geophysical Research-Planets, 114*, E09005, doi:10.1029/2008je003308.

Price, D. M. (1995), Temperature calibration of differential scanning calorimeters, *J Therm Anal, 45*(6), 1285-1296, doi:Doi 10.1007/Bf02547423.

Priscu, J. C. (1998), *Ecosystem dynamics in a polar desert: the McMurdo Dry Valleys, Antarctica*, American Geophysical Union.

Putkonen, J. (1998), Soil thermal properties and heat transfer processes near Ny-Alesund, northwestern Spitsbergen, Svalbard, *Polar research, 17*(2), 165-179.

Putkonen, J., R. Sletten, and B. Hallet (2003), Atmosphere/ice energy exchange through thin debris cover in Beacon Valley, Antarctica, paper presented at Eighth international conference on Permafrost, Zurich, Switzerland.

Robinson, G. R., and J. L. Haas (1983), Heat Capacity, Relative Enthalpy, and Calorimetric Entropy of Silicate Minerals - an Empirical-Method of Prediction, *Am Mineral, 68*(5-6), 541-553.

Romanovsky, V. E., and T. E. Osterkamp (1995), Interannual variations of the thermal regime of the active layer and near-surface permafrost in northern Alaska, *Permafrost and Periglacial Processes*, *6*(4), 313-335, doi:10.1002/ppp.3430060404.

Romanovsky, V. E., and T. E. Osterkamp (1997), Thawing of the active layer on the coastal plain of the Alaskan Arctic, *Permafrost and Periglacial Processes*, *8*(1), 1-22.

Romanovsky, V. E., and T. E. Osterkamp (2000), Effects of unfrozen water on heat and mass transport processes in the active layer and permafrost, *Permafrost and Periglacial Processes*, *11*(3), 219-239, doi:10.1002/1099-1530(200007/09)11:3<219::Aid-Ppp352>3.0.Co;2-7.

Rossbacher, L. A., and S. Judson (1981), Ground ice on Mars: Inventory, distribution, and resulting landforms, *Icarus*, *45*(1), 39-59.

Roth, K., and J. Boike (2001), Quantifying the thermal dynamics of a permafrost site near Ny-Alesund, Svalbard, *Water Resources Research*, *37*(12), 2901-2914.

Schäfer, J. M., H. Baur, G. H. Denton, S. Ivy-Ochs, D. R. Marchant, C. Schluchter, and R. Wieler (2000), The oldest ice on Earth in Beacon Valley, Antarctica: New evidence from surface exposure dating, *Earth and Planetary Science Letters*, *179*(1), 91-99.

Schörghofer, N. (2005), A physical mechanism for long-term survival of ground ice in Beacon Valley, Antarctica, *Geophysical Research Letters*, *32*(19), L19503, doi:10.1029/2005gl023881.

Schörghofer, N., and O. Aharonson (2005), Stability and exchange of subsurface ice on Mars, *Journal of Geophysical Research-Planets*, *110*, E05003, doi:10.1029/2004je002350.

Sizemore, H. G., and M. T. Mellon (2006), Effects of soil heterogeneity on Martian ground-ice stability and orbital estimates of ice table depth, *Icarus*, *185*(2), 358-369.

Sletten, R. S., B. Hallet, and R. C. Fletcher (2003), Resurfacing time of terrestrial surfaces by the formation and maturation of polygonal patterned ground, *Journal of Geophysical Research-Planets*, *108*(E4), 8044, doi:10.1029/2002je001914.

Speirs, J. C., D. F. Steinhoff, H. A. McGowan, D. H. Bromwich, and A. J. Monaghan (2010), Foehn winds in the McMurdo Dry Valleys, Antarctica: The origin of extreme warming events, *Journal of Climate*, *23*(13), 3577-3598, doi:10.1175/2010jcli3382.1.

Sugden, D. E., D. R. Marchant, N. Potter, R. A. Souchez, G. H. Denton, C. C. Swisher, and J. L. Tison (1995), Preservation of Miocene glacier ice in East Antarctica, *Nature*, *376*(6539), 412-414.

Swanger, K. M., and D. R. Marchant (2007), Sensitivity of ice-cemented Antarctic soils to greenhouse-induced thawing: Are terrestrial archives at risk?, *Earth and Planetary Science Letters*, *259*(3), 347-359.

Thomas, L. (2003), Making accurate DSC and MDSC® specific heat capacity measurements with the Q1000 Tzero™ DSC, *TA Bulletin TA310. TA Instruments, New Castle.* *http://www.tainstruments.com/main.aspx*.

Vanderwateren, D., and R. Hindmarsh (1995), East Antarctic Ice-Sheet - Stabilists strike again, *Nature*, *376*(6539), 389-391.

West, A. C., and T. F. Fuller (1996), Influence of rib spacing in proton-exchange membrane electrode assemblies, *J Appl Electrochem*, *26*(6), 557-565, doi:Doi 10.1007/Bf00253453.

Winter, D. F., and J. M. Saari (1969), A Particulate Thermophysical Model of Lunar Soil, *Astrophysical Journal*, *156*(3p1), 1135-1151, doi:Doi 10.1086/150041.

Wood, S. (2011), A General Analytic Model for the Thermal Conductivity of Loose, Indurated or Icy Planetary Regolith, paper presented at Lunar and Planetary Science Conference.

Appendix 3.A. The Finite Difference Method (FDM) and the Finite Volume Method (FVM)

Figure 3.A.1 shows the grid points to be used in the FDM modeling [*Patankar*, 1980].

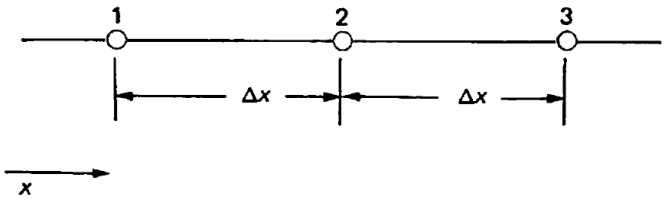

Figure 3.A.1. Grid points used for a one-dimensional Taylor Series expansion.

For grid point 2, located midway between grid points 1 and 3, the Taylor Series expansion gives:

$$\phi_1 = \phi_2 - \Delta x \left(\frac{d\phi}{dx}\right)_2 + \frac{1}{2}(\Delta x)^2 \left(\frac{d^2\phi}{dx^2}\right)_2 - \cdots \tag{3.A.1}$$

$$\phi_3 = \phi_2 + \Delta x \left(\frac{d\phi}{dx}\right)_2 + \frac{1}{2}(\Delta x)^2 \left(\frac{d^2\phi}{dx^2}\right)_2 - \cdots \tag{3.A.2}$$

Adding and subtracting the two equations yield the substitution into the differential equation for the FDM:

$$\left(\frac{d\phi}{dx}\right)_2 = \frac{\phi_3 - \phi_1}{2\Delta x} \tag{3.A.3}$$

$$\left(\frac{d^2\phi}{dx^2}\right)_2 = \frac{\phi_1 - 2\phi_2 + \phi_3}{(\Delta x)^2} \tag{3.A.4}$$

Figure 3.A.2 shows the control volume to be used in the FVM modeling [*Patankar*, 1980]. The grid points are labeled as W, P, and E, and the control volume interfaces are w and e.

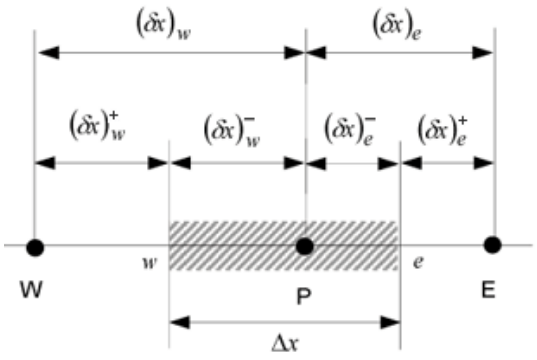

Figure 3.A.2. Control volume for a 1-D situation.

The discretization equation of Equation (3.6) for a fully implicit FVM is:

$$a_P T_P = a_W T_w + a_E T_E + b \tag{3.A.5}$$

where

$$a_E = \frac{k_e}{\delta x_e}, \tag{3.A.6}$$

$$a_W = \frac{k_w}{\delta x_W}, \tag{3.A.7}$$

$$a_P^0 = \Delta x/\Delta t, \tag{3.A.8}$$

$$b = a_P^0 T_P^0, \tag{3.A.9}$$

$$a_P = a_E + a_W + a_P^0, \tag{3.A.10}$$

$$k_e = \left(\frac{1-f_e}{k_P} + \frac{f_e}{k_E}\right)^{-1}, \tag{3.A.11}$$

$$k_w = \left(\frac{1-f_w}{k_P} + \frac{f_w}{k_W}\right)^{-1}, \tag{3.A.12}$$

$$f_e = \frac{(\delta x)_e^+}{(\delta x)_e}, \tag{3.A.13}$$

$$f_w = \frac{(\delta x)_w^+}{(\delta x)_w}. \tag{3.A.14}$$

Where *T* is temperautre, *k* is thermal conductivity, *Δx* is spatial step, and *Δt* is time step. Note that when $\Delta t \to \infty$, this equation reduces to steady state discretization equation.

Appendix 3.B. Comparison of Modeled and Measured Temperature

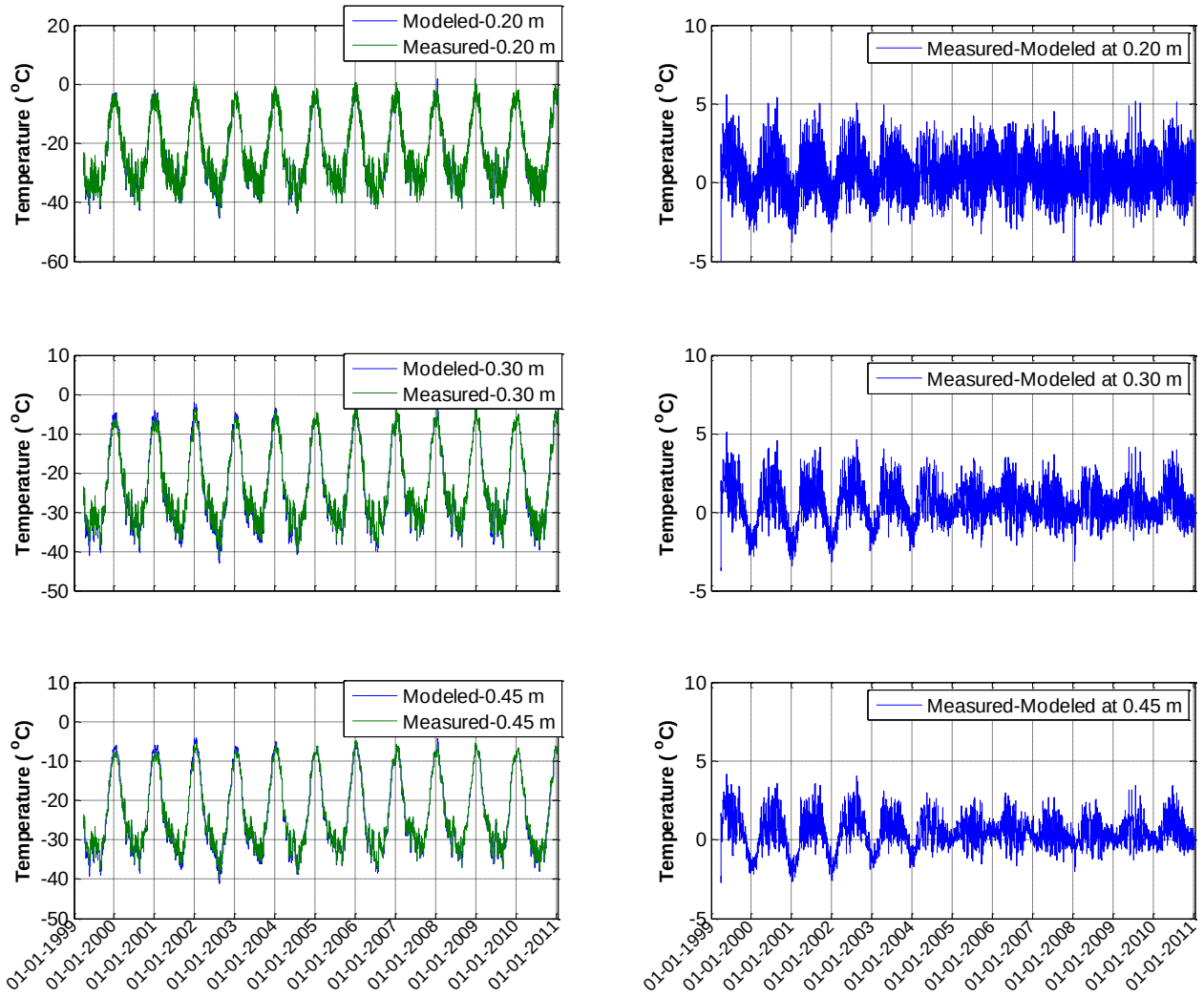

Figure 3.B.1. The FDM modeled and measured temperatures and the differences between them at 0.20 m, 0.30 m, and 0.45 m, respectively.

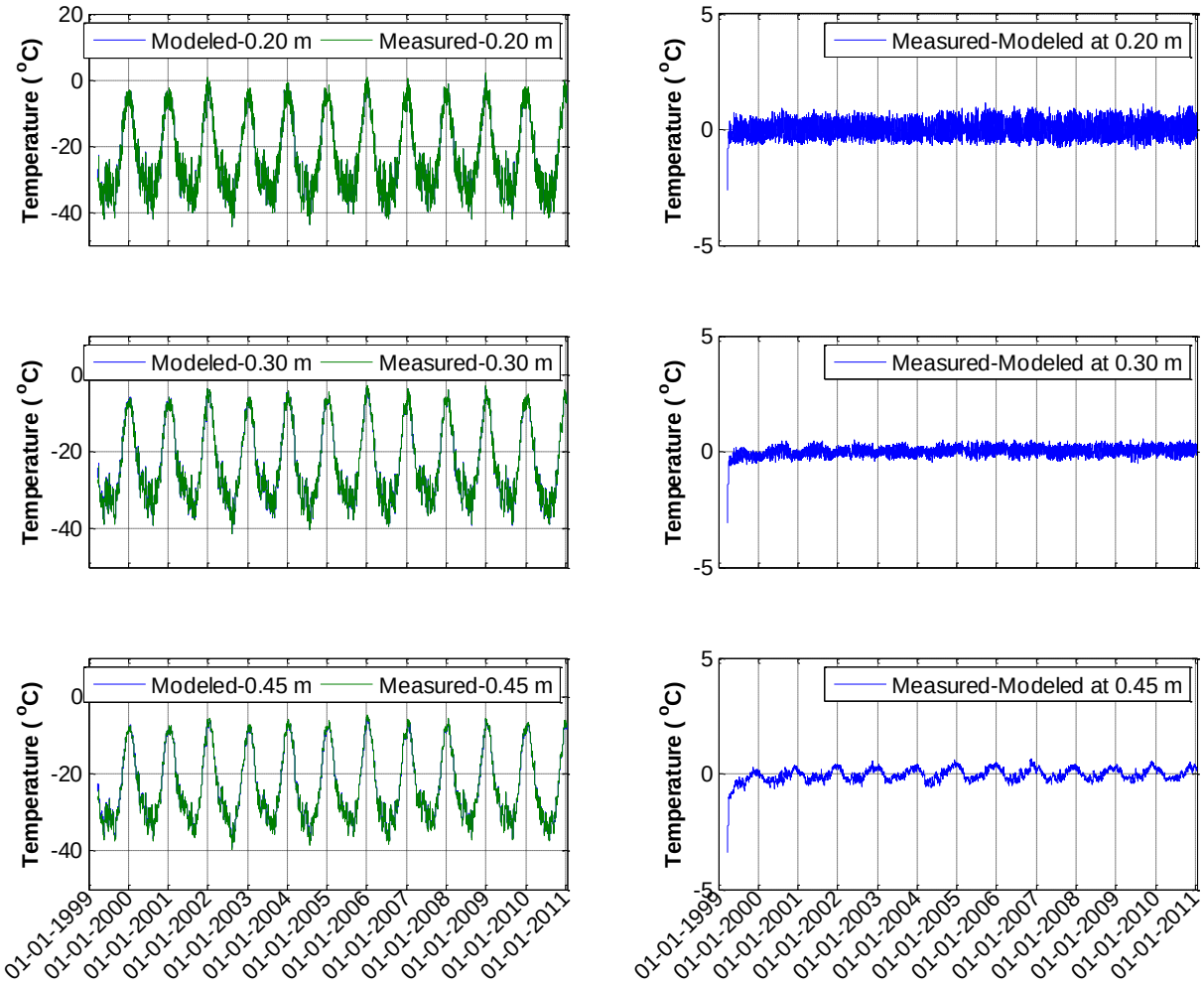

Figure 3.B.2. The FVM modeled and measured temperatures and the differences between them at 0.20 m, 0.30 m, and 0.45 m, respectively using temperature-independent thermal properties.

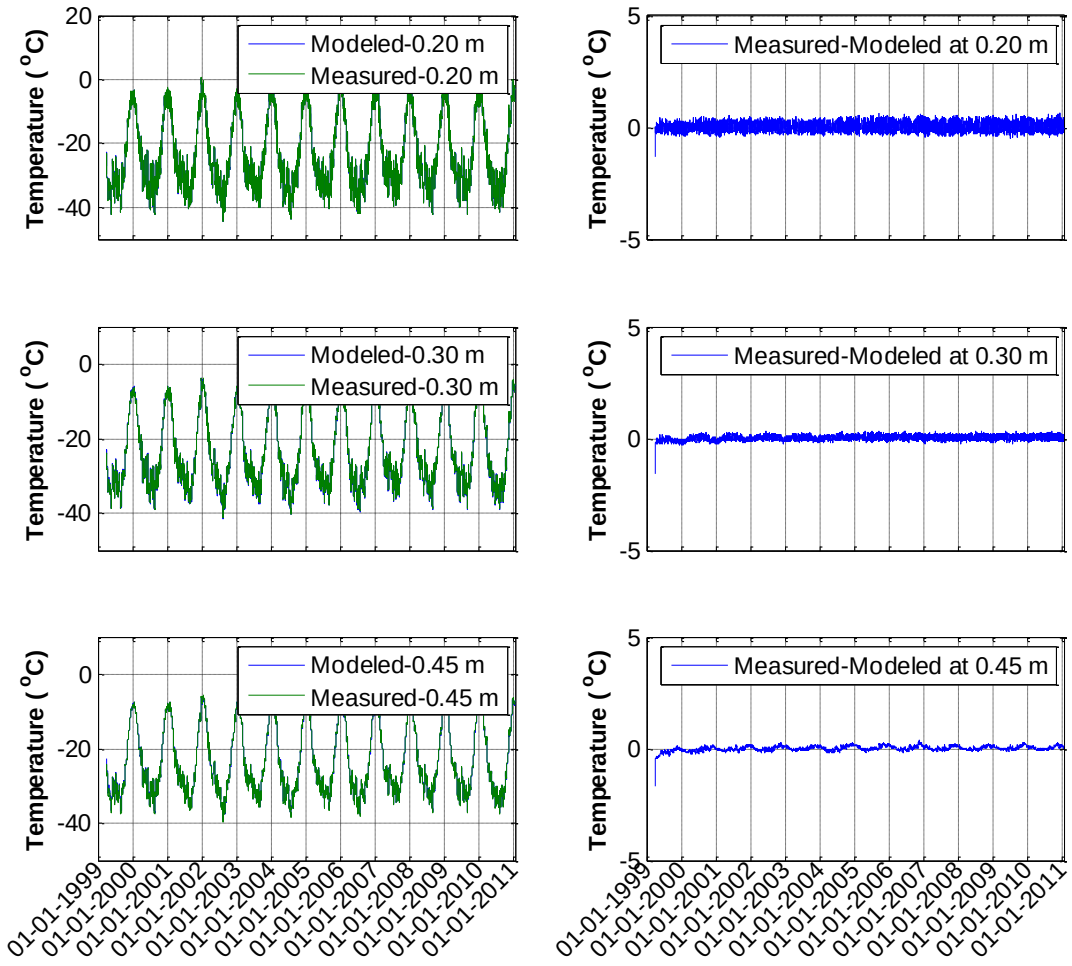

Figure 3.B.3. The FVM modeled and measured temperatures and the differences between them at 0.20 m, 0.30 m, and 0.45 m, respectively using temperature-dependent thermal properties.

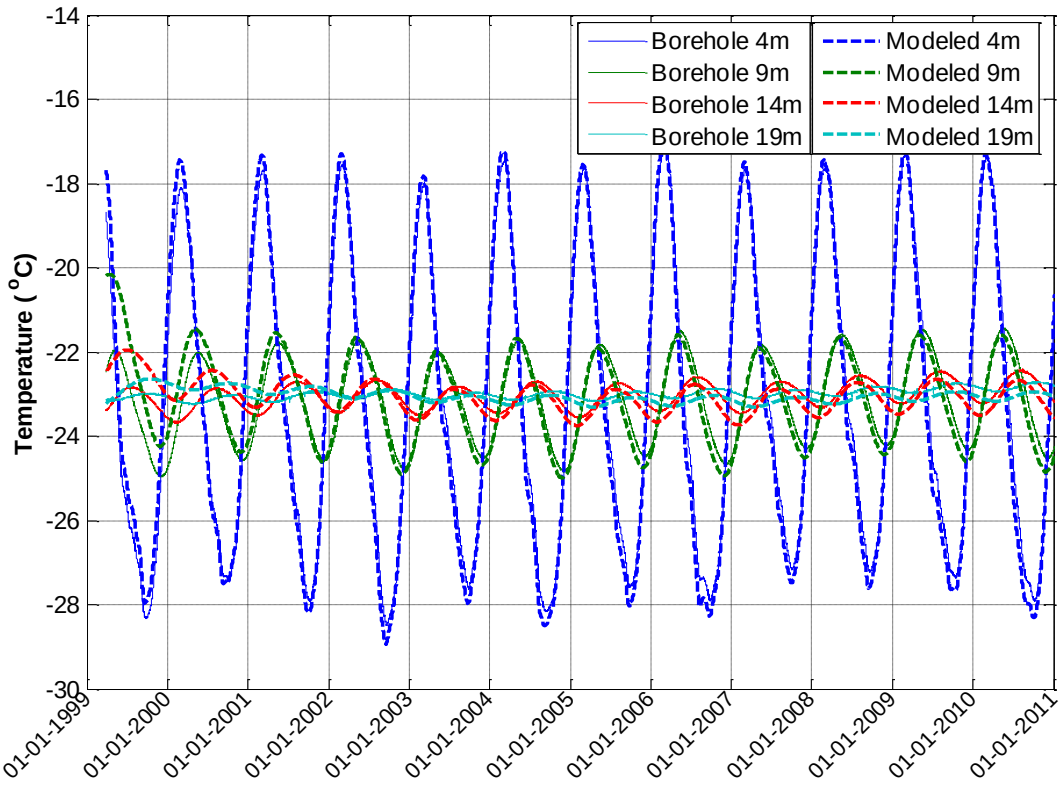

Figure 3.B.4. Comparison between FVM modeled temperature and measured borehole temperature in Beacon Valley at depths of 4 m, 9 m, 14 m, and 19 m.

Chapter 4. Long-term persistence of potential ground ice at Gale Crater, Mars constrained using Curiosity Rover REMS data

The content of this chapter is currently in preparation for publication as:

Liu, L., R. S. Sletten, B. Hallet, M. A. Mischna, and A. R. Vasavada (in prep), Long-term persistence of potential ground ice at Gale Crater, Mars constrained using Curiosity Rover REMS data, *Icarus*.

4.1. Abstract

Surface ice and shallow ground ice in the equatorial region on Mars would be quickly lost to sublimation under current Martian climate conditions; however, if ground ice formed during the last high obliquity of 32 ° approximately 0.5 Ma ago, when ice is believed to have been stable there, residual ice may currently persist below the surface. Ground-based measurements by Curiosity Rover′s Environmental Monitoring Station (REMS) in Gale Crater enable a detailed study of the subsurface transport of heat and water vapor that determines the rate of sublimation. This study is prompted and guided by an analogous investigation in the Dry Valleys of Antarctica where ground ice is currently unstable but has persisted ~0.5 m below the surface for over 1 Ma. A heat and vapor diffusion model is developed to study quantitatively the ground thermal regime and the persistence of potential ground ice in the equatorial region of Mars using the first year of data collected by Curiosity. Based on the derived thermal properties of dry regolith, including thermal inertia values ranging from 300 to 450 J m^{-2} K^{-1} $s^{-1/2}$, diurnal and annual temperature variations propagate to depths of 0.05 m and 1.3 m, respectively. The modeled

rate of water vapor escape from the ground ice to the atmosphere corresponds to a sublimation rate of ~350 m Ma^{-1} for ice at the ground surface; however, the sublimation rate decreases rapidly with depth as the overlying dry regolith thickens. We explore whether interstitial ground ice that formed at Gale Crater ~0.5 Ma ago during the last high obliquity period could currently exist at shallow depths. While this study does not account for the effects of replenishing processes, adsorption, and climate change influenced by obliquity, it highlights the potential long-term persistence of ground ice and implications for future missions on Mars.

4.2. Introduction

Liquid water has been shown to be metastable under current Martian conditions [*Hecht*, 2002; *Martin-Torres et al.*, 2015; *Martínez and Renno*, 2013; *Renno et al.*, 2009; *Zorzano et al.*, 2009]; it would quickly freeze or evaporate in the cold, thin atmosphere. The bulk of Mars' water inventory therefore occurs in the cryosphere, which probably penetrates to depths of several kilometers.

The stability of Martian ground ice has been the focus of numerous studies, and various models have been constructed to predict the global distribution and depth of ice below the surface of Mars assuming that the vapor in the regolith is in equilibrium with the vapor in the atmosphere. Ground ice models range from conceptual descriptions by *Leighton and Murray* [1966], to models including latitudinal dependence [*Fanale*, 1976; *Fanale et al.*, 1986; *Schörghofer*, 2007], to models with both latitudinal and longitudinal dependence [*Mellon and Jakosky*, 1993; 1995; *Mellon et al.*, 1997; *Paige*, 1992]. The most recent models include observed spatial and temporal variations in atmospheric humidity [*Mellon et al.*, 2004; *Schörghofer and Aharonson*, 2005]. The modeling work has focused on the key physical processes responsible for ground ice: vapor diffusion and condensation. These processes predict the spatial distribution of ground ice occurring under a dry regolith. Comparing the model results with observed geographic ice boundaries suggests that the ground ice has adjusted to the atmospheric humidity [*Boynton et al.*, 2002; *Mellon et al.*, 2004]. The past studies have shown that the cryosphere extends to the surface near the poles, but exists below a distinct layer of ice-free regolith at low- to mid-latitudes. Observed distributions of leakage neutrons measured by the Neutron Spectrometer, an instrument that is part of Mars Odyssey spacecraft's Gamma Ray Spectrometer (GRS)

instrument suite, have supported the ground ice distribution predicted by vapor transport models, revealing that the uppermost 50–100 cm of regolith poleward of ~60 ° latitude contains substantial amounts of hydrogen, interpreted to be equivalent to several tens of weight percent water ice [*Feldman et al.*, 2004]; this is consistent with an ice-rich porous regolith. Phoenix landed at 68 °N on Mars and confirmed the existence of ground ice under a layer of an average of 4.6 cm of dry soil [*Mellon et al.*, 2009].

The current Martian climate in the equatorial region, in particular the atmospheric water content and the mean surface and subsurface temperature, dictate that subsurface ice is unstable with respect to sublimation [*Clifford and Hillel*, 1983; *Mellon et al.*, 2004; *Mellon and Jakosky*, 1993; *Schörghofer and Aharonson*, 2005]. This is consistent with the GRS observations [*Feldman et al.*, 2002]. Ground ice present in these regions would sublimate and the water vapor would diffuse through the regolith to the atmosphere, causing the ice table to progressively descend below the surface and eventually vanish. The stability of ice at or near the ground surface is a function of temperature, which is sensitive to the obliquity of the planet's rotation that changes on timescales of ~100 ka; in the past five million years it has reached extremes of 15 ° and 40 ° [*Laskar et al.*, 2004]. Models suggest that at low obliquity, near-surface ice is stable only poleward of about 60 °latitude, but when obliquity is high, near-surface ice can be stable at low latitudes [*Chamberlain and Boynton*, 2007; *Mellon and Jakosky*, 1995]. For example, at an obliquity of 32 ° or higher, ground ice becomes stable globally; this was suggested to have occurred most recently approximately 0.5 Ma ago [*Mellon and Jakosky*, 1995].

Previous studies that have also considered the persistence of ground ice on Mars. *Smoluchowski* [1968] concluded that it could persist for as long as 10^9 years with a

sufficiently thick soil cover by estimating rates of subsurface ice sublimation and molecular diffusion through a soil layer into the atmosphere. *Clifford and Hillel* [1983] calculated the lifetime of equatorial ground ice for various types of soils, and concluded that the longevity of ice would be shortest under warmer soils with larger pores and longest for colder soils with smaller pores; with the latter reaching between 10^8 and 10^9 years is in accord with *Smoluchowski* [1968]. *Fanale et al.* [1986] modeled the thermal and diffusive behavior of a regolith initially saturated with ice and they found that ice was stable poleward of about $\pm 30°$ to $40°$ and that the equatorial regions should be depleted of ice. *Paige* [1992] considered the range of thermal properties observed on Mars and suggested that the stability region of ground ice is closer to the surface and closer to the equator for areas with lower thermal inertia values. If a process replenished the ground ice periodically or continuously, ground ice could have persisted in the equatorial region throughout Martian geologic history.

Morphological observations on the surface of Mars are consistent with the former presence of shallow subsurface water ice [*Balme and Gallagher*, 2009; *Head et al.*, 2003; *Lanagan et al.*, 2001; *Oehler*, 2013; *Reiss et al.*, 2006; *Squyres and Carr*, 1986; *Yakovlev*, 2012]. According to *Aharonson and Schorghofer* [2006], this water ice may be locally preserved, and it could be stable today on pole-facing slopes at low latitudes. Moreover, the Curiosity landing site, Gale Crater′s mound, is predicted to be a hemispheric maximum for snowmelt on Mars [*Kite et al.*, 2013]. The combination of these factors highlights the potential for residual ground ice to persist in Martian equatorial regions, despite the unfavorable current conditions.

The potential existence of ice covered by a dry layer of regolith on Mars in regions where it is not currently stable was motivated by a terrestrial analog for ground ice observed in Beacon Valley, Antarctica, where massive ice is found beneath ~30 cm of dry sandy soil. The ice was first suggested to be more than 8.1 Ma old based on the age of a pocket of volcanic ash found in the sediments above ice [*Sugden et al.*, 1995]. This initial age estimate was challenged based on modeling studies on ice sublimation and vapor diffusion through the dry regolith suggesting that the ice is much younger [*Hindmarsh et al.*, 1998; *Liu et al.*, 2015]. Understanding the dynamics and stability of the ground ice on Earth provides a basis for understanding the evolution of the Martian counterpart, and hence the evolution of the Martian climate.

Here we present a study of the stability and persistence of ground ice at Gale Crater on Mars using in situ climate data collected by Curiosity. We examine the ground thermal regime using a 1-D time-dependent thermal model [*Liu et al.*, in prep] and a vapor diffusion model modified from *Liu et al.* [2015] to calculate rates of ice sublimation and condensation. If deposited 0.5 Ma ago under high obliquity (> 32 °), ground ice could have persisted to the present at a depth of meters, as discussed in Section 4.7. This work provides constraints on the long-term evolution of ground ice at Gale Crater on Mars and is applicable to other regions on Mars.

4.3. Sites Description

Gale Crater, the Mars Science Laboratory (MSL) landing site, is a Martian impact crater ~154 km in diameter, centered near 5 °S, 138 °E. It has an interior mound composed of layered rocks up to ~5 km high known informally as Mt Sharp that may represent the thickest exposed stratigraphic reference section for environmental change on Mars

[*Grotzinger et al.*, 2015; *Grotzinger and Milliken*, 2012]. The crater has been estimated to be Noachian in age (~3.5–3.8 Ga) [*Bridges*, 2001; *Cabrol et al.*, 1999]. In Gale Crater, ground ice is assumed to not be present within the top 1 m of the ground surface [*Feldman et al.*, 2002; *Mellon et al.*, 2004].

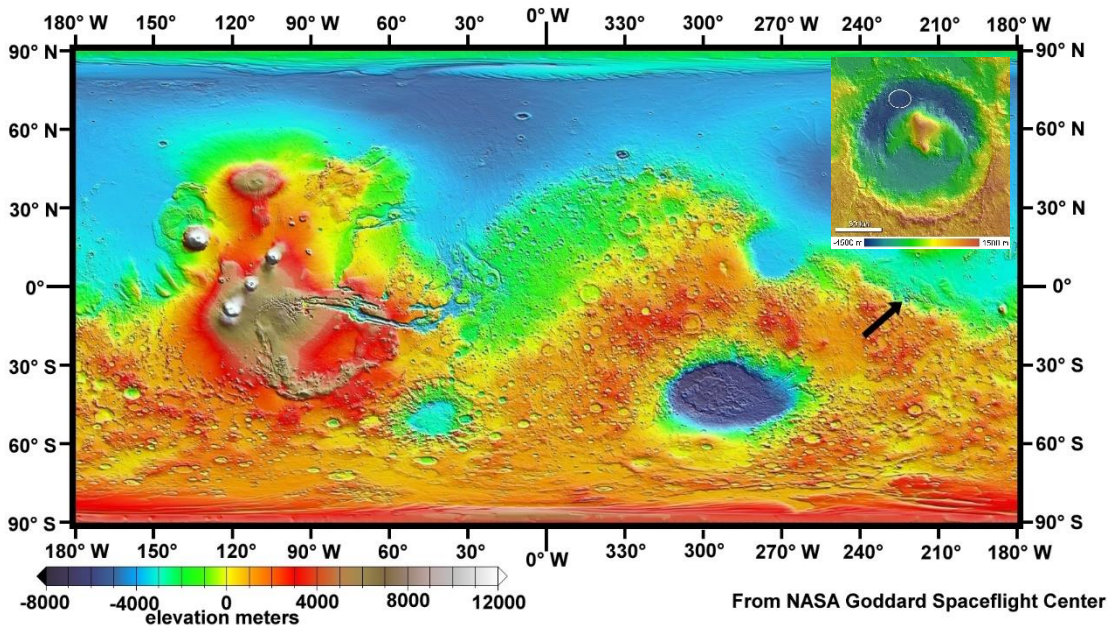

Figure 4.1. Global topographic map of Mars adapted from Smith et al. [1999]. The black arrow marks the location of Gale Crater that is shown in the insert; white circle in the insert marks the landing ellipse of Curiosity Rover.

Curiosity is equipped with a set of analytical and optical instruments [*Grotzinger et al.*, 2012] capable of parameterizing models of the stability and persistence of potential ground ice that may have formed when climatic conditions favored ice formation in the region. Of particular relevance are the Rover Environmental Station (REMS), a suite of sensors designed to study the environmental conditions along the rover traverse, that systematically measures atmospheric pressure, relative humidity, atmospheric temperature, and wind speed. The REMS suite also includes an infrared ground temperature sensor

(GTS) that enhances significantly our knowledge of surface temperature variations on Mars [*Gómez-Elvira et al.*, 2012].

4.4. REMS Measurements

The ~5 min hourly average of REMS measurements of atmospheric temperature, relative humidity (RH), pressure, and ground surface temperature for the first Martian year at Gale Crater are shown in Figure 4.2. Air temperature ranges from 183 K to 277 K with an annual average of 224 K. At Gale Crater, the range of seasonal temperature variation is less prominent than that of diurnal variation that can reach as much as 60 K. Atmospheric RH ranges from 0% to 100%, and it peaks at the beginning of the southern winter. Daily RH values peak between 3 A.M. and 6 A.M. local time. Atmospheric pressure varies from 689 Pa to 969 Pa with the lowest pressures occurring during the southern winter and the highest during the end of the southern spring.

Ground surface temperatures range from 173 K to 288 K with an annual average of 226 K. The offset in the diurnal peaks of ground surface temperature occurring at around sol 120 is the result of the rover moving over a different type of soil: from a sandy soil to fine grained debris sediment [*Martínez et al.*, 2014]. Systematic uncertainties and environmental influences associated with the GTS performance have been discussed by *Hamilton et al.* [2014] and *Martínez et al.* [2014].

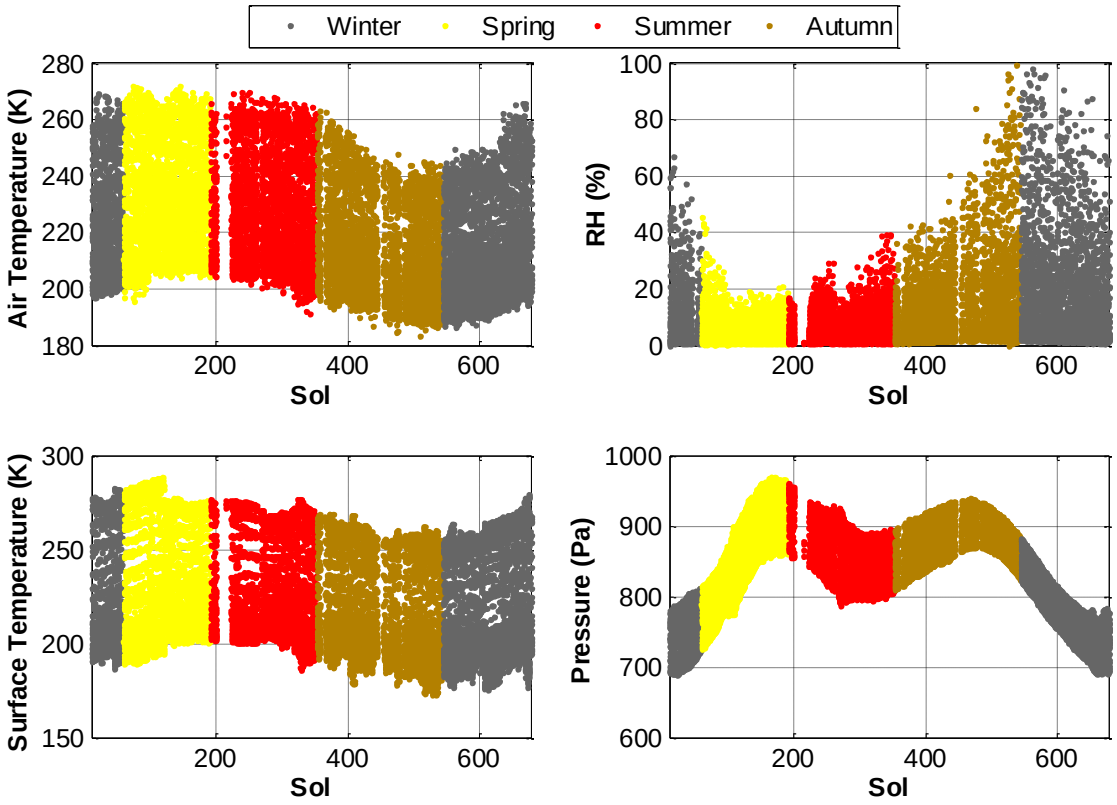

Figure 4.2. REMS measurements of atmospheric temperature, relative humidity (RH), pressure, and ground surface temperature for the first Martian year at Gale Crater.

4.5. Model Description

4.5.1. Subsurface Temperature Modeling

Subsurface temperatures at Gale Crater are modeled using a 1-D thermal diffusion equation assuming that the annual and diurnal fluctuations in soil temperature are driven by atmospheric forcing through surface temperature fluctuations [*Liu et al.*, in prep]. The thermal regime of a laterally uniform soil can be modeled using the general 1-D thermal diffusion equation with no phase change, or other heat transport or generation processes:

$$\rho_m C(T)_m \frac{\partial T}{\partial t} = \frac{\partial}{\partial z}\left(k_m(T)\frac{\partial T}{\partial z}\right) \quad (4.1)$$

where T is temperature (K), t is time (s), k is the thermal conductivity (W m^{-1} K^{-1}), ρC is the volumetric heat capacity (J m^{-3} K^{-1}), z is depth (m), and m refers to the different media types through which heat is conducting (s for the dry soil and i for the ice-cemented soil). Thermal diffusivity ($\alpha = k/\rho C$) reflects the ability of a material to conduct thermal energy relative to its ability to store thermal energy. The ability of the soil to exchange the radiative energy received at the surface with the shallow subsurface and the near-surface air depends on the thermal inertia (I) of the soil. Given a radiative forcing at the surface, the thermal inertia regulates thermal excursions of ground and subsurface temperatures at diurnal and seasonal timescales. The thermal skin depth Δ can be derived from these parameters for temperature variations of period P, this is the depth at which the amplitude of temperature variations decreases to 1/e of the surface value, by equation 4.2 [*Lachenbruch et al.*, 1962]:

$$\Delta = \sqrt{\frac{k}{\rho C}\frac{P}{\pi}} = \sqrt{\alpha\frac{P}{\pi}} = \frac{I}{\rho C}\sqrt{\frac{P}{\pi}} \tag{4.2}$$

The upper boundary condition for the model is set by the REMS GTS measurements. The technical description, design, and in-flight calibration of the REMS GTS are described by *Sebastián et al.* [2010]. Hourly temperature meansuremnt are derived frm the first 5 minutes of 1 Hz measurements that are made each hour during a sol. The temperatures values range from 170 K to 290 K for the first year. The second boundary condition required is the geothermal flux at the lower boundary. For this study, we use 20 mW/m^2 [*Hoffman*, 2001; *Mellon and Jakosky*, 1993; *Solomon and Head*, 1990]. Given that rover is traversing along the surface at Gale Crater and not remaining stationary, the initial condition is updated at the beginning of each sol.

4.5.2. Thermo-physical Properties

Equation (4.1) describes the evolution of the subsurface temperature regime as a function of both thermal conductivity and volumetric heat capacity. The thermal diffusivity of the regolith plays an important role in heat diffusion, as well as in water vapor diffusion, because the rate of vapor diffusion scales with subsurface temperature gradients; however, the values of diffusivity for Martian regolith need to be inferred from other data. Available measurements of the thermal properties of the Martian surface primarily determine the thermal inertia *I*. REMS GTS and surface energy budget estimates of *I* are in the range of 265-450 J m^{-2} K^{-1} $s^{-1/2}$ [*Hamilton et al.*, 2014; *Martínez et al.*, 2014], which is consistent with satellite measurements [*Christensen et al.*, 2013; *Fergason et al.*, 2006; *Mellon et al.*, 2000]. Thermal inertia varies with the types of terrain traversed by the rover, as well as the porosity and particle sizes of the uppermost regolith.

In this study, the temperature effects of both the volumetric heat capacity and thermal conductivity have been taken into account [*Liu et al.*, in prep]. We use I = 300 J m^{-2} K^{-1} $s^{-1/2}$ for sols 1-120 and I = 450 J m^{-2} K^{-1} $s^{-1/2}$ for sols 121-668 (Table 4.1), which are consistent with values estimated for the terrain [*Hamilton et al.*, 2014; *Martínez et al.*, 2014]. The skin depths are then calculated using equation (4.2). On Mars, the dirunal and annual skin depth are approximately 0.05 m and 1.3 m.

Thermal inertia *I* derived from satellite measurements is based on the diurnal cooling rate; therefore, it is an indication of the thermal properties of the upper tens of centimeters of the dry regolith. If ice is present, the thermal conductivity, density, and heat capacity of the regolith all need to be modified. In this study, for the initial condition, it is simply assumed that subsurface ice was distributed evenly in the regolith. The thermal

conductivity *k* of the ice-cemented regolith can be modeled given its volumetric ice content [*Liu et al.*, in prep]; the volumetric heat capacity ρC_p of the ice-cemented regolith can be calculated additively from the heat capacity of the dry regolith and the interstitial ice [*Schörghofer and Aharonson*, 2005].

Table 4.1. Thermal properties of the dry and ice-cemented regolith used in this study at Gale Crater.

	Dry Soil		**Ice-cemented Soil**
	Sol 1-120	Sol 121-668	
Volumetric Heat Capacity ρC_p J m^{-3} K^{-1}	~1.25×10^{6}	~1.50×10^{6}	~2.10×10^{6}
Thermal Inertia I J m^{-2} K^{-1} s$^{-1/2}$	~300	~450	~2290
Thermal Conductivity k W m^{-1} K^{-1}	~0.07	~0.13	~2.5
Thermal Diffusivity α m^2 s^{-1}	~5.8×10^{-8}	~9.0×10^{-8}	~1.2×10^{-6}

4.5.3. Water Vapor Diffusion Modeling

A 1-D water-vapor diffusion model from *Liu et al.* [2015] is used to determine the rate of ice exchange between ground ice and the atmosphere under current climate conditions at Gale Crater. In this model, water vapor diffusion in the system is driven by the gradients of water vapor density; the flux of water vapor is calculated using Fick′s first law:

$$F = -\frac{\varepsilon}{\tau} D_{\text{eff}} \frac{\partial \rho_{\text{v}}}{\partial z} \tag{4.3}$$

where F is the flux of vapor (molecules m^{-2} s^{-1}), D_{eff} is the effective diffusion coefficient of water vapor in Martian air (m^2 s^{-1}), ε is porosity to account for the cross-sectional area of diffusion, and τ is tortuosity accounting for the length of the diffusion pathway. The

water vapor density at depth changes with time as a function of the divergence in the water vapor flux *dF/dz*. Mass conservation can be expressed as [*Hindmarsh et al.*, 1998; *Liu et al.*, 2015; *Schörghofer and Aharonson*, 2005]:

$$\varepsilon \frac{\partial \rho_v}{\partial t} = -\left(\frac{\partial F}{\partial z} + \frac{\partial \theta}{\partial t} + \frac{\partial \sigma}{\partial t}\right) \quad (4.4)$$

where σ and θ are the amounts of condensed and adsorbed water (molecules m_{soil}^{-3}), respectively. Instantaneous vapor transport is calculated without considering water adsorption, which may change vapor density gradient and thus vapor fluxes significantly [*Houben et al.*, 1997; *Jakosky et al.*, 1997; *Schörghofer and Aharonson*, 2005; *Zent et al.*, 1993]. This process will be included in future studies.

The diffusion coefficient, D_{eff}, plays a key role in the diffusion equation, and it is significantly different under Earth and Mars conditions. Similar to other studies, here we assume that diffusion of H_2O molecules through a porous soil can be modeled in two ways, depending on the mean free path of the molecules in the gas and the size of the pores in the soil [*Clifford and Hillel*, 1983; *Clifford and Hillel*, 1986; *Fisher*, 2005; *Mellon and Jakosky*, 1993]. The effective diffusivity D_{eff} of H_2O vapor in a porous soil is expressed as [*Clifford and Hillel*, 1986]:

$$\frac{1}{D_{\mathrm{eff}}} = \frac{1}{D_{\mathrm{AB}}} + \frac{1}{D_{\mathrm{KA}}} \quad (4.5)$$

where D_{AB} is the normal gas diffusivity of water vapor in a host CO_2 atmosphere, and D_{KA} is the Knudsen diffusivity that dominates where the pore sizes are smaller than the mean free path of the water molecules in the host CO_2 air. D_{AB} of H_2O through an atmosphere of CO_2, in units of $m^2\ s^{-1}$, is given by [*Clifford*, 1991; 1993a; *Fisher*, 2005; *Mellon and Jakosky*, 1993]:

$$D_{\mathrm{AB}} = 0.1654 \left(\frac{T}{273.15}\right)^{3/2} \left(\frac{1.013 \cdot 10^{6}}{P}\right) \quad (4.6)$$

where T is the temperature in K, and P is the total surface pressure of the atmosphere in Pa. D_{KA}, in $\mathrm{cm^2\ s^{-1}}$, is estimated as [*Clifford and Hillel*, 1986]:

$$D_{\mathrm{KA}} = \frac{2}{3} r \left(\frac{8\mathrm{R}T}{\pi m_{\mathrm{H_2O}}}\right)^{1/2} \quad (4.7)$$

where r is pore size in cm, R is the universal gas constant (8.314×10^7 ergs $\mathrm{g^{-1}\ mole^{-1}\ K^{-1}}$), T is temperature in K, m_{H2O} is the molecular weight of H_2O. By inserting the constant, this equation can be reduced to:

$$D_{\mathrm{KA}} = 22.85 T^{1/2} r \quad (4.8)$$

where D_{KA} is in units of $\mathrm{m^2\ s^{-1}}$. The effective diffusivity D_{eff} here is assessed using REMS measurements.

4.5.4. Water Vapor Diffusion Coefficient

Figure 4.3a illustrates the calculated effective vapor diffusion coefficient as a function of pore radius under current temperature and pressure conditions at Gale using REMS measurements. The linear region towards smaller pore radii is the Knudsen region, where D_{eff} is proportional to r. The almost constant region with larger pore radii is the normal diffusion region, where D_{eff} is independent of r. Between the two regions, both diffusion processes influence the effective diffusion coefficient. In general, variations in temperature have a small effect, especially in the Knudsen region. For typical Martian conditions, the range of pore sizes has been suggested to be 1−10 μm [*Clifford and Hillel*, 1986; *Fisher*, 2005]. We assume the pore size to be 10 μm for this study. For the measured temperature and pressure range at Gale Crater, the effective diffusion coefficient D_{eff}

ranges from 0.7×10^{-3} to 1.5×10^{-3} m^2 s^{-1} and is in the transition region. Hence, both diffusion processes are taken into account.

The effective diffusion coefficient D_{eff} is a function of both temperature and pressure for a fixed pore size. Figure 4.3b and 4.3c demonstrate the dependence of D_{eff} on temperature and pressure at the surface and 10-m depth. The range of D_{eff} decreases with depth from 0.7×10^{-3} to 1.5×10^{-3} m^2 s^{-1} at the surface to 0.9×10^{-3} to 1.2×10^{-3} m^2 s^{-1} at 10 m depth. D_{eff} increases with the temperature, and it shows a greater range at the surface than at depth (e.g. 10 m in Figure 4.3). D_{eff} decreases with the pressure; it shows a greater variation at the surface.

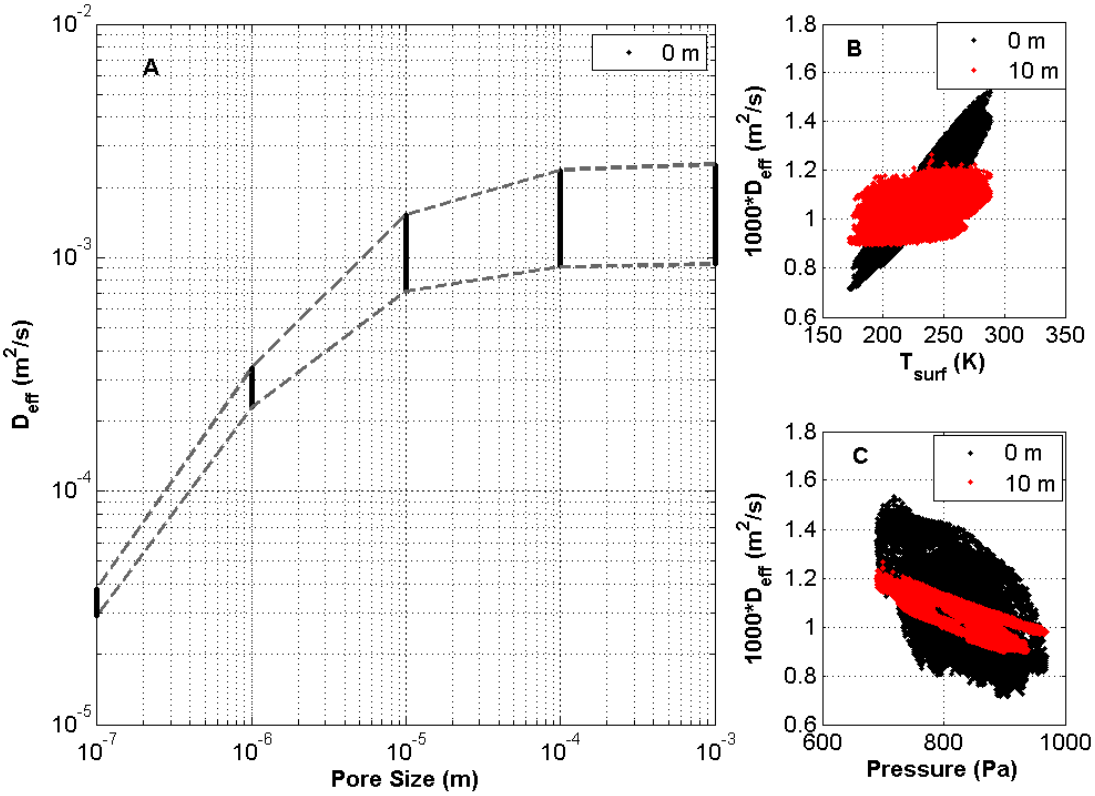

Figure 4.3. (a). The effective vapor diffusion coefficient D_{eff} as a function of pore radius under current temperature and pressure condition at Gale using REMS measurements. The dashed lines delineate ranges of D_{eff} for each pore size. (b). D_{eff} as a function of ground temperature at 0 m and 10 m, respectively. (c). D_{eff} as a function of atmospheric pressure

at 0 m and 10 m, respectively.

4.6. Results

4.6.1. Ground Temperature Profile

Given that the ground structure is unknown, a uniform dry regolith has been assumed here to model the ground temperature profile. The modeled ground temperatures along the Curiosity traverse in Gale Crater for the first year are shown in Figure 4.4, and in greater detail for 1 sol on sols 100 and 500 in Figure 4.5. Temperatures in the upper 0.1 m of the regolith closely track ground surface temperature with dampened and lagged variations. Diurnal variations are negligible below 0.5 m. Seasonal variations are well presented with the same average temperature over depths on each sol. The collapse in GTS measurements around sol 120 is also reflected at depths up to 0.0175 m, but this phenomena disappears at depth 0.05 m.

The daily variations of ground surface temperature change with location and seasonality. On sol 100, MSL Rover was collecting data at Rocknest in the spring. Ground surface temperature ranged from 196 K to 283 K and averaged 235 K (Figure 4.5a). On sol 500, MSL Rover was collecting data at Dingo Gap in the autumn. Ground surface temperature ranges from 185 K to 257 K and averaged 215 K (Figure 4.5b). In addition to the seasonal effect, thermal inertia values of different soils play significant roles. At Rocknest (sol 100), the regolith is sandy and has an estimated thermal inertia of 295 J m^{-2} K^{-1} $s^{-1/2}$, whereas at Dingo Gap (sol 500), fine-grained sediment covers the surface and has an estimated thermal inertia of 450 J m^{-2} K^{-1} $s^{-1/2}$ [*Martínez et al.*, 2014]. Rocknest soil,

with lower thermal inertia, experiences larger temperature oscillations at the surface than the Dingo Gap soil.

The temperature variations attenuate with depth at similar rates despite the differences in thermal inertia (Figure 4.4 and Figure 4.5). They decrease by ~70% at 0.05 m and by ~90% at 0.10 m on all sols, consistent with the calculated diurnal skin depth of 0.05 m. This is largely dictated by the thermal diffusivity and the values used in this model are the same for both before and after sol 120 (Table 4.1). Subsurface temperature is constant at depth of 0.20 m or lower, somewhat deeper than assumed by *Martínez et al.* [2014].

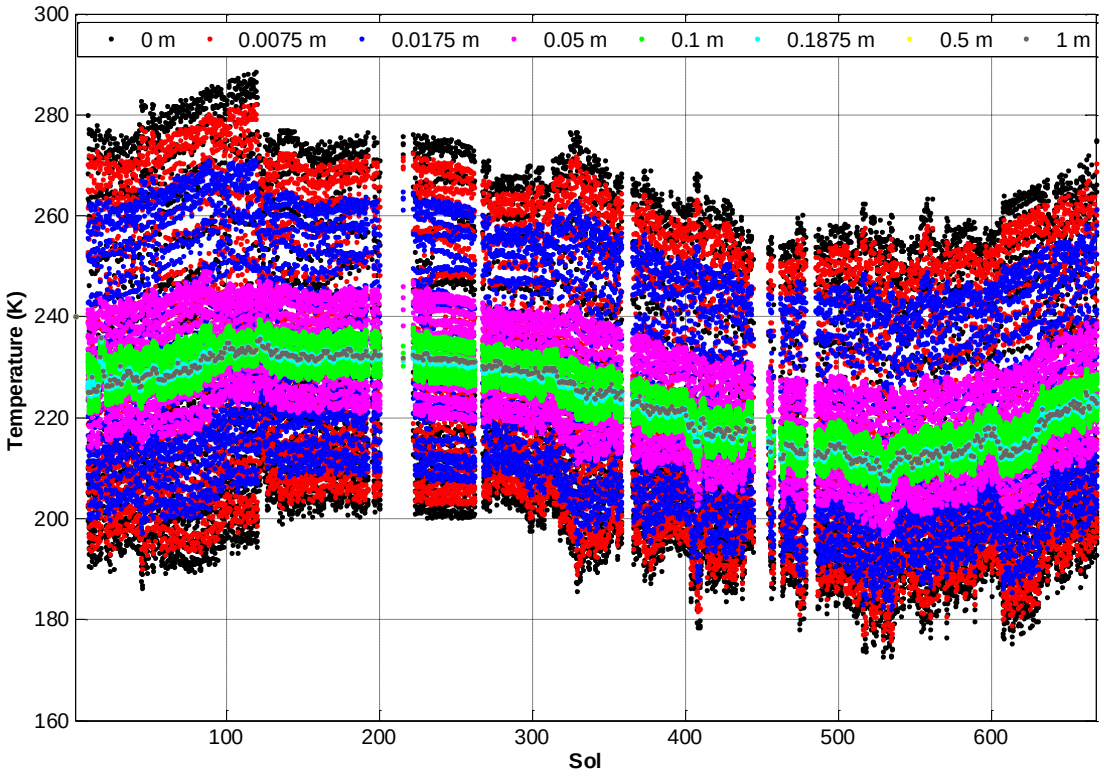

Figure 4.4. Modeled ground temperature for the first Martian year at Gale Crater at depths: 0 m, 0.0075 m, 0.0175 m, 0.05 m, 0.10 m, 0.50 m, and 1 m.

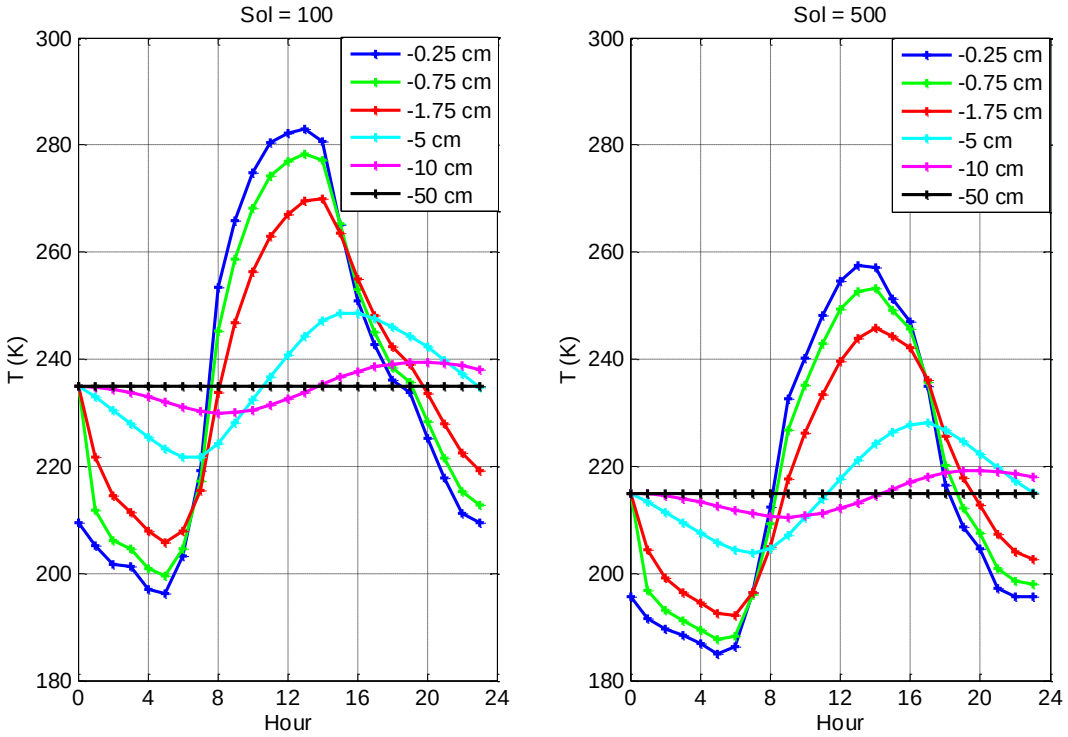

Figure 4.5. Modeled ground temperature for 1 sol at Gale Crater at depths of 0.0025 m, 0.0075 m, 0.0175 m, 0.05 m, 0.10 m, and 0.50 m on sols 100 and 500.

4.6.2. Ground Ice Sublimation Rates

To model the sublimation rate of an un-replenished layer of ground ice at Gale Crater, some initial assumptions are necessary regarding the vertical distribution of ice within the regolith. In this study, it is assumed that ice initially fills the pore space in a single, uniform regolith layer, consistent with other studies of potential or ancient ground ice in the equatorial region of Mars [*Clifford and Hillel*, 1983; *Mellon et al.*, 1997]. As ice sublimates, the front of this ice-rich layer descends below the surface, leaving a layer of dry regolith overlaying the ice-rich layer.

The water vapor flux through the regolith in exchange with the atmosphere is driven by the water vapor density gradient according to equation 4.3. Figure 4.6 shows the water

vapor density in the atmosphere and at the ground surface at Gale Crater calculated from REMS measurements of air temperature, RH, and ground surface temperature. Overall, the water vapor density at the ground surface exceeds that in the atmosphere ~250 folds. There is a tendency for water vapor to escape from the regolith surface to the atmosphere.

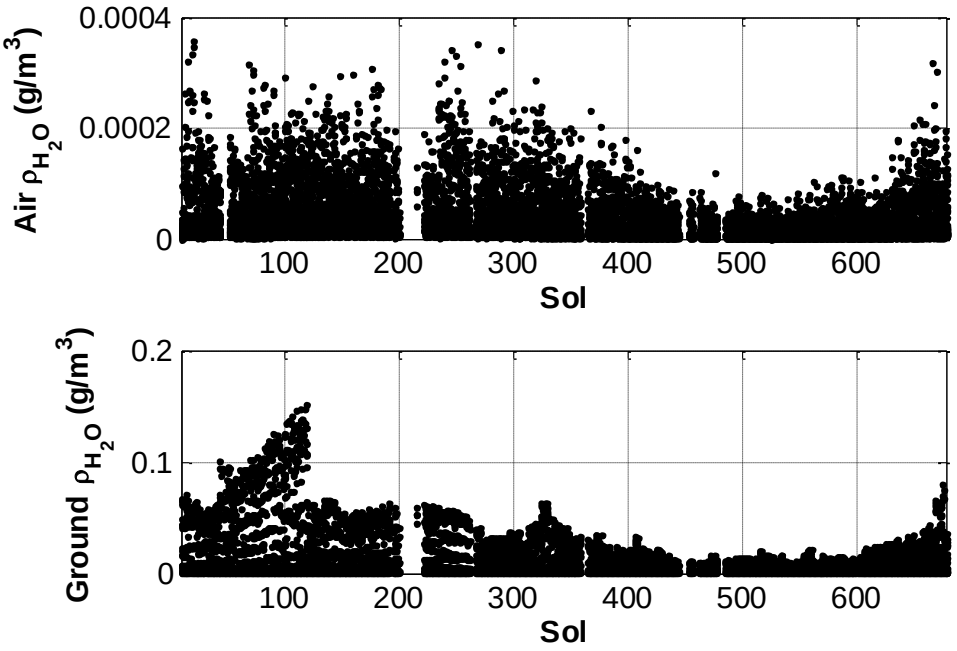

Figure 4.6. Water vapor density in the atmosphere and at the ground surface at Gale Crater.

If the ground ice formed at Gale Crater long ago, as suggested by other studies [*Mellon and Jakosky*, 1995; *Mellon et al.*, 1997], it would have undergone substantial sublimation. Using current climate conditions at Gale Crater, modeled sublimation rates at the dry regolith-ice boundary, as it propagates to depth, are shown in Figure 4.7. The sublimation rate is fastest (~350 m Ma^{-1}) initially when the ice extends up to the ground surface; water vapor migration to the atmosphere is unimpeded. As sublimation continues, the top of the ice-rich regolith drops and an overlying layer of dry regolith forms. The sublimation rate decreases significantly as the porous barrier of dry regolith thickens; the

rate is estimated to be ~1.2 m Ma^{-1} when the top of ground ice layer reaches 1 m, ~0.16 m Ma^{-1} at 10 m, and ~0.035 m Ma^{-1} at 50 m (Figure 4.7).

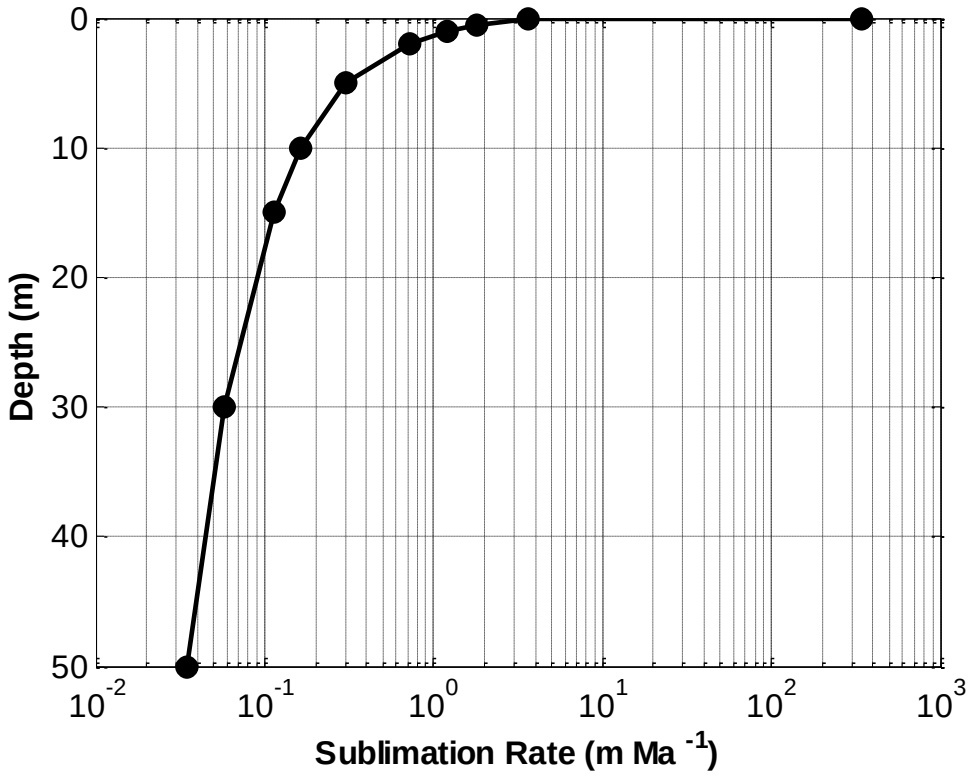

Figure 4.7. Modeled sublimation rates at the interface between dry regolith and ice-rich regolith as the front of the ground ice layer propagates to depth due to ice sublimation (porosity $\varepsilon = 0.3$; pore size $r = 10$ μm).

4.7. Discussion

The modeled sublimation rates versus depth profile shown in Figure 4.7 can be approximated using a second order polynomial expression useful for calculating the temporal evolution of the top of the ground ice (Figure 4.8). If ground ice table initially reached the ground surface, the top of the ground ice descended quickly as the ice sublimates rapidly and then progressively slows down. Considering the obliquity cycle of Mars [*Laskar et al.*, 2004] and the report that ground ice is stable globally when obliquity

is 32 °or higher [*Mellon and Jakosky*, 1995], ice would have been stable below the surface at Gale Crater ~0.5 Ma. Assuming that the regolith was 100% saturated with ice at that time, the model results suggest that this ancient ice would persist to the present day below the ground surface at depths exceeding 2 m. Residual ice-rich regolith would persist at greater depths if the regolith was not initially saturated with ice (Figure 4.8b).

If recharge mechanisms including seasonal surface frost took place during this period of time [*Bapst et al.*, 2014; *Schörghofer and Edgett*, 2006], the sublimation rate would be decreased significantly [*Hagedorn et al.*, 2010; *Liu et al.*, 2015; *Schörghofer*, 2009] and ground ice would be expected closer to the ground surface.

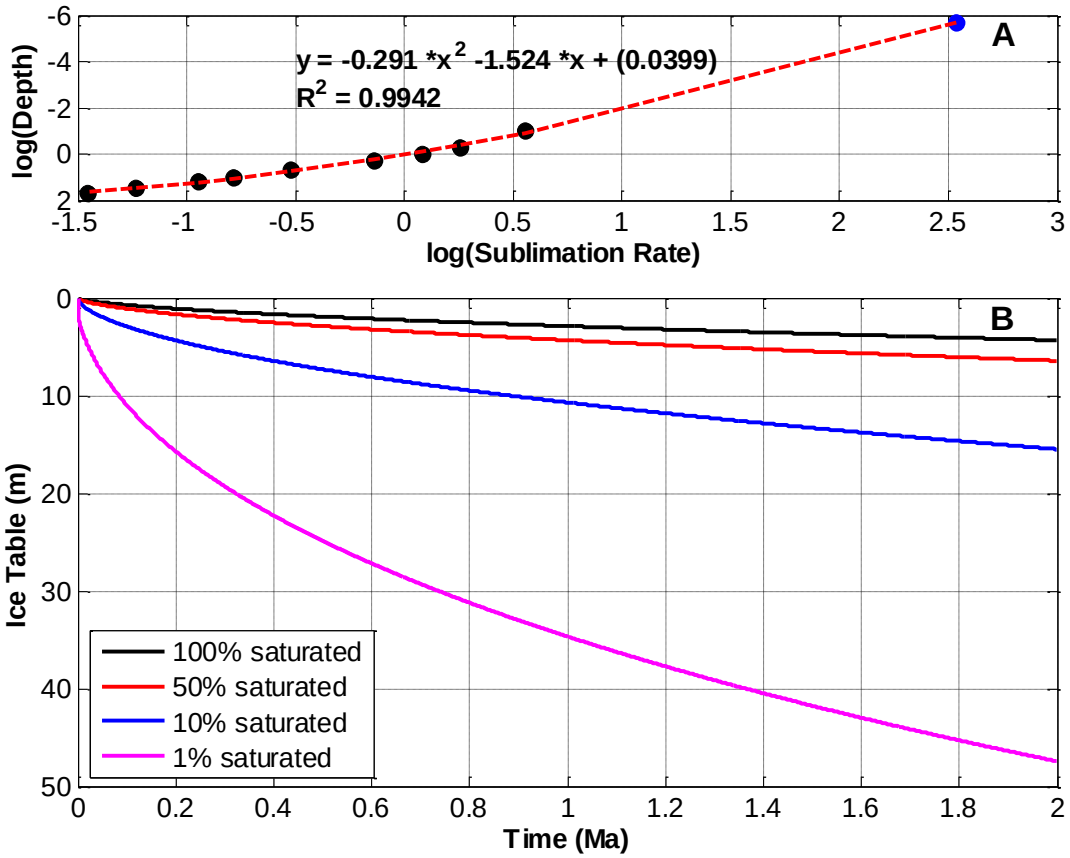

Figure 4.8. (a). Relationship between the sublimation rates and depths. (b). Modeled temporal evolution of the top of the ice-rich regolith for the last 2 Ma for different initial ice contents.

The effect of the adsorbed water on ground ice persistence has not been included in this study. The diurnal and seasonal fluctuations of the temperature and local pressure can produce substantial changes in the adsorptive capacity of the top few meters of the regolith because the amount of adsorbed water in the regolith is a function of both the temperature and the local partial pressure of within the soil pores [*Jakosky*, 1983; *Jakosky et al.*, 1997; *Schörghofer and Aharonson*, 2005; *Zent and Quinn*, 1995]. Therefore, the diffusion of water vapor through the pore system of the near-surface regolith can be significantly damped. On the other hand, according to *Schörghofer and Aharonson* [2005], adsorption does not play a role in the net ice diffusion with periodic changes in the temperature and vapor density and it does not change the mean vapor density profile.

The stability and persistence of the ground ice is dictated by the Martian climate history that is mostly influenced by orbital parameters, in particular the obliquity on time scales of 10^5 Martian years [*Laskar et al.*, 2004]. At an obliquity higher than the present value (25 °), more solar energy is provided to the polar region, which raises the mean annual temperature and prolongs the polar summer season, while less solar energy reaches the mid- and low-latitudes including the equatorial regions, which lowers mean annual temperatures. As a result, this temperature change will accelerate the sublimation of the polar water ice cap [*Jakosky et al.*, 2005; *Mellon and Jakosky*, 1993; 1995; *Toon et al.*, 1980]. The increased atmospheric water abundance can be carried to lower latitudes and could saturate the atmosphere and deposit onto the ground or into the subsurface as ice [*Jakosky and Carr*, 1985; *Mischna et al.*, 2003]. The rate and direction of water vapor diffusion to the atmosphere can be affected. Other studies have shown that water vapor can

diffuse and condense within the near-surface regolith from the atmosphere during periods of high obliquity [*Jakosky and Carr*, 1985; *Jakosky and Mellon*, 2004; *Mellon and Jakosky*, 1995; *Schörghofer*, 2007]. This process acts as periodic replenishment to the ground ice and thus prolongs its persistence.

Ground ice can also be replenished by condensation of water vapor from greater depth driven toward the surface by the geothermal gradient [*Clifford*, 1991; 1993b; *Mellon et al.*, 1997].

The results presented here are conservative estimates of the persistence of ancient ground ice at Gale Crater in the sense that ice could persist closer to the surface than suggested by this study because the model does not include any replenishment mechanisms. Moreover, the model reflects the simple assumption that at the end of the last high obliquity phase, around 0.5 Ma ago, the climate changed abruptly to the modern conditions represented by climate data collected by Curiosity. A more realistic, gradual change in climate would result in slower ground ice sublimation.

4.8. Summary and Conclusions

Martian ground ice has been a subject of extensive investigation due to its fundamental importance as a source of water for microorganisms, a reservoir of paleoclimatic information, and a major component controlling the landscape. The acquisition of hourly climate measurements including air temperature, RH, pressure, and ground surface temperature by REMS enables a detailed investigation of the stability and persistence of ground ice at Gale Crater, in the equatorial region on Mars. This study presents a heat and vapor transport model to examine the ground thermal regime and the dynamics of atmospherically derived ground ice in the present Martian climate.

The thermal model results document the rapid attenuation and lag of ground temperature variations with depth. The attenuation is similar in different terrains despite significant differences in thermal inertia. Diurnal variations of the ground surface temperature change with location and seasonality. The diurnal and annual skin depth are approximately 0.05 m and 1.3 m at Gale Crater, respectively.

Under current climate conditions, water vapor has a tendency to escape from the regolith to the atmosphere. Ice in the regolith would sublimate quickly, especially near the ground surface; the rate of sublimation decreases as the top of the ice-rich regolith descends and the dry regolith above the ice thickens. If ground ice was stable and present at Gale Crater ~0.5 Ma ago at the last high obliquity cycle, residual ice is expected meters below the ground surface at present if the regolith was initially saturated with ice. This study did not account for the effects of potential replenishing processes, adsorption, and gradual climate change influenced by obliquity, all of which may slow the sublimation rate.

Acknowledgements. This material is based upon work supported by the National Science Foundation under grants 0541054, 0636998, and 1341680 and NASA through the Mars Science Laboratory mission via a grant awarded to Malin Space Science Systems. We thank the REMS team for their support of this investigation.

4.9. References

Aharonson, O., and N. Schorghofer (2006), Subsurface ice on Mars with rough topography, *Journal of Geophysical Research-Planets*, *111*(E11), E11007, doi:10.1029/2005je002636.

Balme, M., and C. Gallagher (2009), An equatorial periglacial landscape on Mars, *Earth and Planetary Science Letters*, *285*(1), 1-15.

Bapst, J., J. Bandfield, and S. Wood (2014), Investigating the Timing and Extent of Seasonal Surface Water Frost on Mars with MGS TES, paper presented at Lunar and Planetary Institute Science Conference Abstracts.

Boynton, W. V., et al. (2002), Distribution of hydrogen in the near surface of Mars: Evidence for subsurface ice deposits, *Science*, *297*(5578), 81-85, doi:10.1126/science.1073722.

Bridges, N. (2001), Assessing layered materials in Gale Crater, paper presented at First Landing Site Workshop for the 2003 Mars Exploration Rovers.

Cabrol, N. A., E. A. Grin, H. E. Newsom, R. Landheim, and C. P. McKay (1999), Hydrogeologic evolution of Gale crater and its relevance to the exobiological exploration of Mars, *Icarus*, *139*(2), 235-245.

Chamberlain, M. A., and W. V. Boynton (2007), Response of Martian ground ice to orbit-induced climate change, *Journal of Geophysical Research-Planets*, *112*(E6), E06009, doi:10.1029/2006je002801.

Christensen, P., R. Fergason, C. Edwards, and J. Hill (2013), THEMIS-derived thermal inertia mosaic of Mars: Product description and science results, paper presented at Lunar and Planetary Institute Science Conference Abstracts.

Clifford, S. M. (1991), The role of thermal vapor diffusion in the subsurface hydrologic evolution of Mars, *Geophysical Research Letters*, *18*(11), 2055-2058.

Clifford, S. M. (1993a), A model for the hydrologic and climatic behavior of water on Mars, *Journal of Geophysical Research: Planets (1991–2012)*, *98*(E6), 10973-11016.

Clifford, S. M. (1993b), The role of the geothermal gradient in the emplacement and replenishment of ground ice on Mars, paper presented at Lunar and Planetary Institute Science Conference Abstracts.

Clifford, S. M., and D. Hillel (1983), The stability of ground ice in the equatorial region of Mars, *Journal of Geophysical Research*, *88*(B3), 2456-2474, doi:10.1029/JB088iB03p02456.

Clifford, S. M., and D. Hillel (1986), Knudsen Diffusion - the Effect of Small Pore-Size and Low Gas-Pressure on Gaseous Transport in Soil, *Soil Science*, *141*(4), 289-297, doi:10.1097/00010694-198604000-00006.

Fanale, F. P. (1976), Martian Volatiles - Their Degassing History and Geochemical Fate, *Icarus*, *28*(2), 179-202, doi:10.1016/0019-1035(76)90032-4.

Fanale, F. P., J. R. Salvail, A. P. Zent, and S. E. Postawko (1986), Global distribution and migration of subsurface ice on Mars, *Icarus*, *67*(1), 1-18.

Feldman, W., W. Boynton, R. Tokar, T. Prettyman, O. Gasnault, S. Squyres, R. Elphic, D. Lawrence, S. Lawson, and S. Maurice (2002), Global distribution of neutrons from Mars: Results from Mars Odyssey, *Science*, *297*(5578), 75-78.

Feldman, W. C., et al. (2004), Global distribution of near-surface hydrogen on Mars, *Journal of Geophysical Research-Planets*, *109*(E9), E09006, doi:10.1029/2003je002160.

Fergason, R. L., P. R. Christensen, and H. H. Kieffer (2006), High-resolution thermal inertia derived from the Thermal Emission Imaging System (THEMIS): Thermal model and applications, *Journal of Geophysical Research-Planets*, *111*(E12), E12004, doi:10.1029/2006je002735.

Fisher, D. A. (2005), A process to make massive ice in the martian regolith using long-term diffusion and thermal cracking, *Icarus*, *179*(2), 387-397, doi:10.1016/j.icarus.2005.07.024.

Gómez-Elvira, J., C. Armiens, L. Castañer, M. Domínguez, M. Genzer, F. Gómez, R. Haberle, A.-M. Harri, V. Jiménez, and H. Kahanpää (2012), REMS: the environmental sensor suite for the Mars Science Laboratory rover, *Space science reviews*, *170*(1-4), 583-640.

Grotzinger, J. P., J. Crisp, A. R. Vasavada, R. C. Anderson, C. J. Baker, R. Barry, D. F. Blake, P. Conrad, K. S. Edgett, and B. Ferdowski (2012), Mars Science Laboratory mission and science investigation, *Space science reviews*, *170*(1-4), 5-56.

Grotzinger, J. P., et al. (2015), Deposition, Exhumation, and Paleoclimate of an Ancient Lake Deposit, Gale Crater, Mars, *Science*.

Grotzinger, J. P., and R. E. Milliken (2012), The sedimentary rock record of Mars: distribution, origins, and global stratigraphy, *Sedimentary Geology of Mars*, *102*, 1-48.

Hagedorn, B., R. S. Sletten, B. Hallet, D. F. McTigue, and E. J. Steig (2010), Ground ice recharge via brine transport in frozen soils of Victoria Valley, Antarctica: Insights from modeling delta O-18 and delta D profiles, *Geochimica Et Cosmochimica Acta*, *74*(2), 435-448, doi:10.1016/j.gca.2009.10.021.

Hamilton, V. E., et al. (2014), Observations and preliminary science results from the first 100 sols of MSL Rover Environmental Monitoring Station ground temperature sensor measurements at Gale Crater, *Journal of Geophysical Research-Planets*, *119*(4), 745-770, doi:10.1002/2013je004520.

Head, J. W., J. F. Mustard, M. A. Kreslavsky, R. E. Milliken, and D. R. Marchant (2003), Recent ice ages on Mars, *Nature*, *426*(6968), 797-802.

Hecht, M. H. (2002), Metastability of liquid water on Mars, *Icarus*, *156*(2), 373-386, doi:10.1006/icar.2001.6794.

Hindmarsh, R. C. A., F. M. Van der Wateren, and A. L. L. M. Verbers (1998), Sublimation of ice through sediment in Beacon Valley, Antarctica, *Geografiska Annaler Series a-Physical Geography*, *80A*(3-4), 209-219.

Hoffman, N. (2001), Modern geothermal gradients on Mars and implications for subsurface liquids, paper presented at Conference on the Geophysical Detection of Subsurface Water on Mars.

Houben, H., R. M. Haberle, R. E. Young, and A. P. Zent (1997), Modeling the Martian seasonal water cycle, *Journal of Geophysical Research-Planets*, *102*(E4), 9069-9083.

Jakosky, B. M. (1983), The Role of Seasonal Reservoirs in the Mars Water Cycle .1. Seasonal Exchange of Water with the Regolith, *Icarus*, *55*(1), 1-18, doi:10.1016/0019-1035(83)90046-5.

Jakosky, B. M., and M. H. Carr (1985), Possible Precipitation of Ice at Low Latitudes of Mars during Periods of High Obliquity, *Nature*, *315*(6020), 559-561, doi:DOI 10.1038/315559a0.

Jakosky, B. M., and M. T. Mellon (2004), Water on Mars, *Physics Today*, *57*(4), 71-76.

Jakosky, B. M., M. T. Mellon, E. S. Varnes, W. C. Feldman, W. V. Boynton, and R. M. Haberle (2005), Mars low-latitude neutron distribution: Possible remnant near-surface water ice and a mechanism for its recent emplacement (vol 175, pg 58, 2005), *Icarus*, *178*(1), 291-293, doi:DOI 10.1016/j.icarus.2005.07.002.

Jakosky, B. M., A. P. Zent, and R. W. Zurek (1997), The Mars water cycle: Determining the role of exchange with the regolith, *Icarus*, *130*(1), 87-95.

Kite, E. S., I. Halevy, M. A. Kahre, M. J. Wolff, and M. Manga (2013), Seasonal melting and the formation of sedimentary rocks on Mars, with predictions for the Gale Crater mound, *Icarus, 223*(1), 181-210, doi:10.1016/j.icarus.2012.11.034.

Lachenbruch, A. H., M. C. Brewer, G. W. Greene, and B. Vaughn Marshall (1962), Temperatures in permafrost, paper presented at Temperature; Its Measurement and Control in Science and Industry, Volume 1.

Lanagan, P. D., A. S. McEwen, L. P. Keszthelyi, and T. Thordarson (2001), Rootless cones on Mars indicating the presence of shallow equatorial ground ice in recent times, *Geophysical Research Letters, 28*(12), 2365-2367, doi:10.1029/2001gl012932.

Laskar, J., A. C. M. Correia, M. Gastineau, F. Joutel, B. Levrard, and P. Robutel (2004), Long term evolution and chaotic diffusion of the insolation quantities of Mars, *Icarus, 170*(2), 343-364, doi:10.1016/j.icarus.2004.04.005.

Leighton, R. B., and B. C. Murray (1966), Behavior of Carbon Dioxide and Other Volatiles on Mars, *Science, 153*(3732), 136-144, doi:10.1126/science.153.3732.136.

Liu, L., R. S. Sletten, B. Hagedorn, B. Hallet, C. P. McKay, and J. O. Stone (2015), An enhanced model of the contemporary and long-term (200 ka) sublimation of the massive subsurface ice in Beacon Valley, Antarctica, *Journal of Geophysical Research: Earth Surface*, 120, doi:10.1002/2014JF003415.

Liu, L., R. S. Sletten, B. Hallet, E. D. Waddington, and S. E. Wood (in prep), Soil thermal properties and ground thermal regime above an ancient ground ice body in Beacon Valley, Antarctica, *Journal of Geophysical Research: Earth Surface*.

Martin-Torres, F. J., et al. (2015), Transient liquid water and water activity at Gale crater on Mars, *Nature Geosci, advance online publication*, doi:10.1038/ngeo2412.

Martínez, G., and N. Renno (2013), Water and brines on Mars: current evidence and implications for MSL, *Space Science Reviews*, *175*(1-4), 29-51.

Martínez, G., N. Rennó, E. Fischer, C. Borlina, B. Hallet, M. Torre Juárez, A. Vasavada, M. Ramos, V. Hamilton, and J. Gomez-Elvira (2014), Surface energy budget and thermal inertia at Gale Crater: Calculations from ground-based measurements, *Journal of Geophysical Research: Planets*, *119*(8), 1822-1838.

Mellon, M. T., et al. (2009), Ground ice at the Phoenix Landing Site: Stability state and origin, *Journal of Geophysical Research*, *114*, E00E07, doi:10.1029/2009je003417.

Mellon, M. T., W. C. Feldman, and T. H. Prettyman (2004), The presence and stability of ground ice in the southern hemisphere of Mars, *Icarus*, *169*(2), 324-340, doi:10.1016/J.Jicarus.10.022.

Mellon, M. T., and B. M. Jakosky (1993), Geographic Variations in the Thermal and Diffusive Stability of Ground Ice on Mars, *Journal of Geophysical Research-Planets*, *98*(E2), 3345-3364.

Mellon, M. T., and B. M. Jakosky (1995), The Distribution and Behavior of Martian Ground Ice during Past and Present Epochs (Vol 100, Pg 11781, 1995), *Journal of Geophysical Research-Planets*, *100*(E11), 23367-23370.

Mellon, M. T., B. M. Jakosky, H. H. Kieffer, and P. R. Christensen (2000), High-resolution thermal inertia mapping from the Mars Global Surveyor Thermal Emission Spectrometer, *Icarus*, *148*(2), 437-455, doi:10.1006/icar.2000.6503.

Mellon, M. T., B. M. Jakosky, and S. E. Postawko (1997), The persistence of equatorial ground ice on Mars, *Journal of Geophysical Research-Planets*, *102*(E8), 19357-19369, doi:10.1029/97je01346.

Mischna, M. A., M. I. Richardson, R. J. Wilson, and D. J. McCleese (2003), On the orbital forcing of Martian water and CO2 cycles: A general circulation model study with simplified volatile schemes, *Journal of Geophysical Research-Planets*, *108*(E6), 5062, doi:10.1029/2003je002051.

Oehler, D. Z. (2013), A periglacial analog for landforms in Gale Crater, Mars, in *44th Lunar and Planetary Science Conference*, edited.

Paige, D. A. (1992), The thermal stability of near-surface ground ice on Mars, *Nature*, *356*(6364), 43-45.

Reiss, D., S. Gasselt, E. Hauber, G. Michael, R. Jaumann, and G. Neukum (2006), Ages of rampart craters in equatorial regions on Mars: Implications for the past and present distribution of ground ice, *Meteoritics & Planetary Science*, *41*(10), 1437-1452.

Renno, N. O., et al. (2009), Possible physical and thermodynamical evidence for liquid water at the Phoenix landing site, *Journal of Geophysical Research-Planets*, *114*, doi:10.1029/2009je003362.

Schörghofer, N. (2007), Dynamics of ice ages on Mars, *Nature*, *449*(7159), 192-U192, doi:10.1038/Nature06082.

Schörghofer, N. (2009), Buffering of sublimation loss of subsurface ice by percolating snowmelt: A theoretical analysis, *Permafrost and Periglacial Processes*, *20*(3), 309-313, doi:10.1002/Ppp.646.

Schörghofer, N., and O. Aharonson (2005), Stability and exchange of subsurface ice on Mars, *Journal of Geophysical Research-Planets*, *110*, E05003, doi:10.1029/2004je002350.

Schörghofer, N., and K. S. Edgett (2006), Seasonal surface frost at low latitudes on Mars, *Icarus*, *180*(2), 321-334, doi:10.1016/j.icarus.2005.08.022.

Sebastián, E., C. Armiens, J. Gómez-Elvira, M. P. Zorzano, J. Martinez-Frias, B. Esteban, and M. Ramos (2010), The Rover Environmental Monitoring Station Ground Temperature Sensor: A Pyrometer for Measuring Ground Temperature on Mars, *Sensors-Basel*, *10*(10), 9211-9231, doi:10.3390/S101009211.

Smith, D. E., M. T. Zuber, S. C. Solomon, R. J. Phillips, J. W. Head, J. B. Garvin, W. B. Banerdt, D. O. Muhleman, G. H. Pettengill, and G. A. Neumann (1999), The global topography of Mars and implications for surface evolution, *Science*, *284*(5419), 1495-1503.

Smoluchowski, R. (1968), Mars - Retention of Ice, *Science*, *159*(3821), 1348-1350, doi:DOI 10.1126/science.159.3821.1348.

Solomon, S. C., and J. W. Head (1990), Heterogeneities in the Thickness of the Elastic Lithosphere of Mars - Constraints on Heat-Flow and Internal Dynamics, *J Geophys Res-Solid*, *95*(B7), 11073-11083, doi:10.1029/Jb095ib07p11073.

Squyres, S. W., and M. H. Carr (1986), Geomorphic evidence for the distribution of ground ice on Mars, *Science*, *231*(4735), 249-252.

Sugden, D. E., D. R. Marchant, N. Potter, R. A. Souchez, G. H. Denton, C. C. Swisher, and J. L. Tison (1995), Preservation of Miocene glacier ice in East Antarctica, *Nature*, *376*(6539), 412-414.

Toon, O. B., J. B. Pollack, W. Ward, J. A. Burns, and K. Bilski (1980), The Astronomical Theory of Climatic-Change on Mars, *Icarus*, *44*(3), 552-607, doi:Doi 10.1016/0019-1035(80)90130-X.

Yakovlev, V. (2012), The Ice Nature of the Gale Crater Central Structure, paper presented at Lunar and Planetary Institute Science Conference Abstracts.

Zent, A. P., R. M. Haberle, H. C. Houben, and B. M. Jakosky (1993), A Coupled Subsurface-Boundary Layer Model of Water on Mars, *Journal of Geophysical Research-Planets, 98*(E2), 3319-3337.

Zent, A. P., and R. C. Quinn (1995), Simultaneous Adsorption of CO_2 and H_2O under Mars-Like Conditions and Application to the Evolution of the Martian Climate, *Journal of Geophysical Research-Planets, 100*(E3), 5341-5349, doi:10.1029/94je01899.

Zorzano, M. P., E. Mateo-Marti, O. Prieto-Ballesteros, S. Osuna, and N. Renno (2009), Stability of liquid saline water on present day Mars, *Geophysical Research Letters*, *36*, doi:10.1029/2009gl040315.

Chapter 5. Conclusions and Future Work

5.1. Summary and Conclusions

The dissertation investigates the long-term persistence and stability of the massive ice occurring within decimeters of the ground surface in the McMurdo Dry Valleys of Antarctica and equatorial ice on Mars that has been suggested to have formed during last high obliquity of 32 degrees. First, the evolution of subsurface ice in Beacon Valley was studied using a water-vapor diffusion model constrained by local climate data including episodic snow events and soil temperature measurements to depth. At the same site, a thermal model was developed to calculate the subsurface temperatures driven by the near-surface temperatures as a boundary condition, and validated against the measured subsurface temperatures. Finally, using the validated thermal model to constrain subsurface temperatures on Mars based on surface temperatures from the Curiosity rover, a water-vapor diffusion model was developed for Mars to assess the long-term persistence of the ground ice since the most recent high obliquity changes at ~500 ka.

To determine the rate of water vapor exchange between the massive subsurface ice and the atmosphere in Beacon Valley, an enhanced water vapor diffusion model that accounts for the effects of episodic snow cover and snowmelt events was developed and presented in Chapter 2. This model is founded on 12 years of hourly data on air temperature, relative humidity, and soil temperature. The ice loss from the massive ice body based on a simple vapor-diffusion model averages 0.17 mm a^{-1} during 1999−2011 with most sublimation occurring during the summer season. Accounting for the episodic snow cover and snowmelt events reduces the ice sublimation rate by 30% to 0.11 mm a^{-1}. This model is then extended over the past 200 ka based on the atmospheric temperature reconstructed from the ice core records from nearby Taylor Dome, and a

detailed comparison between measured atmospheric temperature and relative humidity from 1999 to 2011 in Beacon Valley. The latter yielded a defined relationship between the atmospheric temperature and vapor density. The model produces an average sublimation rate of 0.09 mm a^{-1} for the past 200 ka. It was shown that ground surface conditions such as snow cover and snowmelt affect the sublimation rates of subsurface ice; however, under none of the scenarios is the massive subsurface ice in Beacon Valley stable during the past 200 ka. Even with the slowest loss rate, 40 meters of ice would be lost in 1 Ma.

Modeling ground temperatures is essential for vapor diffusion models investigating the ground ice stability when in situ temperature measurements are not available. A study on the soil thermal properties and 1-D heat diffusion process in Beacon Valley was presented in Chapter 3. For the temperature range of −47.9 to 7.5°C at our study site, the heat capacity of the dry soil ranges from 589 to 687 J kg^{-1} K^{-1} with a positive temperature dependence, thermal conductivity ranges from 0.29 to 0.33 W m^{-1} K^{-1}, and thermal diffusivity ranges from 0.30 to 0.32 mm^2 s^{-1} with a negative temperature dependence. The 1-D thermal diffusion model, numerically solved both by the finite difference method (FDM) and finite volume method (FVM), assumes that soil temperature at depth is driven primarily by the surface temperature. The results demonstrated that the FVM modeled results provide a much better fit with average differences range from 0.01°C to 0.03°C at various depths. Seasonal, as well as short-term, fluctuations in temperature are reflected well in the modeled results. In addition to reducing the model error, using temperature-dependent thermal parameters for the dry soil and the massive ground ice provides more realistic constraints on the thermal model. Increasing the thermal conductivity of either the dry soil layer, ground ice layer, or both, will increase the difference between modeled and measured temperature. In contrast to the Arctic where liquid water is present seasonally, the amount of latent heat from episodic

snowmelt and ice sublimation/condensation could alter the temperature up to 10^{-3} °C, which is insufficient to impact the temperature observations.

Our studies on the vapor and heat diffusion process were then applied on Mars (Chapter 4) to understand the ground thermal regime and the dynamics of atmospherically derived ground ice in the present Martian climate, which was made possible by the acquisition of hourly climate measurements including air temperature, RH, pressure, and ground surface temperature by Curiosity REMS. The thermal model results document the rapid attenuation and lag of ground temperature variations with depth. The attenuation is similar in different terrain despite the differences in thermal inertia. Diurnal variations of ground surface temperature change with location and seasonality. The diurnal and annual skin depth are approximately 0.05 m and 1.3 m at Gale Crater, respectively.

Under current climate conditions, water vapor has a tendency to escape from the regolith to the atmosphere. Ice in the regolith would sublimate quickly, especially near the ground surface; the rate of sublimation decreases as the top of the ice-rich regolith descends and the dry regolith above the ice thickens. If ground ice was stable and present at Gale Crater ~0.5 Ma ago at the last high obliquity cycle, residual ice is expected within several meters of the ground surface at present, assuming that the regolith was saturated with ice initially. This study did not account for the effects of potential replenishing processes, adsorption, and climate change influenced by obliquity, all of which may slow the sublimation rate.

5.2. Future Work

Current vapor diffusion models treat soil/regolith as a simple inert, porous material, and indicate that ground ice should sublimate to several meters below the surface within a few thousand

years in the MDV; however, other processes are likely to influence vapor transport. Adsorbed water can affect vapor density, and hence vapor fluxes in ice-free soil. Solutes in soil water lower the freezing point, absorb atmospheric water, and thereby affect the sublimation rate by influencing soil water activity (water availability).

Salts can hydrate and lower the water activity [*Marion and Grant,* 1994] and are abundant on Mars. The occurrence of salts in regolith in dry regions includes homogeneous salt-cemented soil horizons, salt clods, surface efflorescence and encrustations, salt crystals under boulders and cobbles, centimeter to meter thick massive salt bodies, and salt precipitates in bedrock cracks. Salts are common on the surface of Mars [*Toner et al.,* 2014]; carbonates [*Bandfield et al.,* 2003; *Ehlmann et al.,* 2008; *Morris et al.,* 2010], sulfates [*Kounaves et al.,* 2010; *Langevin et al.,* 2005], chlorides [*Ruesch et al.,* 2012], and perchlorates [*Hecht et al.,* 2009] have been detected. In the MDV, more than 30 salts have been described [*Keys,* 1979]. It has been suggested that unfrozen water films on mineral surfaces exist to very low temperatures [*Anderson and Morgenstern,* 1973; *Smith and Tice,* 1988], and it is assumed that most ion migration occurs along these thin water films [*Dickinson and Rosen,* 2003; *Ugolini and Anderson,* 1973]. The thin surface films may contain high solute concentrations and thereby lowers the freezing point of bulk water well below 0 ℃. Previous studies have not focused on the influence of salts on the chemical potential of soil moisture and the stability of subsurface ice. Moreover, standard vapor diffusion models neglect kinetics and assume chemical equilibrium is maintained between the water vapor and hydrated salts. It merits further consideration as to how the hysteresis of the adsorption and desorption of salty soils may affect the transport or water into and out of the soil.

Adsorption of vapor onto mineral surfaces is another important physical process to take into account when modeling the water vapor diffusion through a porous regolith. Water molecules

are lightly bound to the mineral surfaces by van der Waal forces. They are in equilibrium with the surrounding water vapor in the pore space. In turn, this vapor diffuses through the regolith to equilibrate with the atmospheric water vapor [*Jakosky et al.*, 1997; *Zent and Quinn*, 1995]. Adsorption is strongly dependent on the subsurface temperature, soil composition, thermal inertia, albedo, and atmospheric water content. The adsorption or desorption of water can have a significant effect on the instantaneous vapor density, and therefore on gradients in vapor density. Adsorption increases with partial pressure and may influence local vapor density gradients.

We expect that the kinetics of salt hydration/dehydration and water adsorption/desorption have influence on water vapor pressure, and thereby affect ground ice sublimation rates and stability. Most studies have assumed that the adsorption/desorption of water by salts and surfaces are in equilibrium and do not affect the vapor transport over long time periods [*Schörghofer and Aharonson*, 2005]. These studies have not considered the kinetics of these processes, which are known to be slow [*Bryson et al.*, 2008; *Chevrier et al.*, 2008]. Considering the effects of adsorption and salts on the chemical potential of soil water will help improve our estimate of the water activity and therefore the water vapor density gradient driving the sublimation or condensation of ground ice.

5.3. References

Anderson, D. M., and N. Morgenstern (1973), Physics, chemistry, and mechanics of frozen ground: a review, paper presented at Permafrost: The North American Contribution to the Second International Conference, National Academy of Sciences, Washington, DC.

Bandfield, J. L., T. D. Glotch, and P. R. Christensen (2003), Spectroscopic identification of carbonate minerals in the Martian dust, *Science*, *301*(5636), 1084-1087.

Bryson, K. L., V. Chevrier, D. W. G. Sears, and R. Ulrich (2008), Stability of ice on Mars and the water vapor diurnal cycle: Experimental study of the sublimation of ice through a fine-grained basaltic regolith, *Icarus*, *196*(2), 446-458, doi:10.1016/j.icarus.2008.02.011.

Chevrier, V., D. R. Ostrowski, and D. W. G. Sears (2008), Experimental study of the sublimation of ice through an unconsolidated clay layer: Implications for the stability of ice on Mars and the possible diurnal variations in atmospheric water, *Icarus*, *196*(2), 459-476, doi:10.1016/j.icarus.2008.03.009.

Dickinson, W. W., and M. R. Rosen (2003), Antarctic permafrost: An analogue for water and diagenetic minerals on Mars, *Geology*, *31*(3), 199-202.

Ehlmann, B. L., J. F. Mustard, S. L. Murchie, F. Poulet, J. L. Bishop, A. J. Brown, W. M. Calvin, R. N. Clark, D. J. Des Marais, and R. E. Milliken (2008), Orbital identification of carbonate-bearing rocks on Mars, *Science*, *322*(5909), 1828-1832.

Hecht, M., S. Kounaves, R. Quinn, S. West, S. Young, D. Ming, D. Catling, B. Clark, W. Boynton, and J. Hoffman (2009), Detection of perchlorate and the soluble chemistry of martian soil at the Phoenix lander site, *Science*, *325*(5936), 64-67.

Jakosky, B. M., A. P. Zent, and R. W. Zurek (1997), The Mars water cycle: Determining the role of exchange with the regolith, *Icarus*, *130*(1), 87-95.

Keys, J. (1979), *Distribution of salts in the McMurdo Region, with analyses from the saline discharge area at the terminus of Taylor Glacier*, Victoria University of Wellington.

Kounaves, S. P., M. H. Hecht, J. Kapit, R. C. Quinn, D. C. Catling, B. C. Clark, D. W. Ming, K. Gospodinova, P. Hredzak, and K. McElhoney (2010), Soluble sulfate in the martian soil at the Phoenix landing site, *Geophysical Research Letters*, *37*(9), L09201.

Langevin, Y., F. Poulet, J.-P. Bibring, and B. Gondet (2005), Sulfates in the north polar region of Mars detected by OMEGA/Mars Express, *Science*, *307*(5715), 1584-1586.

Marion, G. M., and S. A. Grant (1994), FREZCHEM: A chemical-thermodynamic model for aqueous solutions at subzero temperatures, DTIC Document, pp.

Morris, R. V., S. W. Ruff, R. Gellert, D. W. Ming, R. E. Arvidson, B. C. Clark, D. Golden, K. Siebach, G. Klingelhöfer, and C. Schröder (2010), Identification of carbonate-rich outcrops on Mars by the Spirit rover, *Science*, *329*(5990), 421-424.

Ruesch, O., F. Poulet, M. Vincendon, J. P. Bibring, J. Carter, G. Erkeling, B. Gondet, H. Hiesinger, A. Ody, and D. Reiss (2012), Compositional investigation of the proposed chloride-bearing materials on Mars using near-infrared orbital data from OMEGA/MEx, *Journal of Geophysical Research: Planets (1991–2012)*, *117*(E11), E00J13.

Schörghofer, N., and O. Aharonson (2005), Stability and exchange of subsurface ice on Mars, *Journal of Geophysical Research-Planets*, *110*, E05003, doi:10.1029/2004je002350.

Smith, M. W., and A. R. Tice (1988), Measurement of the unfrozen water content of soils: comparison of NMR and TDR methods, pp.

Toner, J., D. Catling, and B. Light (2014), Soluble salts at the Phoenix Lander site, Mars: A reanalysis of the Wet Chemistry Laboratory data, *Geochimica et Cosmochimica Acta*, *136*, 142-168.

Ugolini, F. C., and D. M. Anderson (1973), Ionic Migration and Weathering in Frozen Antarctic Soils, *Soil Science*, *115*(6), 461-470, doi:10.1097/00010694-197306000-00010.

Zent, A. P., and R. C. Quinn (1995), Simultaneous Adsorption of CO_2 and H_2O under Mars-Like Conditions and Application to the Evolution of the Martian Climate, *Journal of Geophysical Research-Planets*, *100*(E3), 5341-5349, doi:10.1029/94je01899.